Escola de Camins
Escola Tècnica Superior d'Enginyeria de Camins, Canals i Ports
UPC BARCELONATECH

TREBALL FINAL DE MÀSTER

Structural behaviour of compact stainless steel beam-columns subjected to combined loading

Treball realitzat per:
Jordi Durán García

Dirigit per:
Rolando Chacón Flores

Màster en:
Enginyeria de Camins, Canals i Ports de Barcelona

Barcelona, **Juny 2016**

Departament de la Construcció

TABLE OF CONTENT

1. INTRODUCTION

1.1 Background

Stainless steel has been introduced and increasingly utilized in architectural and structural applications due to their good corrosion resistance, ease of maintenance, aesthetic appearance and its mechanical properties which differs from carbon steel.

Ferritic stainless steel represents one of the five stainless steel families and it is characterized by a low nickel content. Nickel is an element whose price is reaching unusual levels and suffers continuous fluctuations in market. So, this makes ferritic stainless steel an attractive material due to its lower and stable price against austenitic and duplex ones, preserving mechanical corrosion resistances. The chemical compositions of different stainless steel grades are listed in the European code EN 10088-1.

The use of stainless steel for construction is contemplated by the design approach presented in EN 1993 1-4, though it is not well established and the design approach, most of times, is based on the indication given by EN 1993 1-1 for carbon steel. The study on buckling behavior of stainless steel and the interaction axial force and bending moment relation will be advantageous to develop the application rules on stainless steel.

It is important to study the applicability of the expressions proposed in EN 1993 for carbon steel to stainless steel elements. This work pretends to study this applicability in stainless steel columns. Different research works are being developed in order to achieve a better knowledge of stainless steel behavior.

This research belongs to a vaster study on ferritic stainless steel in which, experimental, numerical and theoretical approaches are performed not only in compact sections but also in slender sections. In this project research, groups from CTU in Prague and UPC have developed joint collaboration during 2016.

1.2 Thesis objectives

The main objective of the thesis is to increase the fundamental understanding of the behaviour of stainless steel, especially ferritic one, beam-columns subjected to combined axial load and bending moment and then to verify the European Standard design method. This study is done for compact sections Class 1 and Class 2.

The development of the current thesis has also more objectives:

- To perform a validation of the model and procedure that is going to be used in this thesis with some research tests which are just done or in process to be submitted.
- To study the influence of the strain hardening parameter in ferritic stainless steel.
- To develop various numerical models in order to reproduce their response adopting different cross-sections and lengths members.

- These models, realized with Abaqus code, shall be compared with the results given by the designed formulae of EN 1993-1-4 and some proposals of research done at UPC (Universitat Politècnica de Catalunya) and the Imperial College of London in order to investigate the efficiency of the interaction factors coefficients used in such method with the purpose to strengthen their reliability.
- To carry out a parametric study for ferritic stainless steel and then to make a comparison with the European buckling curves.

1.3 Thesis outline

This chapter contains a brief introduction to the background of stainless steel and its engineering applications in the construction industry. This section summarizes the main aspects of these tasks and analyses and how they are included and organized in the contents of the thesis. This document is divided into seven chapters.

Chapter 2 provides a broad review of previous studies that are relevant to this thesis, in general for stainless steel and in particular for ferritic stainless steel. It also provides a summary of the existing design standards and formulas used in this research work.

Chapter 3 presents the description of the used numerical models. Firstly, it is decided to indicate some general information about the Finite Element Method (FEM). Then, the constitutive equation and the material modelling have been defined.

In chapter 4, a validation of the model to use in this thesis is performed. This validation is done firstly with an experimental study on ferritic stainless steel RHS and SHS beam-columns previously done by Arrayago et al. (2015). Then, as a part of join collaboration with CTU in Prague, a cross-section validation for a Class 1 and a Class 4 is done. Finally, a validation of the strain hardening exponent is done for a ferritic stainless steel in order to observe how this parameter makes to change the final results of the analysis.

Chapter 5 presents numerical studies of the buckling behaviour of ferritic, austenitic and duplex stainless steel SHS under combined compression and bending moment linear along the length member. The main objective of this chapter is to study how the interaction factor *k* of different previously research proposals works through different slendernesses. The obtained experimental data are employed to assess the accuracy of the current codified design codes.

Chapter 6 focuses on a parametric study with ferritic stainless steel conducted to generate more beam-column data over a wide range of cross section sizes and slendernesses. Then, with the European curve for buckling it is compared the results obtained and validated if these results are safe enough or not.

Chapter 7 ends with a summary of the important findings of this research, conclusions and suggestions for further works.

2. STATE OF ART

In this section we will see a short description of stainless steel and its properties. Furthermore, it is going to be described in particular the ferritic stainless steel, the cross-sectional classification, the ultimate capacity predictions for all loading types taken into account in this Master Thesis and some previous research works regarding stainless steel members subjected to the combined loading in question.

2.1 Stainless steel

Stainless steel has been introduced and increasingly utilized in architectural and structural application due to their good corrosion resistance, ease of maintenance, aesthetic appearance, and its mechanical properties which differs from carbon steel.

Unlike carbon steel which has an elastic response, with a clearly defined yield point, followed by a yield plateau and a moderate degree of strain hardening, stainless steel has predominantly non-linear stress-strain behaviour with significant strain hardening. The stainless steel design standards have been developed largely in-line and refer to carbon steel design guidelines, even though they were both different on its mechanical behaviour. The study on buckling behaviour of stainless steel and the interaction axial force and bending moment relation will then be advantageous to develop the application rules on stainless steel.

First of all, it will be described what stainless steel consist of, which elements are part of it and which is the contribution they offer to the generic behaviour of the material. The purpose it to perceive where the ferritic category of stainless steel comes from and its properties.

All stainless steel contains principally iron and a minimum of 10.5% chromium. This last reacts with oxygen and humidity in the environment to form a protective, adherent and coherent oxide film which envelops the whole surface of the material. This oxide film is very thin (2-3 nanometres) and exhibits a truly remarkable property: when it is damaged, it self-repairs since chromium in the steel reacts rapidly with oxygen and humidity in the environment to reform the oxide layer. If the content of chromium enhances beyond the minimum (10.5%), a greater corrosion resistance will be achieved. Adding an 8% or more of nickel, this resistance may be further improved and a wide range of properties can be provided. Therefore, the addition of molybdenum further increases corrosion resistance (in particular, resistance to pitting corrosion), while nitrogen increases mechanical strength and enhances pitting resistance.

The selection of a particular type of stainless steels generally depends on the requirements which a particular application requires. In most cases, the primary requirement is corrosion resistance, followed by tarnish and oxidation resistance. The austenitic stainless steel, with its high content of chromium, is usually required in very high or very low temperatures, because of its significant corrosion resistance, higher than the lower chromium ferritic or martensitic stainless steel.

2.1.1 Types of stainless steel

The stainless steel family has several branches, which may be differentiated in many different ways, such as: areas of application, alloying elements used in their production or the metallurgical phases they present in their microscopic structures. The main types of stainless steel are the ferritic, martensitic, austenitic and duplex stainless steel, where the last one consist of a mixture of ferritic and austenitic crystalline structures.

Within each of these groups, there are several grades of stainless steel, defined according to their compositional ranges. These compositional ranges are defined mainly in European and USA standards.

According to Design Manual for Structural Stainless Steel (April 2006) [CEN, 2006] each stainless steel has a unique corresponding steel number. For example, grade 304L has a steel number 1.4307, where:

- The number 1 denotes steels.
- The number 43 denotes one group of stainless steel (in this case basic chromium-nickel austenitic steels).
- 07 is individual grade identification.

The steel name system provides some understanding of the steel composition. The name of the steels number 1.4307 is X2CrNi18-9, where:

- X denotes high alloy steel.
- 2 is % of carbon multiplied by 100.
- CrNi are the chemical symbols of main alloying elements.
- 18-19 is the % of main alloying elements.

Within the specified range, the stainless steel grade exhibits a wide range of properties.

a) Ferritic stainless steels (e.g. grades 1.4003) consist of chromium (typically 12.5% or 17%) and iron. Ferritic stainless steels are essentially nickel-free (important advantage from the rest of stainless steel grades for structural use). These materials contain very little carbon and are non-heat treatable, but exhibit superior corrosion resistance than martensitic stainless steels and possess good resistance to oxidation. They are ferromagnetic and, although subjected to an impact transition at low temperatures, possess adequate formability. Their thermal expansion and other thermal properties are similar to conventional steels, but with higher fire resistance in general (in fact, all types of stainless steels are better than carbon steel when talking about fire). Ferritic stainless steels are readily welded in thin sections, but suffer grain growth with consequential loss of properties when welded in thicker sections.

b) Martensitic stainless steels (e.g. grades 1.4006, 1.4028 and 1.4112) consist of carbon (0.2-1.0%) chromium (10.5-1%) and iron. These materials may be heat treated, in a similar manner to conventional steels, to provide a range of mechanical properties, but

offer higher harden-ability and have different heat treatment temperatures. Their corrosion resistance may be described as moderate (i.e. their corrosion performance is poorer than other stainless steels of the same chromium and alloy contents). They are ferromagnetic, subjected to an impact transition at low temperatures and possess poor formability. Their thermal expansion and other thermal properties are similar to conventional steels. They may be welded with caution, but cracking can be a feature when matching filler metals are used.

c) Austenitic stainless steels (e.g. grades 1.4301 and 1.4833) consist of chromium (16-26%), nickel (6-12%) and iron. Other alloying elements (e.g. molybdenum) may be added or modified according to the desired properties that are defined in the standards to produce derivative grades. The austenitic group contains more grades that are used in greater quantities, than any other type of stainless steel. Austenitic stainless steels exhibit superior corrosion resistance to both ferritic and martensitic stainless steel. Corrosion performance may be varied to suit a wide range of service environments by careful alloy adjustment e.g. by varying the carbon or molybdenum content. These materials cannot be hardened by heat treatment and are strengthened by work-hardening. They offer excellent formability and their response to deformation can be controlled by chemical composition. They are not subjected to an impact transition at low temperatures and possess high toughness to cryogenic temperatures. They exhibit greater thermal expansion and heat capacity, with lower thermal conductivity than other stainless or conventional steels. They are generally readily welded, but care is required in the selection of consumables and practices for more highly alloyed grades. Austenitic stainless steels are often described as non-magnetic, but may become slightly magnetic when machined or worked.

d) Duplex stainless steels (e.g. grade 1.4462) consist of chromium (18-26%), nickel (4-7%), molybdenum (0-4%), copper and iron. These stainless steels have a micro-structure consisting of austenite and ferrite, which provides a combination of the corrosion resistance of austenitic stainless steels with greater strength. Duplex stainless steels are weldable, but care must be exercised to maintain the correct balance of austenite and ferrite. They are ferromagnetic and subjected to an impact transition at low temperatures. Their thermal expansion lies between that of austenitic and ferritic stainless steels, while other thermal properties are similar to plain carbon steels. Formability is reasonable, but higher forces than those used for austenitic stainless steels are required.

The austenitic stainless steels and the duplex stainless steels are generally the more useful groups for structural applications.

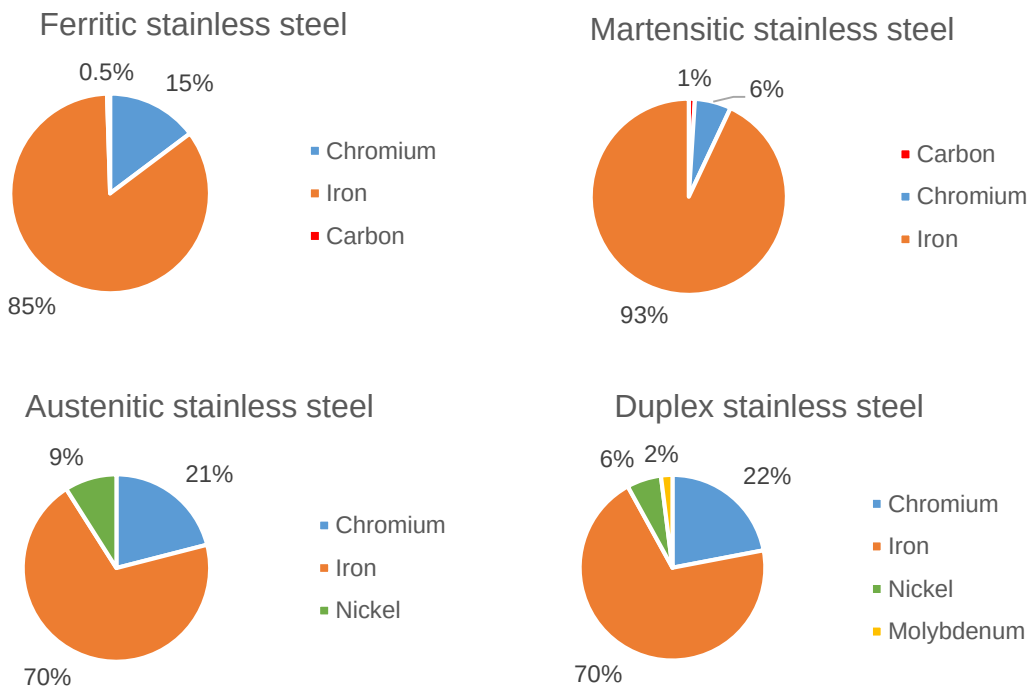

Figure 2.1. Classification of stainless steels according to alloying elements content

2.1.2 Effect of each alloying element on structure and properties

In this section it is explained how each of the alloying elements contribute to the global behaviour of the stainless steel and what would happen if its content is varied.

- Chromium is by far the most important alloying element in stainless steel production. A minimum of 10.5% chromium is required for the formation of a protective layer of chromium oxide on the steel surface. Chromium is described as ferritic stabilizer.
- Nickel improves general corrosion resistance and prompts the formation of austenite. Stainless steels with 8-9% nickel have a fully austenitic structure and exhibit superior welding and working characteristics to ferrite stainless steels.
- Molybdenum increases resistance to both local and general corrosion. It is added to martensitic stainless steels to improve high temperature strength.
- Nitrogen increases strength and enhances resistance to localized corrosion. It is austenite former.
- Cooper increases general corrosion resistance to acids and reduces the rate of work-hardening. It is austenitic stabilizer.
- Carbon enhances strength, but may have an adverse effect on corrosion resistance by the formation of chromium carbides. It is an austenitic stabilizer.
- Titanium may be used to stabilize stainless steel against inter-granular corrosion. Titanium carbides are formed in preference to chromium carbide and thus localized depletion of chromium is prevented. These elements are ferrite stabilizers.

- Sulphur is added to improve the machinability of stainless steels. As a consequence, sulphur-bearing stainless steels exhibit reduced corrosion resistance.
- Cerium, a rare earth metal, improves the strength and adhesion of the oxide film at high temperatures.
- Manganese is an austenitic former, which increases the solubility of nitrogen in the steels and may be used to replace nickel in nitrogen-bearing grades.
- Silicon improves resistance to oxidation and is also used in special stainless steels exposed to highly concentrated sulphuric and nitric acids. Silicon is a ferrite stabiliser.

2.1.3. Stress and strain behaviour

The stress-strain behaviour of stainless steels differs from that of carbon steels in a number of respects. The most important difference is in the shape of the stress-strain curve. Whereas carbon steels typically exhibit linear elastic behaviour up to the yield stress and a plateau before strain hardening is encountered, stainless steel has a more rounded response with no well-defined yield stress (see Figure 2.2). Therefore, stainless steel "yield" strengths are generally quoted in terms of a proof strength defined for a particular offset permanent strain (conventionally the 0.2% strain).

Note that Figure 2.2 shows typical experimental stress-strain curves. The curves shown are representative of the range of material likely to be supplied and should not be used in design.

Stainless steels can absorb considerable impact without fracturing due to their excellent ductility and their strain hardening characteristics.

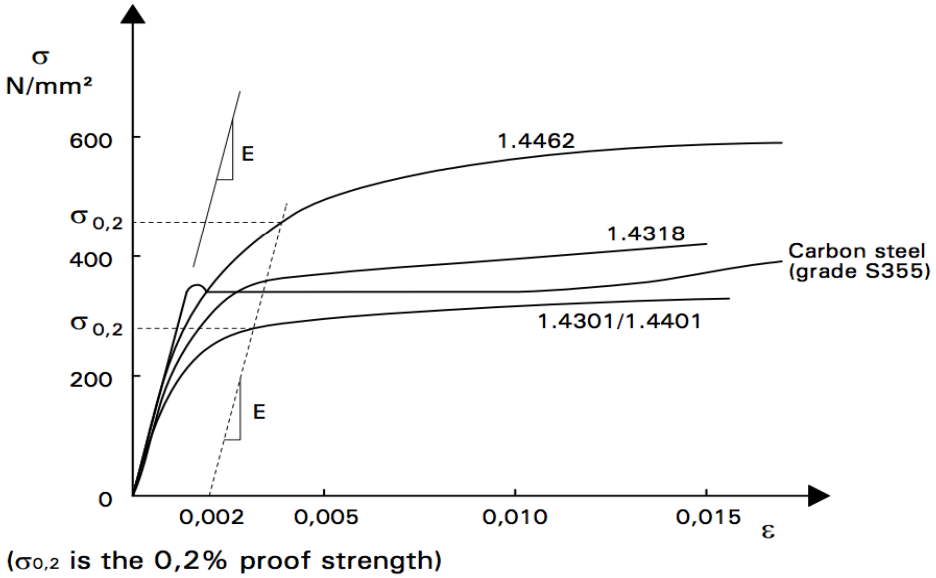

Figure 2.2. Typical stress-strain curves for stainless steel and carbon steel in the annealed condition [CEN, 2006].

There are factors can change the form of the basic stress-train curve for any given grade of stainless steel. These factors are:

Cold working

Strength levels of austenitic and duplex grades are enhanced by cold working. Associated with this enhancement is a reduction in ductility but his normally is of slight consequence due to the initial high values of ductility, especially for the austenitic stainless steels.

As stainless steel is cold worked, it tends to exhibit non-symmetry of tensile and compressive behaviour and anisotropy (different stress-strain characteristics parallel and transverse to the rolling directions). The degree of asymmetry and anisotropy depends on the grade, level of cold working and manufacturing.

The price of cold worked stainless steel is slightly higher than the equivalent annealed material, depending on the grade, product form and level of cold working.

Strain-rate sensitivity

Strain-rate sensitivity is more pronounced in stainless steels than in carbon steels. That is, a proportionally greater strength can be realized at fast strain rated for stainless steel than for carbon steel.

Heat treatment

Annealing, or softening, reduces the strength enhancement and the anisotropy.

2.1.4. Stainless steels used profiles

The applications for cold formed stainless steel profiles such as rectangular hollow sections (RHS) and square hollow sections (SHS) are plenty, particularly in industrial, commercial and residential construction. They are also commonly used in the mechanical and fabricating industries, the agricultural industry, and mining industry and simply for signage. Stainless steel RHS have such universal uses because they are durable and easy to prepare for welding or joining. Stainless steel RHS are practical and aesthetic elements, what makes them highly sought after and a functional solution to modern building needs and requirements.

2.1.5. Standards

American standards SEI/AISI “Specification for design of cold worked stainless structural members”, covers the three traditional ferritic steel grades, as well as South African standards and Australian standards. Eurocode corresponding to stainless steel, EN 1993-1-4 [CEN, 2006], is applicable for these three grades of ferritic stainless steels: 1.4003, 1.4016 and 1.4512. Even so, in some cases the specifications have been obtained and contrasted only for austenitic and duplex stainless steel grades, and therefore in some cases specific guideline is missing for ferritic stainless steel. Besides, in many aspects EN 1993-1-4 refers to part of Eurocode EN 1993-1-1 which has not been validated for ferritic stainless steels. There is not enough information

regarding to structural aspects, neither fire resistance, atmospherical corrosion resistance, welded and screwed unions resistance for its use in construction.

2.1.6. Life cycle cost

Stainless steels are usually considered as an expensive material, but this is because only the initial cost is taken into account.

Stainless steels are 100% recyclable without any loss in quality no matter how many times the process is repeated. When products reach the end of their useful lives, 90% of the stainless steel is collected and recycled. Stainless steels are durable and have low maintenance costs due to their corrosion resistance. There is no coating or painting requirement and normal maintenance would simply be occasional cleaning.

The durability and ease of maintenance compensate for the sometimes higher initial purchasing costs and it is often the least expensive choice in a life cycle costing comparison. This ability to provide long-term performance with a minimum of downtime and cost associated with maintenance is determined by calculating the material's life cycle cost (LCC). Life cycle costing (LCC) is a technique developed for identifying and quantifying all costs, initial and ongoing, associated with a project or installation over a given period. In general terms, the total LCC can be broken down into component:

LCC = Acquisition Cost + Fabrication and Installation Cost + Maintenance Cost (periodic) + Replacement Cost (periodic) + Cost of Lost Production (periodic) – Residual (Scrap) Value.

In the next Figure 2.4 it is possible to see the comparison between stainless steel and mild steel (a cheaper material if it talks about initial costs) in a water mixing tank.

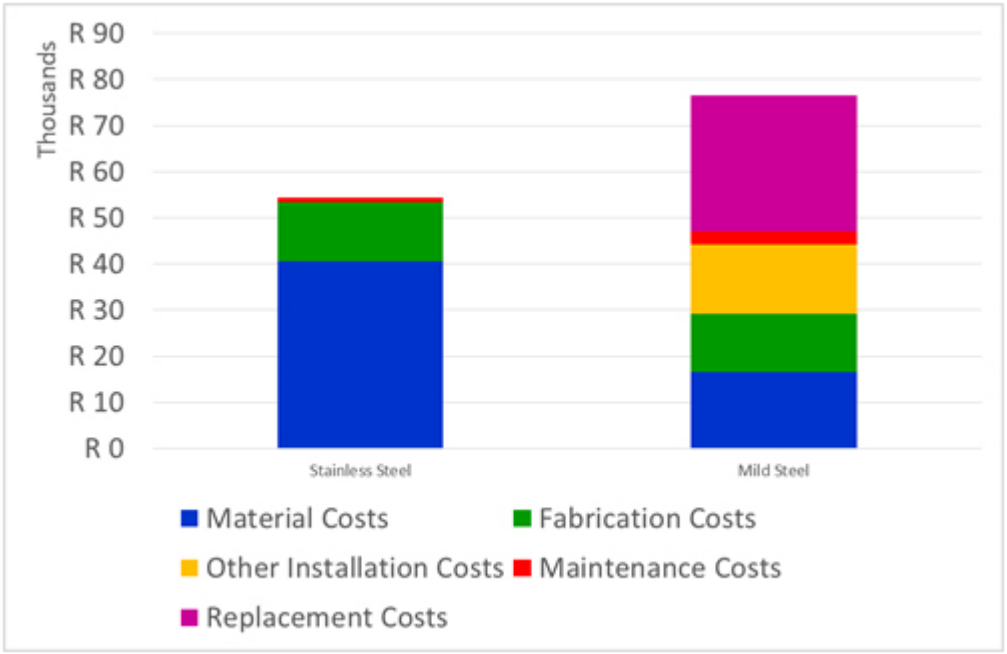

Figure 2.4. Comparison of the total costs between carbon and stainless steel [sassda, Southern Africa stainless steel development association]

2.2. Ferritic stainless steel

It is important to remark that ferritic stainless steels differ from the other families in the absence of nickel. Depending on the content of chromium, molybdenum and other elements contained, it shows us different corrosion resistances and weldability.

There are five groups of ferritic grades depending on the proportion range of its elements as shown in the following Figure 2.5:

Figure 2.5. Groups of ferritic grades [Satyendra, 2014. http://www.ispatguru.com]

- Group 1: This group of ferritic has the lowest chromium content and is the least expensive. It is perfect for non-corrosive conditions. In this context, it has a longer life than carbon style.
- Group 2: It is the most widely used group, having higher content of chromium. It is appropriate to have an intermittent contact with the water but in non-corrosive conditions.
- Group 3: The difference between this group and group 2 is that this one presents better weldability and formability thanks to the stabilizers. The quantity of chromium is similar to group 2.
- Group 4: This group has added molybdenum for extra corrosion resistance. It is corrosion resistant and has a wide range of uses.
- Group 5: These are grades with very high chromium content besides molybdenum, which makes them as corrosion resistant in highly corrosive environments as titanium metal.

Nickel is an element which price is reaching unprecedented levels and suffers continuous fluctuations in market.

Figure 2.6. Nickel price evolution in $ [http://www.infomine.com]

This makes ferritic stainless steel an attractive material due to its lower and stable price against the austenitic ones. Thereby, it is interesting to extend ferritic stainless steel application to structural purposes because in addition to economic reasons, it presents some suitable properties. Ferritic stainless steel also presents all the aforementioned advantages over carbon steel in terms of corrosion resistance and lower lifecycle cost but the absence of nickel provides some extra advantages over the austenitic grades as it has been pointed out before.

Ferritic grades have good mechanical properties (250-330 MPa), with higher yielding stress than austenitic stainless steels and similar elongation properties to carbon steel. They are easier to cut and work than austenitic than the main differences over austenitic grades are their thermal expansion, thermal conductivity and magnetism.

The thermal expansion coefficient of ferritic stainless steels is much lower than in austenitic, similar to carbon steel, so they distort less when heated. This presents some useful advantages in welding and this property is being analysed as part of an energy saving strategy in which the thermal capacity of the ferritic stainless steel is mobilized in floor slabs for example. The magnetic nature of ferritic stainless steels was initially considered as a disadvantage for the working and welding processes but the magnetism of theses grades is now considered one of its major assets, having many potential uses. In addition, it does not need any protection layers as painting and it is easier to recycle than galvanized steels.

Ferritic stainless steels are not widely covered by the stainless steel Standards but some research is being done in order to include them in the most important specifications. American standards SEI/AISI covers three traditional ferritic steel grades 1.4003, 1.4016 and 1.4512, as well as South African and Australian standards.

The European Standard EN 1993-1-4 [CEN, 2006] corresponding to stainless steels also covers the same three ferritic grades. Anyway, theses specifications have been obtained for different austenitic and duplex stainless steel grades and some research needs to be conducted in order to study their applicability to the ferritic stainless steels.

As it was commented in 2.1.3 Stress and Strain Behaviour, the stainless steel is a material with suitable mechanical properties for structural applications but its nonlinear stress-strain behaviour makes it different from carbon steel. Actual modelling techniques require defining an

analytical expression to describe this nonlinear stress-strain relationship through a material model.

In last decades various material models have been developed in order to reproduce stainless steel behaviour and some of them are in included in European Standards. All these models have derived from the general expression proposed by Ramberg-Osgood [Ramberg and Osgood, 1943] with Hill's modification. The basic equation is presented in Equation (2.1):

$$\varepsilon = \frac{\sigma}{E} + 0.002\left(\frac{\sigma}{\sigma_{0.2}}\right)^{n} \tag{2.1}$$

where:

E is the initial elastic modulus (Young's modulus)

$\sigma_{0.2}$ is the proof stress corresponding to a 0.2% plastic strain.

The non-linear parameter n is usually considered by the following Equation (2.2):

$$n = \frac{\ln(20)}{\ln\left(\frac{\sigma_{0.2}}{\sigma_{0.01}}\right)} \tag{2.2}$$

where $\sigma_{0.01}$ is the 0.01% proof stress.

The basic Ramberg-Osgood [Ramberg and Osgood, 1943] formulation has been shown to be capable of accurately representing different regions of the stress-strain curve, depending on the choice of the *n* parameter, but to be generally incapable of accurately representing the full stress-strain curve with a single value of *n*. This observation led to the development of various two-stages Ramber-Osgood models that were capable of providing a single continuous representation of the strain curve of stainless steel from the onset of loading to the ultimate tensile stress. Mirambell-Real [Mirambell and Real, 2000] proposed a two-stage model based on the Ramberg-Osgood expression, but defining a second curve for stresses above the 0.2% proof stress, with a new reference system, denoted ($\sigma^* - \varepsilon^*$) and presented in Figure 2.7, where the transformation of the variables to the new reference system from the original one is defined in Equations (2.3) and (2.4), where $\sigma_{0.2}$ is the total strain at the 0.2% proof stress.

$$\sigma^* = \sigma - \sigma_{0.2} \tag{2.3}$$

$$\varepsilon^* = \varepsilon - \varepsilon_{0.2} \tag{2.4}$$

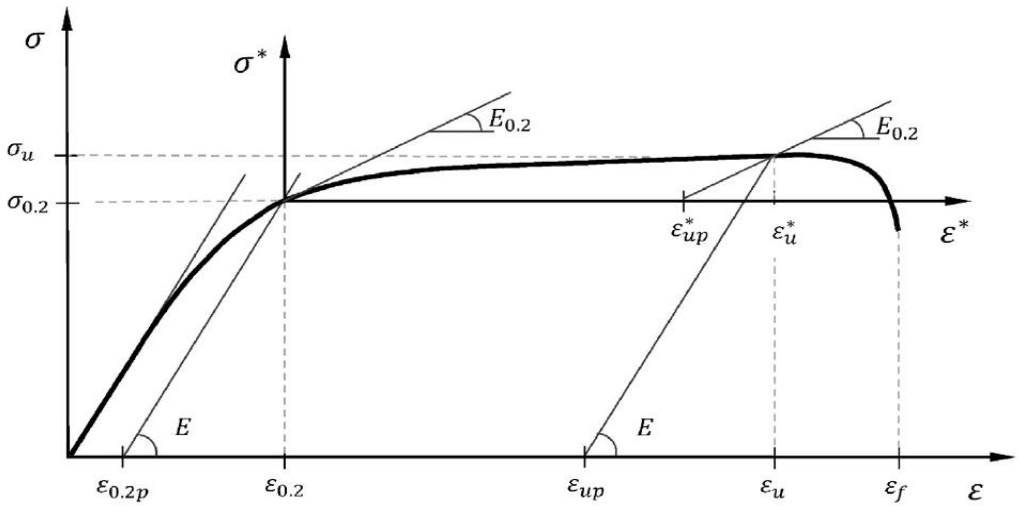

Figure 2.7. Typical stress-strain curve with definitions of key material parameters [Arrayago et al., 2015]

Figure 2.7 shows a typical stainless steel stress-strain curve where both the general ($\sigma - \varepsilon$) and the new ($\sigma^* - \varepsilon^*$) reference system are plated, together with the key symbols used in the material modeling expressions. The parameter ε_{up} is the ultimate plastic strain and ε_f is the strain at fracture, both expressed in the general reference system. The remaining symbols are as previously defined.

The second curve can be defined as established in Equation (2.5) in terms of $\sigma^* - \varepsilon^*$ reference system and according to Equation (2.6) if the general ($\sigma - \varepsilon$) system is considered, with an additional strain hardening exponent, *m*, for the second stage. Equation (2.1) continued to apply for stresses less than or equal to the 0.2% proof stress

$$\varepsilon^* = \frac{\sigma^*}{E_{0.2}} + \varepsilon^*_{up}\left(\frac{\sigma^*}{\sigma^*_u}\right)^m \quad \text{for} \quad \sigma > \sigma_{0.2} \tag{2.5}$$

$$\varepsilon^* = \frac{\sigma-\sigma_{0.2}}{E_{0.2}} + \left(\varepsilon_u - \varepsilon_{0.2} - \frac{\sigma_u-\sigma_{0.2}}{E_{0.2}}\right)\left(\frac{\sigma-\sigma_{0.2}}{\sigma_u-\sigma_{0.2}}\right)^m + \varepsilon_{0.2} \quad \text{for} \quad \sigma > \sigma_{0.2} \tag{2.6}$$

where $E_{0.2}$ is the tangent modulus at the 0.2% proof stress, given by Equation (2.7), σ^*_u and ε^*_{up} are the ultimate strength and ultimate plastic strain according to the new reference system, σ_u and ε_{up} are the ultimate strength and total strain in terms of the general system and $\sigma_{0.2}$ is the total strain at the 0.2% proof stress.

$$E_{0.2} = \frac{E}{1+0.002n\frac{E}{\sigma_{0.2}}} \tag{2.7}$$

In order to reduce the number of required input parameters, the two-stage Ramberg-Osgood [Ramberg and Osgood, 1943] model was simplified by Rasmussen [Rasmussen, 2003], leading

to the revised expression for $\sigma>\sigma_{0.2}$, given by Equation (2.8). This equation assumes that the ultimate plastic strain ε_{up}^{*} in terms of the second reference system is equal to the general ultimate total strain ε_u, as expressed in termination of the second strain hardening parameter *m*, the ultimate strain and the ultimate strength, as given in Equations (2.10) and (2.12a-2.12b) respectively, effectively reducing the number of required input parameters to the three basic Ramberg-Osgood parameters (E, $\sigma_{0.2}$ and *n*). This proposal was included in EN 1993-1-4 Annex C [CEN, 2006] for the modelling of stainless steel material behaviour.

$$\varepsilon = \frac{\sigma-\sigma_{0.2}}{E_{0.2}} + \varepsilon_u \left(\frac{\sigma-\sigma_{0.2}}{\sigma_u-\sigma_{0.2}}\right)^m + \varepsilon_{0.2} \quad \text{for} \quad \sigma > \sigma_{0.2} \tag{2.8}$$

$$\varepsilon_{up}^{*} = \varepsilon_u - \varepsilon_{0.2} - \frac{\sigma_u-\sigma_{0.2}}{E_{0.2}} \cong \varepsilon_u \tag{2.9}$$

$$m = 1 + 3.5\frac{\sigma_{0.2}}{\sigma_u} \tag{2.10}$$

$$\varepsilon_u = 1 - \frac{\sigma_{0.2}}{\sigma_u} \tag{2.11}$$

$$\frac{\sigma_{0.2}}{\sigma_u} = 0.20 + 185\frac{\sigma_{0.2}}{E} \tag{2.12a}$$

2.12a for austenitic and duplex stainless steels.

$$\frac{\sigma_{0.2}}{\sigma_u} = \frac{0.20+185\frac{\sigma_{0.2}}{E}}{1-0.0375(n-5)} \tag{2.12b}$$

2.12b for all stainless steel alloys.

Then, the material model proposed by Mirambell and Real [Mirambell and Real, 2000] was also modified by Gardner and Ashraf [Gardner and Ashraf, 2006], Equation (2.9), in order to improve the accuracy of the model at low strains (less than approximately 10%) and to allow the model to be applied also to the description of compressive stress-strain behaviour. The modifications involved used of the 1% proof stress instead of the ultimate stress in the second stage of the model, leading to Equation (2.13). Hence, the revised curve passes through the 1% proof stress $\sigma_{1.0}$ and corresponding total strain $\varepsilon_{1.0}$, but strains are not limited to $\varepsilon_{1.0}$, and the model provides excellent agreement with experimental stress-strain data for strains up to 10% both in tension and compression. The second strain hardening exponent was denoted $n_{0.2,1.0}$. This model provides excellent agreement with measured stress-strain curves in both tension and compression and is accurate for the prediction of stress-strain behaviour in structural purposes where strains are not very high.

$$\varepsilon = \frac{\sigma-\sigma_{0.2}}{E_{0.2}} + \left(\varepsilon_{1.0} - \varepsilon_{0.2} - \frac{\sigma_{1.0}-\sigma_{0.2}}{E_{0.2}}\right)\left(\frac{\sigma-\sigma_{0.2}}{\sigma_{1.0}-\sigma_{0.2}}\right)^{n_{0.2,1.0}} + \varepsilon_{0.2} \quad \text{for} \quad \sigma_{0.2} < \sigma < \sigma_u \qquad (2.13)$$

However, advanced numerical modelling requires a great knowledge of stainless steel behaviour with a better fit of the stress-strain curves over a wide strain range, especially for cold-forming processes. Quach [Quach et al., 2008] proposed a three-stage material model, based in the true stress and strain values and using the three basic Ramberg-Osgood parameters, adequate for cold-formed materials. This model uses the Ramberg-Osgood [Ramberg and Osgood, 1943] Equation 2.1, for the first stage up to the yielding stress, assumes the Gardner and Ashraf [Gardner and Ashraf, 2006] proposal, Equation (2.13), for the second stage and proposed a new expression for the third stage up to the 2% true proof stress.

Then, a new three-stage model, based on the Ramberg-Osgood [Ramberg and Osgood, 1943] equation for each stage but with a new reference system, has been developed by VTT (Finland), UPC (Catalonia) and Université de Liege (Belgium) [Hradil et al., 2003]. This model has been developed to fit experimental curves up to the ultimate strain.

The study presented in [Real et al., 2014] compares the three-stages models with the two-stages models. The conclusions of this study are that the three-stage models provide most accurate fit to experimental stress-strain curves at high strain but it is necessary to entry a high number of parameters and taking into account that two-stages models are also shown excellent agreement with experimental results. So it is better to use two-stage models with as so it is the best balance between accuracy and practicality.

2.3. Cross-sectional classification

In principle, stainless steel cross-sections classify the same as carbon steel. Sections are classified as Class 1, 2 or 3 depending on the limits set out in EN 1993-1-4 [CEN, 2006], and the sections which do not meet the criteria for Class 3 sections are classified as Class 4. Four classes of cross-section are defined as follows:

Class 1 cross-sections are those which can form a plastic hinge with the rotation capacity required from plastic analysis.

Class 2 cross-sections are those which can develop their plastic moment resistance, but have limited rotation capacity.

Class 3 cross-sections are those in which the calculated stress in the extreme compression fibre of the steel member can reach its yield strength, but local buckling is liable to prevent development of the plastic moment resistance.

Class 4 cross-sections are this in which local buckling will occur before the attainment of yield stress in one or more parts of the cross-section.

The classification of a cross-section depends on the highest (least favourable) class of its constituent parts that are partially or wholly in compression. It should be noted that the cross-section classification can vary according to the proportion of moment or axial load present and thus can vary along of a member.

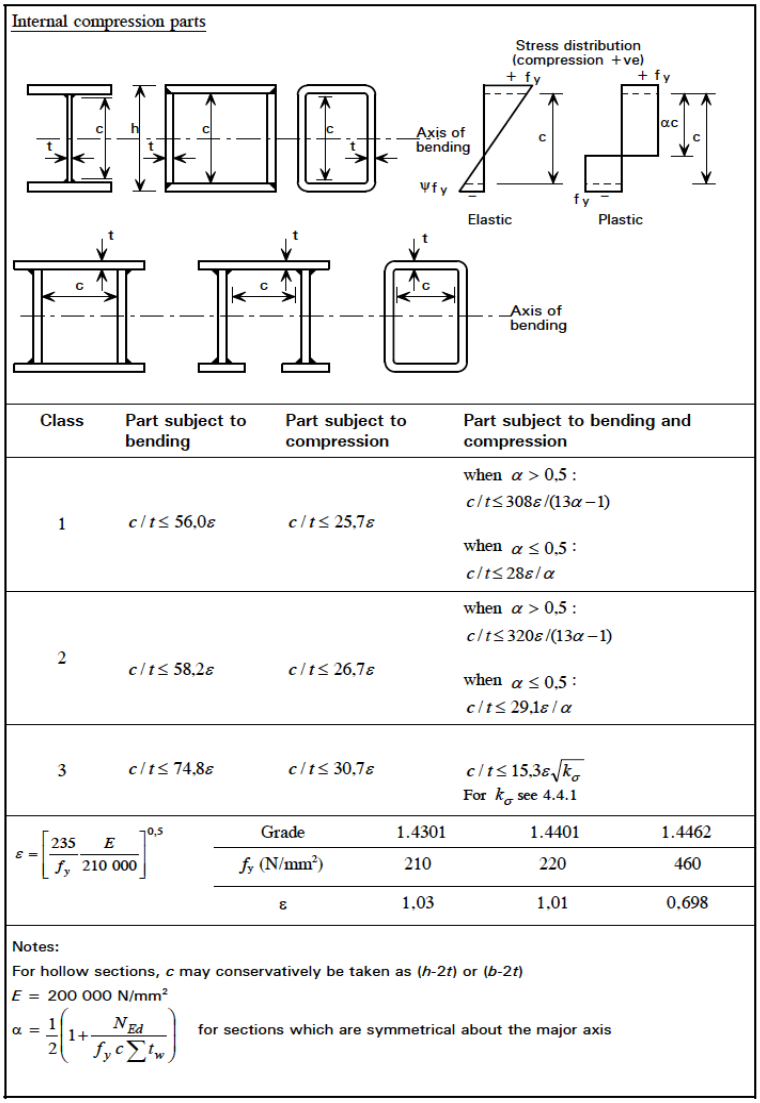

Internal compression parts

Class	Part subject to bending	Part subject to compression	Part subject to bending and compression
1	$c/t \le 56{,}0\varepsilon$	$c/t \le 25{,}7\varepsilon$	when $\alpha > 0{,}5$: $c/t \le 308\varepsilon/(13\alpha - 1)$ when $\alpha \le 0{,}5$: $c/t \le 28\varepsilon/\alpha$
2	$c/t \le 58{,}2\varepsilon$	$c/t \le 26{,}7\varepsilon$	when $\alpha > 0{,}5$: $c/t \le 320\varepsilon/(13\alpha - 1)$ when $\alpha \le 0{,}5$: $c/t \le 29{,}1\varepsilon/\alpha$
3	$c/t \le 74{,}8\varepsilon$	$c/t \le 30{,}7\varepsilon$	$c/t \le 15{,}3\varepsilon\sqrt{k_\sigma}$ For k_σ see 4.4.1

$$\varepsilon = \left[\frac{235}{f_y}\frac{E}{210\,000}\right]^{0,5}$$

Grade	1.4301	1.4401	1.4462
f_y (N/mm²)	210	220	460
ε	1,03	1,01	0,698

Notes:
For hollow sections, c may conservatively be taken as $(h\text{-}2t)$ or $(b\text{-}2t)$
E = 200 000 N/mm²
$\alpha = \frac{1}{2}\left(1 + \frac{N_{Ed}}{f_y c \sum t_w}\right)$ for sections which are symmetrical about the major axis

Figure 2.8. Maximum width-to-thickness ratios for compression parts [CEN, 2006]

Nevertheless, some recent experimental research works in ferritic stainless steel rectangular and square hollow section elements reported by Afshan and Gardner [Afshan and Gardner, 2013], concluded that some of the class limits proposed by Gardner and Theofanous [Gardner and Theofanous, 2008] overestimate the capacity of some of the cross-sections when concerning to Class 1 cross-sections. This might be caused due to the lower ultimate strain or ductility shown by ferritic grades, which make them not that deformable as austenitic and duplex stainless steels.

The calibration of the class limits for internal elements subjected to compression can be experimentally assessed by conducting stub column (pure compression without any global instability) and bending tests. The limit between Class 3 and Class 4 can be easily determined by

comparing the experimental ultimate capacities N_u with the plastic axial resistance N_{pl} of the cross section, as defined in Equation (2.14), where A is the cross-sectional area and $\sigma_{0.2}$ is the average proof stress corresponding to a 0.2% plastic strain.

$$N_{pl} = A \cdot \sigma_{0.2} \tag{2.14}$$

When the experimental ultimate capacity is higher than the plastic axial resistance ($N_u > N_{pl}$), the cross-section is fully effective in compression, so it can be classified as Class 3 or better. If $N_u < N_{pl}$, the cross-section will be classified as Class 4. Bending moment tests also allow for an experimental cross-sectional classification. In fact, Class 1, 2 and 3 limits are analysed from the bending experimental results. Cross-sections are defined as Class 3 or better if the ultimate bending capacity is higher than the M_{el} elastic moment capacity, defined in Equation (2.15). When the cross-section is able to resist a bending moment higher than M_{el} but fails before reaching the M_{pl} plastic moment capacity, given by Equation (2.16), the cross-section is classified as Class 3.

$$M_{el} = W_{el} \cdot \sigma_{0.2} \tag{2.15}$$

$$M_{pl} = W_{pl} \cdot \sigma_{0.2} \tag{2.16}$$

2.4. Flexural Buckling

The expressions for the prediction of the ultimate capacity of stainless steel columns currently codified in EN 1993-1-4 [CEN, 2006] and the new proposals are presented herein. Additionally, the expressions for the consideration of beams-columns (axial compression and bending moment interaction) through interaction facts are also considered, both in Standards and recent research works.

2.4.1. Stainless steel members subjected to axial load

For design of columns according to EN 1993-1-4 [CEN, 2006], the specific behaviour of stainless steel has been accounted for just by specifying different buckling curves and the ultimate capacity $N_{b,Rd}$ is calculated from:

$$N_{b,Rd} = \frac{\chi A \sigma_{0.2}}{\gamma_{M1}} \tag{2.17}$$

in which the flexural buckling reduction factor is:

$$\chi = \frac{1}{\phi + \sqrt{\phi^2 - \bar{\lambda}^2}} \leq 1.0 \tag{2.18}$$

and:

$$\phi = 0.5\left[1 + \alpha\left(\bar{\lambda} - \bar{\lambda}_0\right) + \bar{\lambda}^2\right] \tag{2.19}$$

$$\bar{\lambda} = \sqrt{\frac{A\sigma_{0.2}}{N_{cr}}} \tag{2.20}$$

where A is the cross-sectional area (for Class 4 slender sections, the effective are is used), $\sigma_{0.2}$ is the 0.2% proof stress, N_{cr} is the elastic critical buckling load, α is the imperfection factor, $\bar{\lambda}_0$ is the limiting slenderness factor and $\bar{\lambda}$ is the relative slenderness. For all members, EN 1993-1-4 [CEN, 2006] establishes that α =0.34 and α =0.20.

2.4.2. Stainless steel members subjected to combined load

In addition to satisfying the requirements of cross-sectional resistance at every point along the length of the member and the general requirements for beam members, interaction effects should be considered between compressive loads and bending moments.

- **Axial compression and uniaxial major axis moment:**

To prevent premature buckling about the major axis:

$$\frac{N_{Ed}}{(N_{b,Rd})_{min}} + k_y \left(\frac{M_{y,Ed} + N_{Ed} e_{Ny}}{\frac{\beta_{W,y} W_{pl,y} \sigma_y}{\gamma_{M1}}} \right) \leq 1 \tag{2.21}$$

To prevent premature buckling about the minor axis (for members subject to lateral-torsional buckling):

$$\frac{N_{Ed}}{(N_{b,Rd})_{min1}} + k_{LT} \left(\frac{M_{y,Ed} + N_{Ed} e_{Ny}}{M_{b,Rd}} \right) \leq 1 \tag{2.22}$$

- **Axial compression and uniaxial minor axis moment:**

To prevent premature buckling about the minor axis:

$$\frac{N_{Ed}}{(N_{b,Rd})_{min}} + k_z \left(\frac{M_{z,Ed}+N_{Ed}e_{Nz}}{\frac{\beta_{W,z} W_{pl,z}\sigma_z}{\gamma_{M1}}} \right) \leq 1 \qquad (2.23)$$

- **Axial compression and biaxial moments:**

All members should satisfy:

$$\frac{N_{Ed}}{(N_{b,Rd})_{min}} + k_y \left(\frac{M_{y,Ed}+N_{Ed}e_{Ny}}{\frac{\beta_{W,y} W_{pl,y}\sigma_y}{\gamma_{M1}}} \right) + k_z \left(\frac{M_{z,Ed}+N_{Ed}e_{Nz}}{\frac{\beta_{W,z} W_{pl,z}\sigma_z}{\gamma_{M1}}} \right) \leq 1 \qquad (2.24)$$

Members potentially subject to lateral-torsional buckling should also satisfy:

$$\frac{N_{Ed}}{(N_{b,Rd})_{min1}} + k_{LT} \left(\frac{M_{y,Ed}+N_{Ed}e_{Ny}}{M_{b,Rd}} \right) + k_z \left(\frac{M_{z,Ed}+N_{Ed}e_{Nz}}{\frac{\beta_{W,z} W_{pl,z}\sigma_z}{\gamma_{M1}}} \right) \leq 1 \qquad (2.25)$$

In the above expressions:

e_{Ny} and e_{Nz} are the shifts in the neutral axes when the cross-section is subject to uniform compression

N_{Ed}, $M_{y,Ed}$ and $M_{z,Ed}$ are the design values of the compression force and the maximum moments about the y-y and z-z axis along the member, respectively

$(N_{b,Rd})_{min}$ is the smallest value of Nb,Rd for the following three buckling modes: flexural buckling about the z axis, torsional buckling and torsional-flexural buckling

$\beta_{W,z}$ and $\beta_{W,z}$ are the values of β_W determined for the y and z axes respectively in which:

β_W = 1 for Class 1 or 2 cross-sections

β_W = W_{el}/W_{pl} for Class 3 cross-sections

β_W = W_{eff}/W_{pl} for Class 4 cross-sections

$W_{pl,y}$ and $W_{pl,z}$ are the plastic module for the y and z axes respectively

$M_{b,Rd}$ is the lateral-torsional buckling resistance

k_y, k_z, k_{LT} are the interaction factors, where k_{LT} is equal to 1.0.

$$k_y = 1.0 + 2(\bar{\lambda} - 0.5)\frac{N_{Ed}}{N_{b,Rd,y}} \quad \text{but} \quad 1.2 \leq k_y \leq 1.2 + 2\frac{N_{Ed}}{N_{b,Rd,y}} \tag{2.26}$$

$$k_z = 1.0 + 2(\bar{\lambda} - 0.5)\frac{N_{Ed}}{(N_{b,Rd})_{min1}} \quad \text{but} \quad 1.2 \leq k_y \leq 1.2 + 2\frac{N_{Ed}}{(N_{b,Rd})_{min1}} \tag{2.27}$$

2.5. Design formulae

In this chapter it is explained the different formulae that we used in the thesis in order to carry out the procedure validation and the behaviour of stainless steel columns combined bending and axial load.

2.5.1. EN 1993 1-4 (2006)

The European code EN 1993-1-4 [CEN, 2006] for stainless steel gives the following indications for members which are subjected to combined bending and axial compression. They should satisfy the following conditions to prevent premature buckling about the major axis (case that we studied), Equation (2.28):

$$\frac{N_{Ed}}{N_{b,rd}} + k\frac{M_{Ed}+N_{Ed}\cdot e_{Ny}}{M_{b,rd}} \leq 1 \tag{2.28}$$

where:

- e_{Ny} is the shift in the neutral axes when cross-section is subjected to uniform compression;
- N_{Ed} and M_{Ed} are the design values of the compression force and the maximum moments along the member, respectively;
- k is the interaction factor:

$$k = 1 + 2(\bar{\lambda} - 0.5)\frac{N_{Ed}}{N_{b,rd}} \quad \text{but} \quad 1.2 \leq k \leq 1.2 + 2\frac{N_{Ed}}{N_{b,rd}} \tag{2.29}$$

where the minimum value 1.2 is worth mentioning, which usually derives into overconservative capacity predictions since the full, bending capacity of the cross-section cannot be reached for low axial compression values.

The calculations have been developed through Microsoft Office Excel and Abaqus, and, as for the previous chapter, it was settled to consider as steel yielding stress f_y and Young's modulus E equal to 200 GPa. This scheme has been followed for a value of partial safety factor γ_{M1} equal to 1.0.

The Equation (2.28) has to be satisfied during the design of stainless steel members subjected to combined axial and bending loads. On the other hand, our aim was to make a comparison of the different interaction factors depending on the material analysed.

The term $N_{Ed}e_{Ny}$ is always taken as null because the elements which have been managed present double-symmetrical sections and the shifts of the neutral axes when cross-section is subjected to uniform compression are null.

2.5.2 Research performed at Imperial College (Zhao, 2015)

EN 1993 1-4 gives the following indications for members which are subjected to combined bending and axial compression. They should satisfy the following conditions to prevent premature buckling about the major axis (case studied), Equation (2.28). Ou Zhao [Zhao, 2015] propose an interaction factor k different from the one proposed by EN 1993-1-4 [CEN, 2006]:

$$k = 1 + D_1\left(\bar{\lambda} - D_2\right)n_b \leq 1 + D_1(D_3 - D_2)n_b \tag{2.30}$$

where D_1 and D_2 are the coefficients which define the linear relationship between the interaction factor *k* and the slenderness $\bar{\lambda}$ in the low member slenderness range, while D_3 is a limit value, beyond which the interaction factor *k* remains constant.

The values of D_1 and D_2 for each axial compressive load level (n_b) were determined following a regression fit of Equation (2.29) to the corresponding numerically derived results over the member slenderness range from 0.2 and 1.2, while the final D_1 and D_2 coefficients were taken as the average calculated values for all the considered load levels. Then, the limit value of D_3 was determined based on the fit of Equation (2.29) to the FE derived results corresponding to low axial compressive load levels ($n_b \leq 0.4$). Table 2.1 reports the values of D_1, D_2 and D_3 for each stainless steel grade.

Grade	D_1	D_2	D_3
Austenitic	2.0	0.3	1.3
Duplex	1.5	0.4	1.4
Ferritic	1.3	0.45	1.6

Table 2.1. Proposed coefficients for interaction curves for different material grades [Zhao, 2015]

2.5.3 Research performed at UPC (Arrayago et al., 2015)

Regarding design expressions for the evaluation of stainless steel beam-columns, different approaches can be found in Standards. Nevertheless, compression and bending moment interaction verifications are usually presented as interaction expressions with the same general expression, given by Equation (2.28), and a certain interaction factor *k*. The differences among these expressions basically lay on the definition of this interaction factor *k*.

Several interaction expressions available in the literature consider the shape of the bending moment diagram through the μ parameter, and were based in the proposal published by Lopes et al. (2009), which is given by Equation (2.31) when A=B=1.

$$k = A - B \cdot \frac{\mu N_{Ed}}{N_{b,rd}} \tag{2.31}$$

This expression was calibrated for I beams-columns considering different stainless steel grades and bending moment diagrams and was the recalibrated for stainless steel SHS and RHS elements by Jandera and Syamsuddin (2014) with A=B=1.2 and by Arrayago et al. (2015) with A=1 and B=0.92. So, in this chapter, it is used this last Arrayago et al.'s expression in order to evaluate the interaction of axial compression and bending moment.

To determine the values of the μ parameter the following Equation (2.32) should be used.

$$\mu = (0.97\beta_M - 2.11)\bar{\lambda} + 0.44\beta_M + 0.09 \tag{2.32}$$

Finally, the equivalent uniform moment factor β_M can be determined in function of the bending diagram shape, according to the Equation (2.33):

$$\beta_M = 1.8 - 0.7\psi \tag{2.33}$$

where, ψ is the distribution of bending moment and is equal to 1.0 in this thesis.

It is important to remark that when Arrayago et al. (2015) performed the research, they supposed the imperfection amplitudes due to they do not have them. Instead of adopting the traditional L/1500, it was applied expressions from EN 1993-1-1 which gave some imperfections higher than L/1500, so the Equation was calibrated. Hence, this fact can give results which are unsafe (below the ideal value 1.0). In this thesis it has proceed to observe how this calibration of the equation really affects to the final result.

2.5.4 Simplified Method from Structural Steel Code EAE (2012)

The stability of flexural and compression double symmetrical uniform cross-section, not susceptible to distortion, must be checked as it is presented below.

The verification of the elements in a structural system can be carried out on the analysis of individual elements of a single span extracted from the system The second order effects of translational systems should be taken into account. For axial compression and bending moments, the Equation (2.34) must be verified.

$$\frac{N_{Ed}}{N_{b,rd}} + \frac{1}{1-\frac{N_{Ed}}{N_{cr}}} \cdot \frac{C_m \cdot M_{Ed}}{M_{b,rd}} \leq 1.0 \tag{2.34}$$

In this case, the interaction factor k is expressed in Equation (2.35)

$$k = \frac{C_m}{1-\frac{N_{Ed}}{N_{cr}}} \tag{2.35}$$

where $C_m$is the equivalent uniform bending factor, referred to the bending axis, which takes into account the bending moment distribution.

$$C_m = 0.6 + 0.4\psi \tag{2.36}$$

where, as it is explained in before, ψ is equal to 1.0.

In order to obtain the critical load of Euler, N_{cr}, it is used FE in Abaqus instead of the Euler's equation.

2.6 Previous experimental programs

The literature review conducted for this thesis also included a wide collection experimental programs reported by international research groups. The collected data included flexural buckling tests not only in ferritic, but in other stainless steel families and grades. The experimental results will be included in future studies regarding cross-sectional classification, bending design methods and flexural buckling predicting expressions.

Table X presents the different flexural buckling tests gathered from the literature, specifying the cross-section type (SHS, RHS, CHS and Channel), the number of conducted tests, the material grade and the corresponding stainless steel family. A total of 140 flexural buckling test results have been collected, which will be included in future studies.

Reference	Cross-section type	Number of Tests	Grade	Family
Afshan and Gardner (2013)	RHS	8	1.4003	Ferritic
	SHS	3	1.4003	
	SHS	4	1.4509	
Becque and Rasmussen (2006)	Channel	10	1.4003	
	Channel	9	1.4016	
Arrayago, Real and Mirambell (2016)	SHS	5	1.4003	
	RHS	7	1.4003	
Gardner and Nethercot (2004b)	SHS	8	1.4301	Austenitic
	RHS	14	1.4301	
Gardner, Tajla and Baddoo (2006)	RHS	12	1.4318	
Liu and Young (2003)	SHS	12	1.4301	
Rasmussen and Hancock (1993a)	SHS	8	1.4301	
	CHS	10	1.4301	
Becque and Rasmussen (2006)	Channel	10	1.4301	
Liu and Young (2006)	SHS	12	1.4462	Duplex
	RHS	8	1.4462	
Theofanus and Gardner (2009)	SHS	6	1.4162	Lean Duplex
	SHS	6	1.4162	
Total		152		

Table 2.2. Collected flexural buckling tests [Pizzi, 2014]

3. NUMERICAL MODEL

The model used during this present thesis is based on the finite element method (FEM) since is extensively demonstrated that could be considered a method able to give the efficiency, accuracy and versatility necessary to solve non-linear problems in engineering.

This chapter includes the presentation of the general basis of numerical model made to simulate the structural behaviour of stainless steel column, which has been created in Abaqus finite element program. It takes into account both geometrical and material non-linearity.

3.1. General principles of the finite element method

This widely settled method, that got many applications in different fields, consists in the approximation of continuum problems through their discretization into a finite number of elements which are connected by a finite number of points, that are defined nodes. It is important to remark that the principal unknown parameter of the general problem is the displacements of the defined nodes. Then, once the displacement of any point of the finite element is known, it is possible to obtain the values of stress and strain settling the equilibrium and compatibility equations and, in addition, the material constitutive stress-strain relationships.

The main steps to follow in a finite element modelization are:

- Discretization of the element object of the structural analysis

The first step consists in to discretize the continuum unto a finite number of elements that can be of different shape, for example one-dimensional, two-dimensional or three-dimensional. As already said on the elements generated are interconnected through a discrete number of nodal points, whose displacement represents the basic unknown parameter of the problem.

- Definition of the displacement function

A set of functions are chosen to define the state of displacement within each finite element and on its boundaries in terms of its nodal displacements. These are known as shape functions $\underline{N}^e$, whose aim is to link the vector that represents the nodal displacement of the element $\underline{u}^e$, with the vector $\underline{a}^e$ which represents the nodal displacements for the particular element, where *e* represents a generic finite element.

$$\underline{u}^e = \underline{N}^e \cdot \underline{a}^e \tag{3.1}$$

- Strain distribution

The second step lets to determine the value of the strains at any point, once the displacements are known at all points. In this case the displacement function $\underline{S}^e$ define the connection between the strain distribution $\underline{\varepsilon}^e$ and the nodal displacement $\underline{a}^e$:

$$\underline{\varepsilon}^e = \underline{S}^e \cdot \underline{N}^e \cdot \underline{a}^e \tag{3.2}$$

- Stress distribution

The constitutive matrix, $\underline{D^e}$, give us the relationship between stresses and strains.

$$\underline{\sigma^e} = \underline{D^e} \cdot \underline{\varepsilon^e} \tag{3.3}$$

- Equivalent nodal force determination

This step consists in to apply the principle of Virtual Works, that lets to make body forces statically equivalent to the actual boundary stresses and distributed body forces. Then, the procedure consists in to impose a virtual nodal, displacement, which has to be compatible with the boundary conditions, and then, to equate the internal and external work done by the forces and stresses during the imposed displacement.

- General equilibrium

In this last step it is necessary to impose that the external nodal force is equal to the total of the nodal forces. So, after assembling the different parts, the global equation of the structure is:

$$\underline{f} = \underline{K} \cdot \underline{a} \tag{3.4}$$

where $\underline{K}$ is the assembled matrix rigidity of the structure, and $\underline{a}$ and $\underline{f}$ are the nodal displacements vector and the nodal forces vector, respectively.

Having solved this system of equations and consequently obtained the nodal displacements, the strain and stress distributions can be determined by the application of the mathematical expressions presented previously in this chapter.

3.2. Structural elements analyzed and type of elements used

A Finite Element model was made in software Abaqus. Nine nodes reduced integration shell elements S9R5 for the models square hollow sections (SHS) The quadratic definition of the S9R5 element allowed more accurate corner geometry. The nodes of the end-sections were connected by rigid elements to their centroid. At that point, the axial load was applied on the end and the bending moment on both ends. Then, at both ends, the displacement was restrained but the rotation was free. The member was also prevented from the weak axis buckling along the middle of both flanges. This allowed no torsion of the column.

The fully non-linear (GMNIA, geometrically and materially nonlinear analysis with initial imperfections) analysis was performed. The amplitude for global imperfection was L/1000, where L is the pinned column length. For the local buckling, we used a formula explained in chapter 5.2.

3.3. Constitutive equation and material modelling

3.3.1 Elastic-Plastic behaviour

The Abaqus library provides us a wide range of linear and non-linear material models, the most of which are usually required for common and practical applications. Since the constitutive models are mathematical equations that, together with equilibrium and compatibility equations, are absolutely essential to determine the relations between stresses, strains and displacements in a structure, it is necessary to evaluate them accurately. Thus, it is important to analyse the features of the materials and the geometry of structures in order to choose the constitutive model which better reproduces the real behaviour of the material that is purpose of the analysis. The behaviour of the material is defined elastic plastic when it shows an elastic behaviour for low range of stresses that let it to recover completely the strains originated during the loading process. Otherwise, when the stress exceeds a particular level of stress, the strains produced during the process of loading are not completely recovered. Therefore, the stress which separates the elastic behaviour to the plastic one is known as yielding stress and the total strain can be summarized in the following formula:

$$\varepsilon = \varepsilon_{el} + \varepsilon_{pl} \tag{3.5}$$

where ε_{el} is the recoverable elastic strain and ε_{pl} represents the unrecoverable plastic strain which remains after the unloading.

3.3.2 Stainless steel

As it is commented in chapter *2.2.1. Material models*, the main difference between carbon and stainless steel is in their stress-strain relationship. Whereas the carbon steel has linear elastic behaviour with a clearly defined yielding stress, stainless steel shows a rounded and anisotropic strain-stress response without a well-defined yield point. In order to work properly with stainless steel, it is useful to have and analytical expression to study and design structural elements. EN 1993-1-4 recommends to use the Ramberg-Osgood expression [Ramberg and Osgood, 1943] to model the non-linear stress-strain relationship:

$$\varepsilon = \frac{\sigma}{E_0} + 0.002\left(\frac{\sigma}{\sigma_{0.2}}\right)^n \tag{3.6}$$

where $\sigma_{0.2}$ is the yielding stress, taken as the 0.2% proof stress, E_0 is the material Young's modulus and *n* is a strain hardening exponent related with the material non-linearity degree.

Although Equation (3.6) represents a good approximation of the actual stress-strain curves in stainless steel, is useful to remark that at higher strains this model tends to overestimate the material strength. For this reason, it is advisable to use a two adjoining curves used by Mirambell and Real [Mirambell and Real, 2000], which take the basic Ramberg-Osgood [Ramberg and Osgood, 1943] curve until the 0.2% proof stress and add a new expression over this point. This new Equation (3.8) is the same that Equation (2.6).

$$\varepsilon = \frac{\sigma}{E} + 0.002\left(\frac{\sigma}{\sigma_{0.2}}\right)^{n} \qquad \sigma < \sigma_{0.2} \tag{3.7}$$

$$\varepsilon = \frac{(\sigma-\sigma_{0.2})}{E_{0.2}} + \left(\varepsilon_u - \varepsilon_{0.2} - \frac{\sigma_u-\sigma_{0.2}}{E_{0.2}}\right)\cdot\left(\frac{\sigma-\sigma_{0.2}}{\sigma_u-\sigma_{0.2}}\right)^{m} + \varepsilon_{0.2} \qquad \sigma_{0.2} < \sigma < \sigma_u \tag{3.8}$$

where σ_u is the ultimate material strength, ε_u is the plastic ultimate strength, and $\varepsilon_{0.2}$ and $E_{0.2}$ are the total strain and the tangent modulus at the 0.2% proof stress respectively; *m* is a strain hardening exponent that can be defined by the ultimate strength and another intermediate point.

Talking about the strain hardening exponent, there are recent studies involving the examination of austenitic and ferritic stainless steel stress-strain curves (Real et al.,2014; Arrayago et al.,2013) and it is found that this parameter, Equation (2.10) provides higher values for the second strain hardening exponent than those obtained from curve fitting. A revised expression, given by Equation (3.9), was therefore proposed for all stainless steel grades, based on least squares regression:

$$m = 1 + 2.8\frac{\sigma_{0.2}}{\sigma_u} \tag{3.9}$$

Overall, the new proposal provides more accurate predictions for the second strain hardening parameter *m* than existing formula Equation (2.10) and is therefore recommended for code inclusion.

For the plastic ultimate strength, we have different formulas depending on the material that we are using:

- Ferritic

$$\varepsilon_u = 0.6\cdot\left(1 - \frac{\sigma_{0.2}}{\sigma_u}\right) \tag{3.10}$$

- Austenitic and Duplex

$$\varepsilon_u = \left(1 - \frac{\sigma_{0.2}}{\sigma_u}\right) \tag{3.11}$$

Then, the elastic tangent modulus at 0.2% proof stress is:

$$E_{0.2} = \frac{E}{1+0.002\cdot n\cdot\frac{E}{\sigma_{0.2}}} \tag{3.12}$$

where E is the Young's modulus, 200 GPa for this thesis.

3.3.3 Corners: Constitutive law

The Abaqus model was conceived to take into account the strength enhancements induced during cold forming. The variation of the mechanic characteristics along the sections is due to the hardening of the material during the deformation. The operation of cold forming induces an increase of the yielding stress of the material. The smaller the interior radius is, the greater is the increase of resistance. At the increase of the resistance follows a decrease of resilience which makes the material brittle. The Abaqus model was performed in order to contemplate the strength enhancements in the corner regions of cold formed components.

For the model validation we took into consideration that the properties of the flat and corner sections are different, so each part had his own characteristics, but in the parametric study we considered that both flat and corner sections had the same properties.

4. VALIDATION

4.1. Introduction

In this section it is explained that the model used in order to carry out this thesis must be validated before used it, so with this purpose, the results from the documents of *Arrayago, Real, Mirambell- Experimental study on ferritic stainless steel RHS and SHS beams-columns* [Arrayago et al., 2016] are used in order to verify our model. After that, with Rodríguez (2016), a procedure validation about the model has been done. A Class 1 (SHS 60x60x3) and a Class 4 (SHS 80x80x2) has been analysed with different materials (ferritic, duplex and austenitic stainless steel) and then the results were shared and compared in order to verify that the procedure used was correct and the model is ready to start with the structural behaviour of the beams-columns.

4.2. Model Validation

This experimental programme was conducted in the *Laboratori de Tecnologia d'Estructures Luis Agulló*, in the Department of Construction Engineering at *Universitat Politècnica de Catalunya* by the framework project of ferritic stainless steel, where the flexural buckling and beam-column response of ferritic stainless steel RHS and SHS members was analysed. The studied ferritic grade was EN 1.4003.

In this experiment, it is tested two SHS (S1 and S2) and three RHS (S3, S4 and S5). The different cross-sections (in mm) were:

S1	**S2**	**S3**	**S4**	**S5**
80x80x4	60x60x3	80x40x4	120x80x3	70x50x2

Table 4.1. Model validation cross-sections [Arrayago et al., 2016]

The information about the specimens to be tested was accurately measured before testing in order to analyse correctly the experimental results. Thus, the material behaviour, geometrical definition and initial imperfections were carefully defined and are showed in the following Table 4.2, where *F* is the flat section and *C* is the corner section. It is considered flat and corner sections with different properties.

Tests	E (MPa)	$\sigma_{0.05}$ [MPa]	$\sigma_{0.2}$ [MPa]	σ_u [MPa]	ε_u[%]	ε_f[%]	n	m
S1-F	173992	467	521	559	8.2	21.7	12.4	2.3
S1-C	170049	441	577	645	1.1	7.9	5.0	5.4
S2-F	186896	433	485	505	6.8	30.9	12.2	2.6
S2-C	178049	459	555	587	1.0	10.1	7.9	5.2
S3-F	181632	467	507	520	3.6	21.0	16.4	2.5
S3-C	183684	434	558	601	1.0	7.0	5.9	4.5
S4-F	176704	391	430	490	12.6	27.1	14.6	2.3
S4-C	194611	457	540	583	1.0	10.1	7.6	4.8
S5-F	179568	381	418	480	13.8	26.8	15.3	2.4
S5-C	186026	466	552	575	1.1	6.5	8.0	4.6

Table 4.2. Average material properties from coupon tensile test [Arrayago et al., 2016]

All coupons were tested in accordance with the specifications in ISO6892-1 and the mechanization of the coupons and the execution of the tensile tests were performed in acerinox (Figure 4.1).

(a) Testing of S3-F coupon and tested flat coupon

(b) Testing of S2-C coupon and tested corner coupon

Figure 4.1. Tensile coupon test on flat and corner coupons respectively [Arrayago et al., 2016]

Each section was tested with only axial compression and axial compression and bending moment. The following table 4.3 shows us the tests that were conducted per each section:

SECTION	TEST
S1	CC
	EC-1
	EC-2
S2	CC
	EC-1
S3	CC
	EC-1
S4	CC
	EC-1
S5	CC
	EC-1
	EC-2

Table 4.3. Tests conducted for each section [Arrayago et al., 2016]

As it is explained before, these tests have been developed by the framework project of ferritic stainless steel at UPC (Catalonia). Initial global imperfections are an important aspect to be considered in order to define the adequate position of each specimen during the tests. Thus, the magnitude and distribution of the initial bow of each specimen was carefully measured by a laser device. This laser recorded measurements every 100 mm and at mid-height section. The maximum global imperfection amplitude w_o of each specimen is presented in Table 4.4.

Specimen	L [mm]	H [mm]	B [mm]	t [mm]	R_{ext} [mm]	w_o [mm]
S1-CC	1495	79.6	80.2	3.9	7.0	0.81
S1-EC1	1495	80.1	80.3	3.9	7.3	1.25
S1-EC2	1498	79.9	80.3	4.0	7.5	1.38
S2-CC	1500	60.3	60.2	2.9	5.9	0.66
S2-EC1	1500	60.0	60.2	3.0	5.9	0.69
S3-CC	1500	80.0	40.0	3.8	6.8	0.85
S3-EC1	1500	80.0	40.0	3.8	6.5	0.89
S4-CC	1500	119.8	79.8	2.9	7.2	1.21
S4-EC1	1500	119.8	79.6	3.0	7.2	1.58
S5-CC	1500	70.0	49.6	2.0	4.4	1.09
S5-EC1	1500	70.0	49.9	2.0	4.2	1.32
S5-EC2	1500	70.1	49.9	2.0	4.3	1.35

Table 4.4. Measured dimensions for the tests specimens [Arrayago et al., 2016]

Consequently, all these parameters are introduced into our model and run it using the Abaqus software, based on FEM (Finite Element Method). The results of the tests are summarised in the Table 4.5:

SPECIMEN	ARRAYAGO (kN)	ABAQUS (kN)	DIFFERENCE (%)
S1-CC	447.50	458,75	2.51
S1-EC1	256.00	265,19	3.59
S1-EC2	193.50	205,15	6.02
S2-CC	173.10	208,83	20.64
S2-EC1	79.90	93,62	17.17
S3-CC	130.20	155,96	19.78
S3-EC1	76.40	87,15	14.07
S4-CC	364.50	371	1.78
S4-EC1	222.80	199,27	-10.56
S5-CC	97.40	111,48	14.45
S5-EC1	62.40	66,13	5.98
S5-EC2	44.30	51,2	15.57

Table 4.5. Tests results

From this analyse, it is possible to extract the mean value of the difference, 9.25%, and the standard deviation, 9.25.

As it is observed in the previous table, the difference between the load calculated by Arrayago and the one obtained by Abaqus are relatively high. So, it was proceeded to revise the model and change some of the initial parameters.

As it is said in Arrayago et al. (2016), although the nominal length of each specimen was 1500 mm, the effective length of the system L_e equal to the distance between knife-edges will be considered in the following analysis. Hence, the thickness of both end plates and the bearing plates need to be added to the length of the specimens, which will be L_e=1600 mm.

So the tests are recalculated again and this time the results obtained are better than with L=1500 mm. In the following table 4.6 it is possible to see this main differences:

		L=1500 mm		L=1600 mm	
SPECIMEN	**ARRAYAGO (kN)**	**ABAQUS (kN)**	**DIFFERENCE (%)**	**ABAQUS (kN)**	**DIFFERENCE (%)**
S1-CC	447,5	458,75	2,51	442,41	1,14
S1-EC1	256,0	265,19	3,59	253,47	0,99
S1-EC2	193,5	205,15	6,02	197,16	1,89
S2-CC	173,1	208,83	20,64	197	13,81
S2-EC1	79,9	93,62	17,17	88,65	10,95
S3-CC	130,2	155,96	19,78	139,18	6,90
S3-EC1	76,4	87,15	14,07	80,98	5,99
S4-CC	364,5	371	1,78	369,31	1,32
S4-EC1	222,8	199,27	-10,56	192,31	13,68
S5-CC	97,4	111,48	14,46	103,44	6,20
S5-EC1	62,4	66,13	5,98	62,22	0,29
S5-EC2	44,3	51,2	15,58	48,46	9,39

Table 4.6. Tests results with effective length

In this case, the mean value obtained is of 6.05% and the standard deviation 5.02. In the following Table 4.7 we are capable to observe the difference between the first length of 1500 mm and the effective length of the system, 1600 mm.

	L=1500 mm	**L=1600 mm**
Average (%)	9.25	6.05
Standard deviation	9.25	5.02

Table 4.7. Comparison of average and standard deviation of both tests

4.2.1 Concluding remarks

If the effective length is taken into account, the results for each specimen improve considerably. The difference between Arrayago and Abaqus is reduced a 3.2% and the standard deviation 4.23, assuring then a better model for the future study of the ferritic stainless steel. Therefore, the effective length needs to be taken into account in the future analysis. As we have the standard deviation under a 10%, the model is accepted as good enough in order to perform the analysis.

The numerical model exploited has been demonstrated to be an adequate tool to reproduce the behaviour of plate elements loaded in compression. So, it has been showed that it is possible to adopt it in the different analyses that it is going to carry out in the following chapters.

4.3 Procedure Validation

As it is explained in the introduction of this chapter, a verification of the procedure to use in this thesis is carried out together with Rodríguez (2016). Two square hollow section are analysed, one in Class 1 (60x60x3) and the other in Class 4 (80x80x2). Only one material for Class 1 is used (ferritic stainless steel) and three different materials for Class 4 in order to carry out this validation, which are ferritic, duplex and austenitic stainless steel. The characteristics of these materials are proposed in the following Table 4.8:

Material	$\sigma_{0.2}$ (MPa)	σ_u (MPa)	n
Austenitic	220	520	7.0
Duplex	480	660	8.0
Ferritic	210	380	14.0

Table 4.8. Main characteristics of materials [Zhao, 2015]

It is important to remark that we used a value of Young's modulus of 200 GPa and Poisson's ratio of 0.3.

From results displayed in plots and figures, the results obtained in Rodriguez (2016) and the present work are compared. Some conclusions related to this validation are pointed out.

4.3.1 Procedure Validation by EN 1993-1-4

In chapter 2.5.1. it is explained the formulation to use for EN 1993-1-4 [CEN, 2006]. So, the calculation of the interaction Equation (2.28) is worked out and then the results are compared.

- Compact section Class 1

The Figure 4.2 represents how the Equation (2.28) works with ferritic stainless steel with a varying slenderness in Class 1 (SHS 60x60x3).

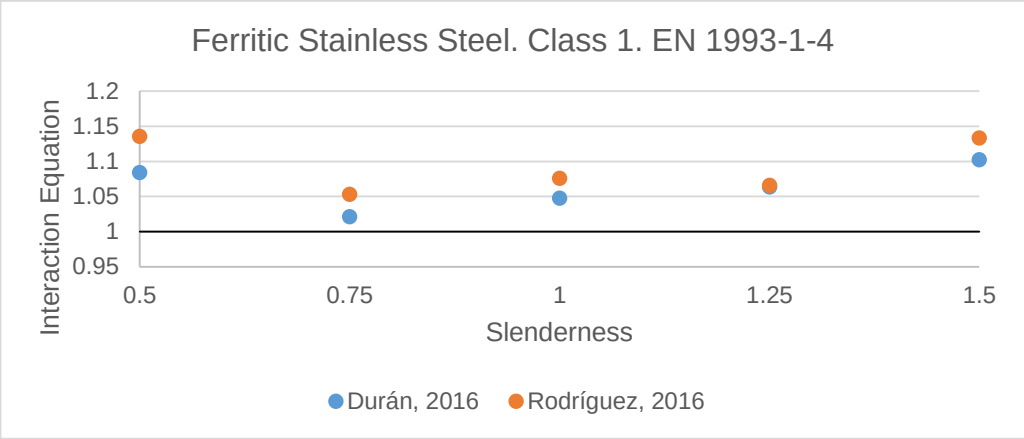

Figure 4.2. Durán and Rodríguez results. Ferritic stainless steel. Class 1. EN 1993-1-4

In Table 4.9 it is represented the mean average and standard deviation for the ferritic stainless steel material for both Durán and Rodríguez results.

		FERRITIC
Durán results	Mean Average	1.0638
	Standard deviation	0.0315
Rodríguez results	Mean Average	1.0933
	Standard deviation	0.0389

Table 4.9. Durán and Rodríguez's results. Ferritic stainless steel. Class 1. EN 1993-1-4

- Slender section Class 4

Figures 4.3-4.5 represent how the interaction Equation (2.28) works with different materials (ferritic, duplex and austenitic stainless steel) with a varying slenderness in Class 4 (SHS 80x80x2), using the interaction factor *k* of EN 1993-1-4.

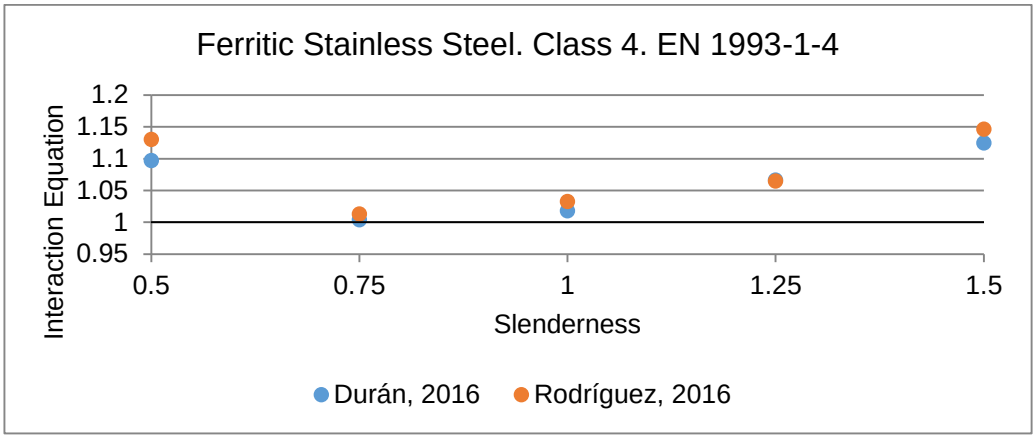

Figure 4.3. Durán and Rodríguez results. Ferritic stainless steel. Class 4. EN 1993-1-4

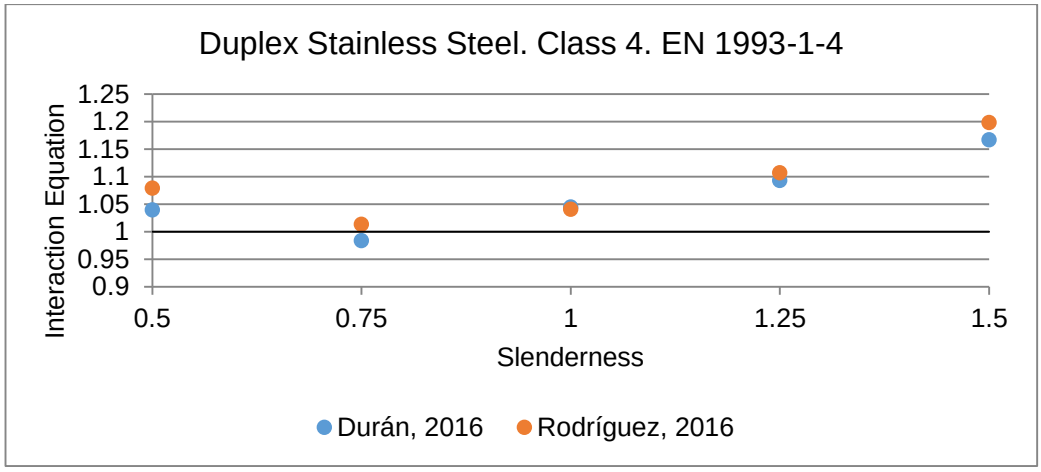

Figure 4.4. Durán and Rodríguez results. Duplex stainless steel. Class 4. EN 1993-1-4

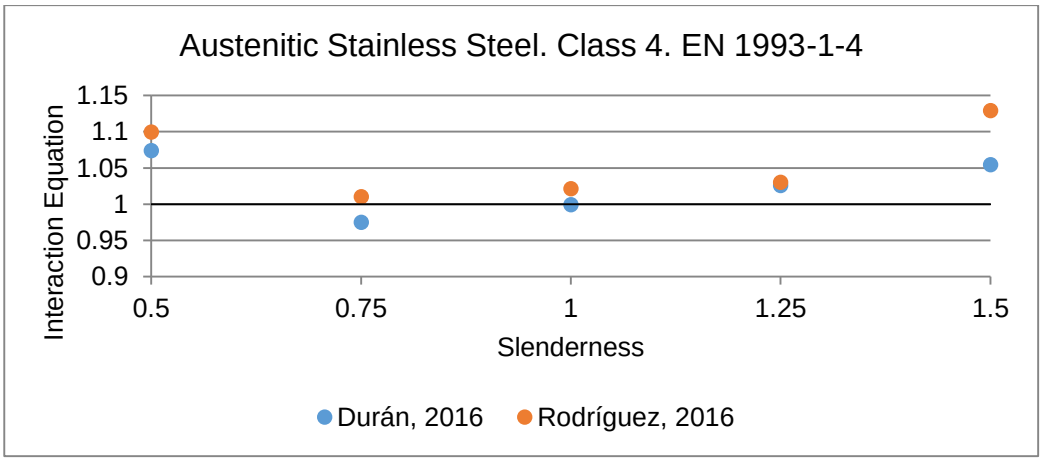

Figure 4.5. Durán and Rodríguez results. Austenitic stainless steel. Class 4. EN 1993-1-4

In Table 4.10 it is represented the mean average and standard deviation for this three materials for both Durán and Rodriguez results.

		FERRITIC	DUPLEX	AUSTENITIC
Durán results	Mean Average	1.0624	1.0656	1.0259
	Standard deviation	0.0511	0.0687	0.0399
Rodríguez results	Mean Average	1.0776	1.0879	1.0583
	Standard deviation	0.0588	0.0714	0.0529

Table 4.10. Durán and Rodríguez results. Ferritic, duplex and austenitic stainless steel. Class 4. EN 1993 1-4

4.3.2 Procedure Validation by Zhao (2015)

In chapter 2.5.2. it is explained the designed formulae to use the interaction factor *k* for Zhao (2015), a research performed at Imperial College in London. So, the calculation of the interaction Equation (2.28) is worked out and then the results are compared.

- Compact section Class 1

The Figure 4.6 represents how the Equation (2.28) works with ferritic stainless steel with a varying slenderness in Class 1 (SHS 60x60x3).

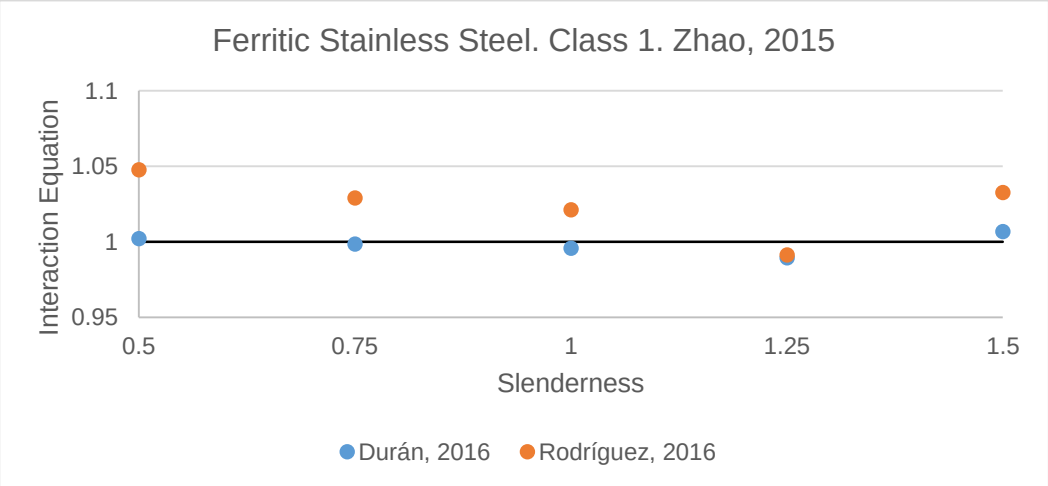

Figure 4.6. Durán and Rodríguez results. Ferritic stainless steel. Class 1. Zhao, 2015

In Table 4.11 it is represented the mean average and standard deviation for ferritic stainless steel material for both Durán and Rodríguez results.

		FERRITIC
Durán results	Mean Average	0.9985
	Standard deviation	0.0065
Rodríguez results	Mean Average	1.0243
	Standard deviation	0.0208

Table 4.11. Durán and Rodríguez results. Ferritic stainless steel. Class 1. Zhao, 2015

- Slender section Class 4

The Figures 4.7-4.9 represent how the interaction Equation (2.28) works with different materials (ferritic, duplex and austenitic stainless steel) with a varying slenderness in Class 4 (SHS 80x80x2), using the interaction factor *k* of Zhao (2015).

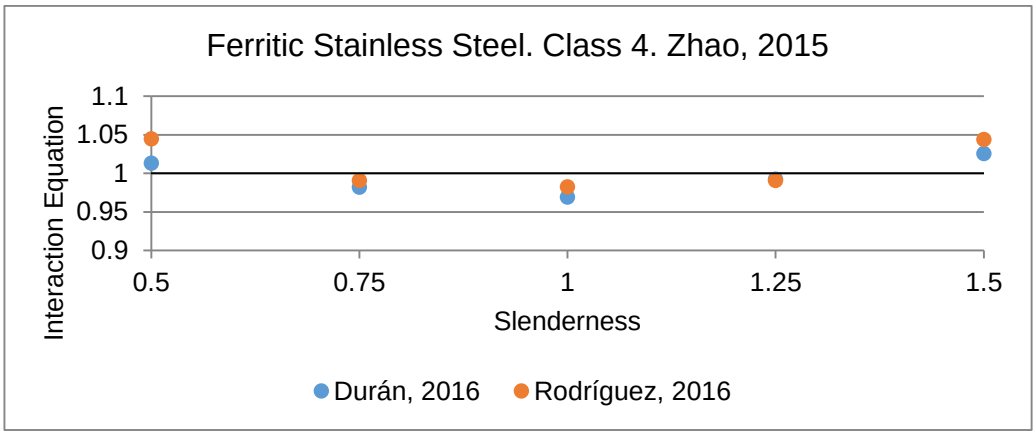

Figure 4.7. Durán and Rodríguez results. Ferritic stainless steel. Class 4. Zhao, 2015

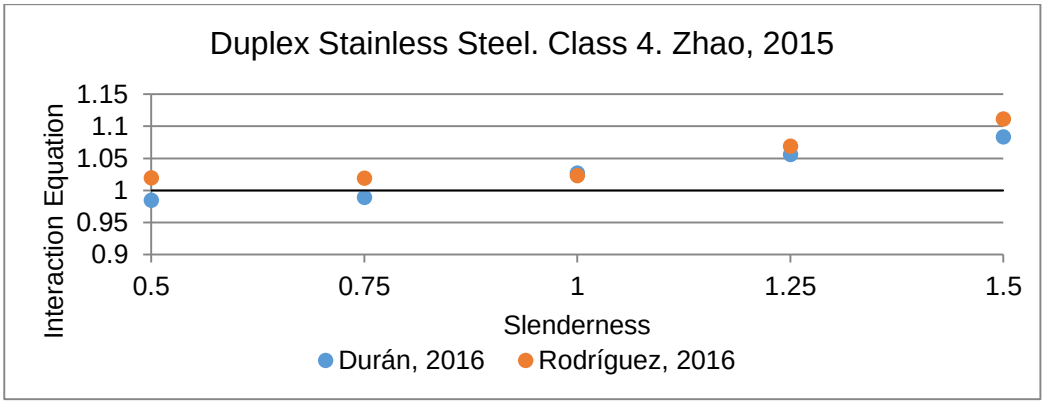

Figure 4.8. Durán and Rodríguez results. Duplex stainless steel. Class 4. Zhao, 2015

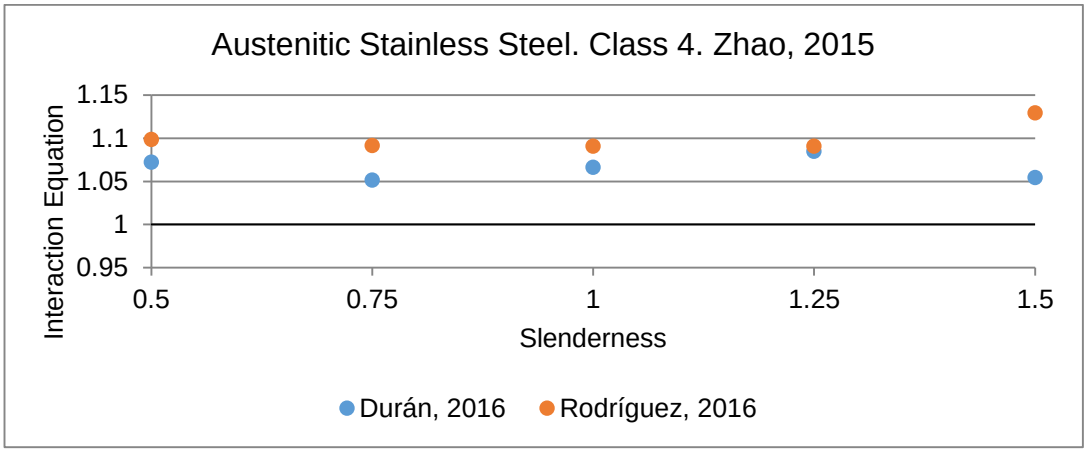

Figure 4.9. Durán and Rodríguez results. Austenitic stainless steel. Class 4. Zhao, 2015

In Table 4.12 it is represented the mean average and standard deviation for this three materials for both Durán and Rodriguez's results.

		FERRITIC	DUPLEX	AUSTENITIC
Durán results	Mean Average	0.9966	1.0277	1.0661
	Standard deviation	0.0023	0.0427	0.0136
Rodríguez results	Mean Average	1.0107	1.0481	1.100
	Standard deviation	0.0310	0.0166	0.0166

Table 4.12. Durán and Rodríguez results. Ferritic, duplex and austenitic stainless steel. Class 4. Zhao, 2015

4.3.3 Procedure Validation by Arrayago et al. (2015)

In chapter 2.5.3. it is explained the designed formulae to use the interaction factor *k* for the research performed at UPC (Arrayago et al., 2015). So, the calculation of the interaction Equation (2.28) is worked out and then the results are compared.

- Compact section Class 1

The Figure 4.10 represents how the Equation (2.28) works with ferritic stainless steel and with a varying slenderness in Class 1 (SHS 60x60x3).

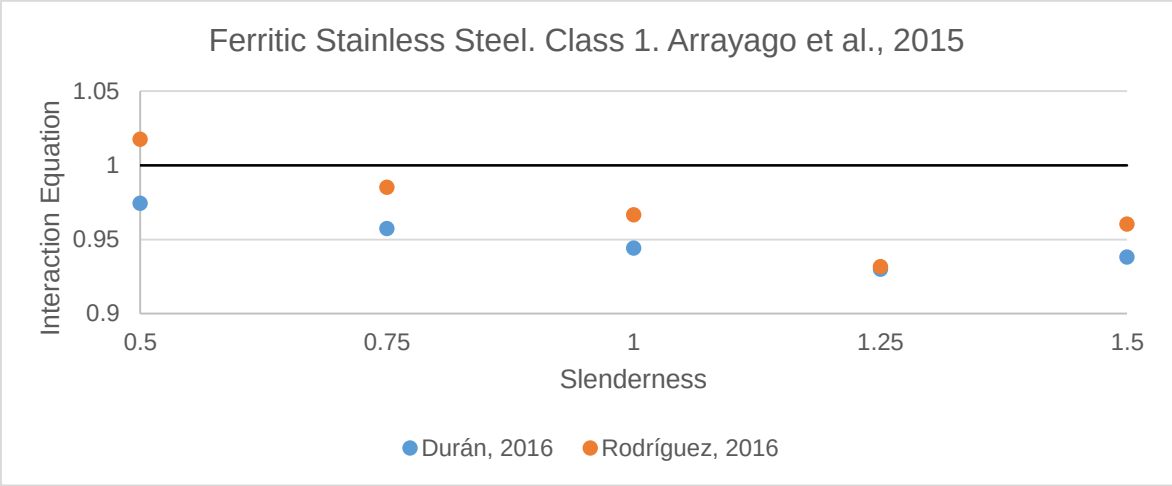

Figure 4.10. Durán and Rodríguez results. Ferritic stainless steel. Class 1. Arrayago et al., 2015

In Table 4.13 it is represented the mean average and standard deviation for ferritic stainless steel material for both Durán and Rodríguez results.

		FERRITIC
Durán results	Mean Average	0.9488
	Standard deviation	0.0174
Rodríguez results	Mean Average	0.9724
	Standard deviation	0.0318

Table 4.13. Durán and Rodríguez results. Ferritic stainless steel. Class 1. Arrayago et al., 2015

- Slender section Class 4

The Figures 4.11-4.13 represent how the interaction Equation (2.28) works with different materials (ferritic, duplex and austenitic stainless steel) with a varying slenderness in Class 4 (SHS 80x80x2), using the interaction factor *k* for the research performed at UPC (Arrayago, 2015).

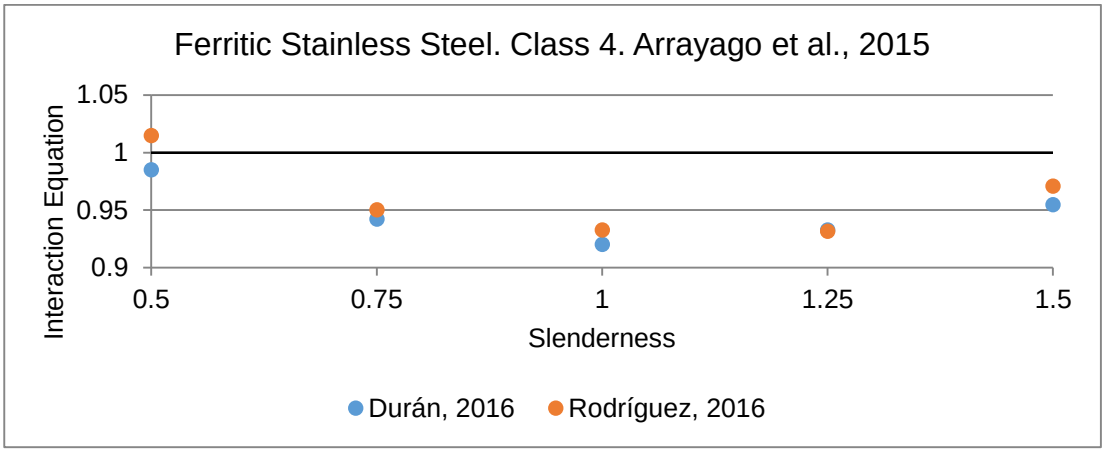

Figure 4.11. Durán and Rodríguez results. Ferritic stainless steel. Class 4. Arrayago et al., 2015

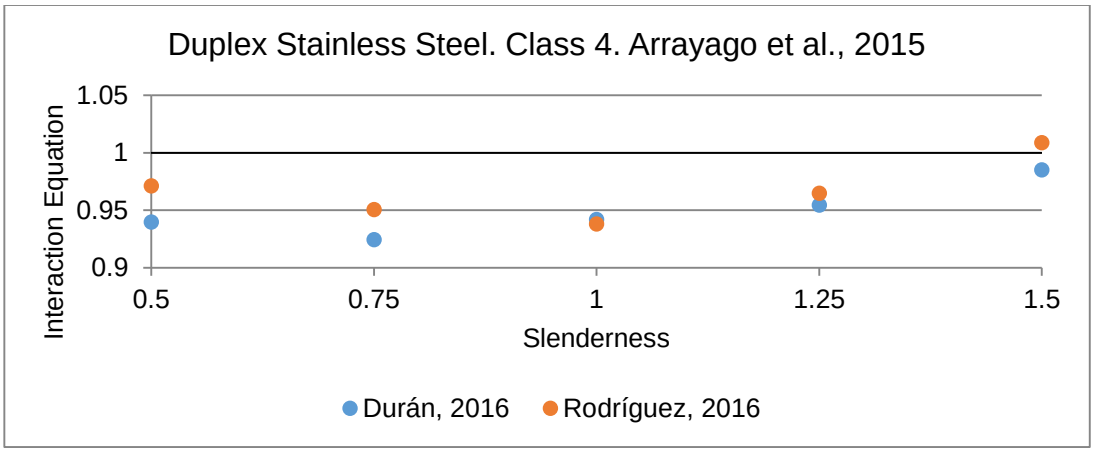

Figure 4.12. Durán and Rodríguez results. Duplex stainless steel. Class 4. Arrayago et al., 2015

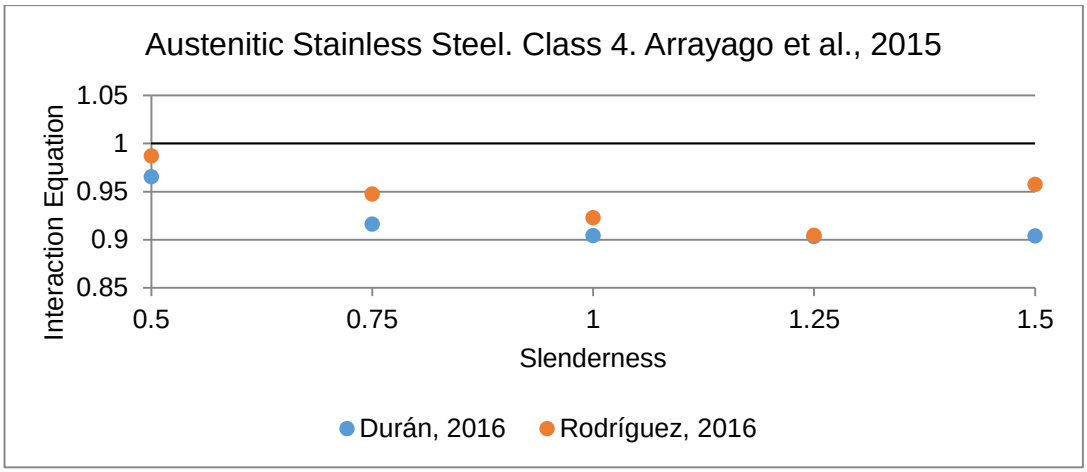

Figure 4.13. Durán and Rodríguez results. Austenitic stainless steel. Class 4. Arrayago et al., 2015

In Table 4.14 it is represented the mean average and standard deviation for this three materials for both Durán and Rodriguez results.

		FERRITIC	DUPLEX	AUSTENITIC
Durán results	Mean Average	0.9472	0.9491	0.9187
	Standard deviation	0.0248	0.0227	0.0267
Rodríguez results	Mean Average	0.9601	0.9667	0.9439
	Standard deviation	0.0345	0.0269	0.0318

Table 4.14. Durán and Rodríguez results. Ferritic, duplex and austenitic stainless steel. Class 4. Arrayago et al., 2015

4.3.4 Concluding remarks

Below there is a Table 4.15 where there are all the mean averages and standard deviations for the different classes and materials for Durán and Rodríguez results.

			Durán results		Rodríguez results	
Formulation	**Cross-section**	**Material**	**Mean A.**	**Standard D.**	**Mean A.**	**Standard D.**
EN 1993 1-4	Class 1	Ferritic	1.064	0.032	1.093	0.039
	Class 4	Ferritic	1.062	0.051	1.078	0.059
		Duplex	1.065	0.069	1.087	0.071
		Austenitic	1.026	0.040	1.058	0.053
Zhao, 2015	Class 1	Ferritic	0.998	0.006	1.024	0.021
	Class 4	Ferritic	0.997	0.023	1.011	0.031
		Duplex	1.028	0.043	1.048	0.041
		Austenitic	1.066	0.014	1.100	0.017
Arrayago et al. 2015	Class 1	Ferritic	0.945	0.017	0.972	0.032
	Class 4	Ferritic	0.947	0.025	0.960	0.034
		Duplex	0.949	0.023	0.966	0.027
		Austenitic	0.919	0.027	0.944	0.032

Table 4.15. Comparison Durán and Rodríguez results for procedure validation

As it could be observed in Table 4.15, for EN 1993-1-4 and Zhao (2015) the results are really similar, whether through Class 1 or Class 4 and for the different stainless steel materials. Values obtained are very near to 1.0, so this are results good enough in order to carry out the behavior of stainless steel beam-columns. But for Arrayago et al. (2015), the results vary 0.2-0.3 in the mean average. These are not bad results but, just to remark, it is obtained better outcomes with Eurocode and Zhao (2015) formulation than with Arrayago formulation (2015). This difference could exist because when Arrayago et al. (2015) performed the research, they supposed the imperfection amplitudes due to they do not have them. In order to adopt the traditional L/1500, it was applied expressions from EN 1993-1-1 which gave some imperfections higher than L/1500, so the Equation was calibrated.

4.4 Strain hardening exponent validation

In this chapter, a validation of the strain hardening exponent *n* is done. This parameter is described in Equation (2.2) and it is used in material equations. This validation is done using a cross-section Class 1 (60x60x3 mm) and another one for Class 2 (100x100x3 mm). I wanted to observe how this change of parameter affected at the final results of the interaction formulas. For this validation procedure, a ferritic stainless steel for both sections with the characteristics parameter of strain hardening exponent for ferritic, n=14, and then n=7, which is the typical strain hardening exponent parameter in austenitic stainless steels, is used, but with all the other characteristics of the ferritic stainless steel.

In the following figures 4.13.a and 4.13.b it is possible to observe how this change affects to the $\sigma_{nom} - \varepsilon_{true,pl.}$ curve.

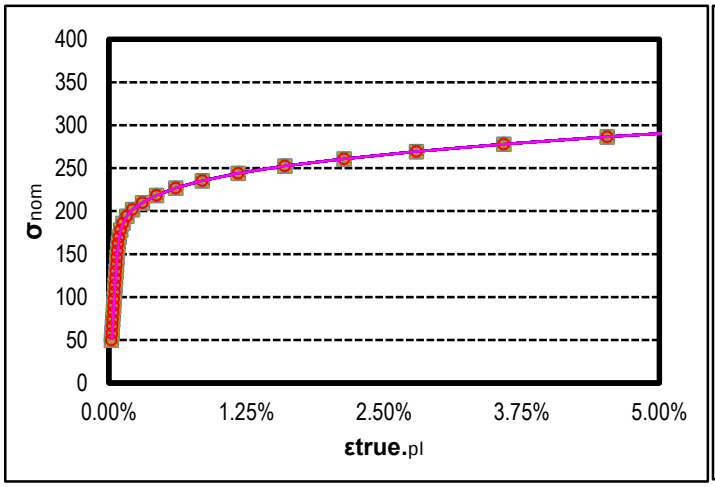

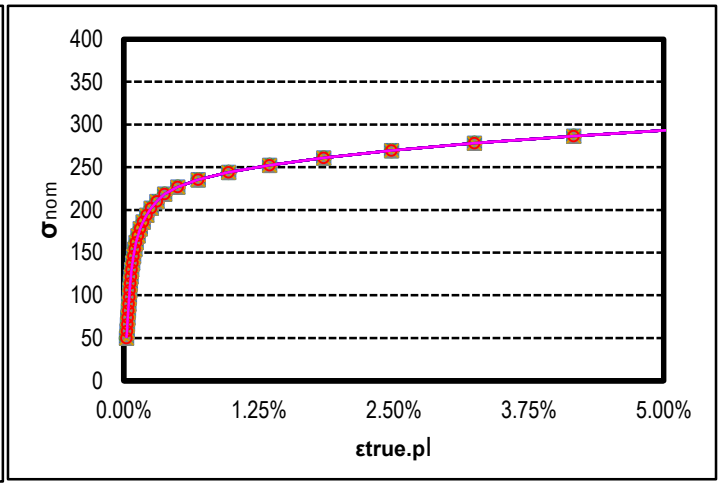

Figure 4.13a Strain hardening exponent n=14 *Figure 4.13b* Strain hardening exponent n=7

Figure 4.13. Strain hardening exponent

It is possible to observe that with the strain hardening exponent equals to 14 in ferritic stainless steel, for less strain we will have a nominal stress higher. But when we have higher strains (between 1.25% and 5.00%) we will have the same nominal stress for both n=14 and n=7 cases. In order to obtain the results, an analysis is carried out with the interaction Equation (2.28) with the interaction factor *k* for EN 1993-1-4, Zhao (2015), Arrayago et al. (2015) and Simplified Method from Structural Steel Code EAE formulae explained in the previous chapter.

4.4.1. Strain hardening exponent by EN 1993-1-4

In chapter 2.5.1. it is explained the formulation to use for EN 1993-1-4. So, the calculation of the interaction Equation (2.28) is worked out and then the results are compared.

- Compact section Class 1

The Figure 4.14 represents how the Equation (2.28) works with ferritic stainless steel with a varying slenderness in Class 1 (SHS 60x60x3).

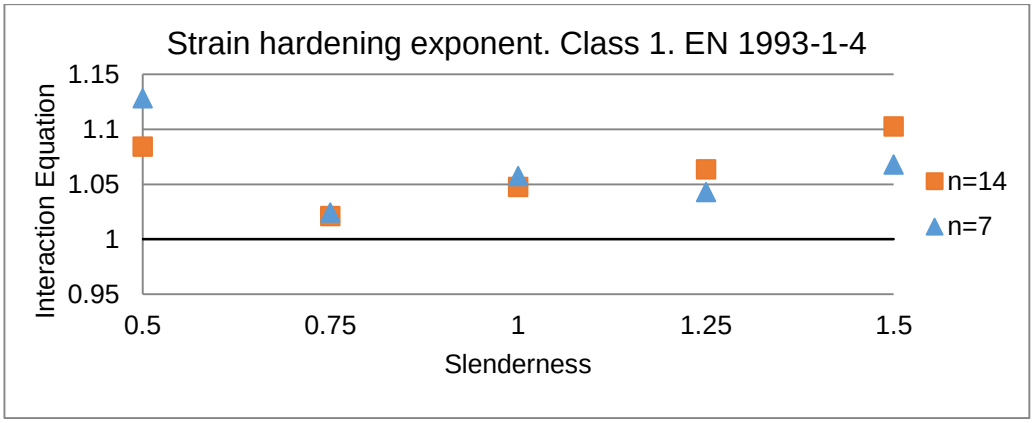

Figure 4.14. Comparison strain hardening exponent by EN 1993 1-4. Class 1

The next Table 4.16 shows the mean average and the standard deviation for both strain hardening exponent.

n	Mean Av.	Standard D.
14.0	1.0638	0.0316
7.0	1.0642	0.0393

Table 4.16. Comparison strain hardening exponent by EN 1993 1-4. Class 1

- Compact section Class 2

The *Figure 4.15* represents how the Equation (2.28) works with ferritic stainless steel with a varying slenderness in Class 2 (SHS 100x100x3).

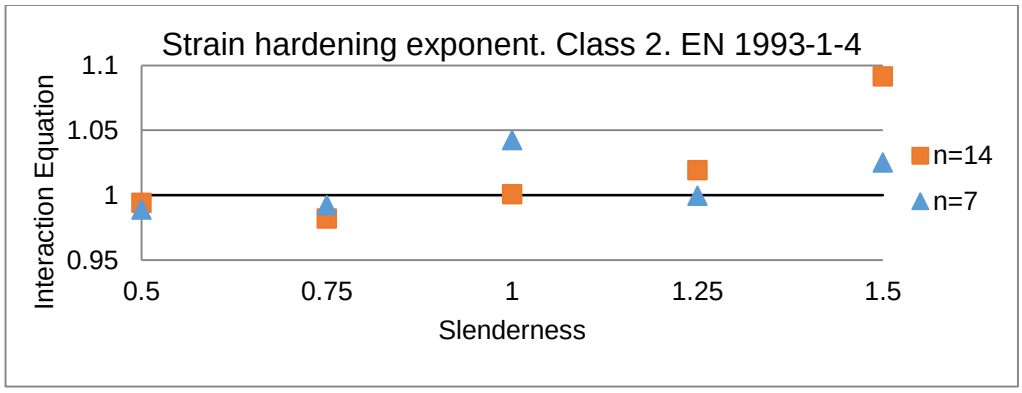

Figure 4.15. Comparison strain hardening exponent by EN 1993 1-4. Class 2

The next Table 4.17 shows the mean average and the standard deviation for both strain hardening exponent.

n	Mean Av.	Standard D.
14.0	1.0175	0.0436
7.0	1.010	0.0231

Table 4.17. Comparison strain hardening exponent by EN 1993 1-4. Class 2

4.4.2. Strain hardening exponent by Zhao (2015)

In chapter 2.5.2. it is explained the designed formulae to use the interaction factor *k* for Zhao (2015). So, the calculation of the interaction Equation (2.28) is worked out and then the results are compared.

- Compact section Class 1

The Figure 4.16 represents how the Equation (2.28) works with ferritic stainless steel with a varying slenderness in Class 1 (SHS 60x60x3).

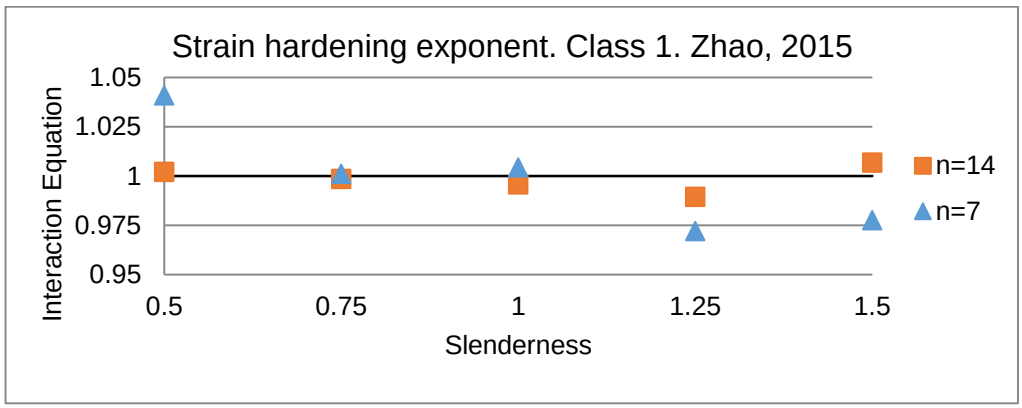

Figure 4.16. Comparison strain hardening exponent by Zhao, 2015. Class 1

The next Table 4.18 shows the mean average and the standard deviation for both strain hardening exponent.

n	Mean Av.	Standard D.
14.0	0.998	0.0065
7.0	0.999	0.027

Table 4.18. Comparison strain hardening exponent by Zhao, 2015. Class 1

- Compact section Class 2

The Figure 4.17 represents how the Equation (2.28) works with ferritic stainless steel with a varying slenderness in Class 2 (SHS 100x100x3).

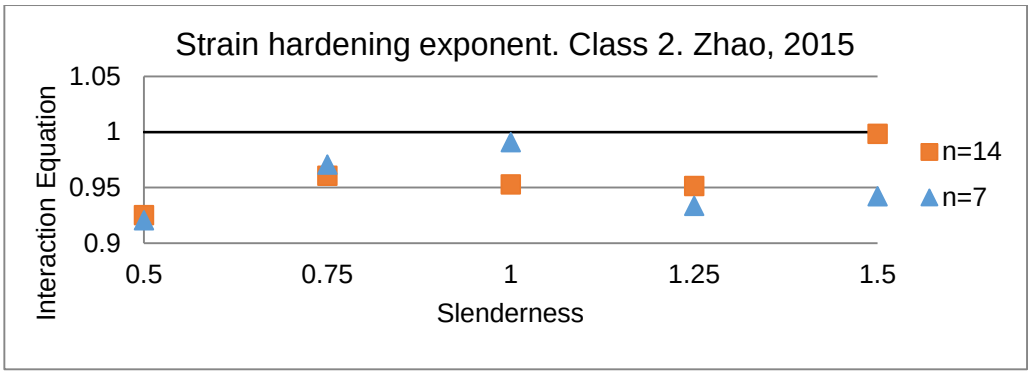

Figure 4.17. Comparison strain hardening exponent by Zhao, 2015. Class 2

The next Table 4.19 shows the mean average and the standard deviation for both strain hardening exponent.

n	Mean Av.	Standard D.
14.0	0.9578	0.0263
7.0	0.9517	0.0286

Table 4.19. Comparison strain hardening exponent by Zhao, 2015. Class 2

4.4.3. Strain hardening exponent by Arrayago et al. (2015)

In chapter 2.5.3. it is explained the designed formulae to use the interaction factor *k* for Arrayago et al., (2015). So, the calculation of the interaction Equation (2.28) is worked out and then the results are compared.

- Compact section Class 1

The Figure 4.18 represents how the Equation (2.28) works with ferritic stainless steel and with a varying slenderness in Class 1 (SHS 60x60x3).

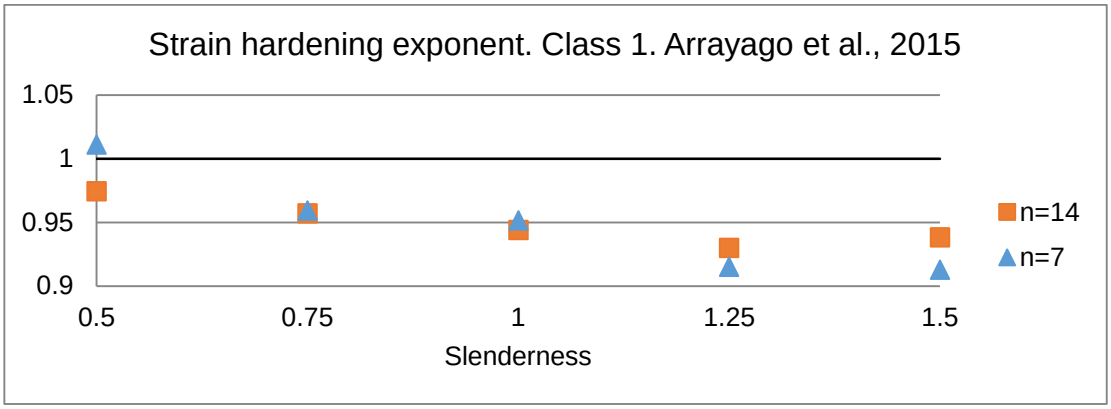

Figure 4.18. Comparison strain hardening exponent by Arrayago et al., 2015. Class 1

The next Table 4.20 shows the mean average and the standard deviation for both strain hardening exponent.

n	Mean Av.	Standard D.
14.0	0.9489	0.017
7.0	0.9501	0.040

Table 4.20. Comparison strain hardening exponent by Arrayago et al., 2015. Class 1

- Compact section Class 2

The Figure 4.19 represents how the Equation (2.28) works with ferritic stainless steel with a varying slenderness in Class 2 (SHS 100x100x3).

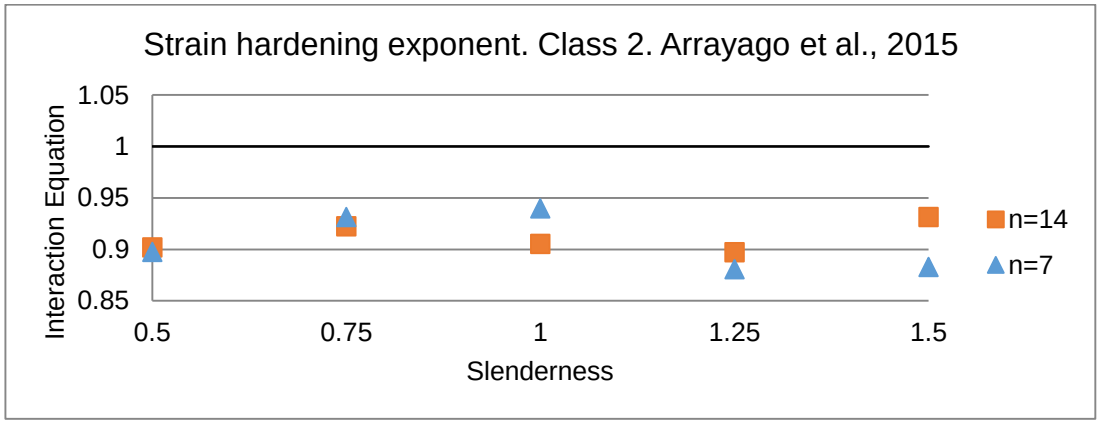

Figure 4.19. Comparison strain hardening exponent by Arrayago et al., 2015. Class 2

The next Table 4.21 shows the mean average and the standard deviation for both strain hardening exponent.

n	Mean Av.	Standard D.
14.0	0.9118	0.0146
7.0	0.9066	0.0275

Table 4.21. Comparison strain hardening exponent by Arrayago et al., 2015. Class 2

4.4.4. Strain hardening exponent by Simplified Method.

In chapter 2.5.4. it is explained the formulation to use for Simplified Method from Structural Steel Code EAE. So, the calculation of the interaction Equation (2.28) is worked out and then the results are compared.

- Compact section Class 1

The Figure 4.20 represents how the Equation (2.34) works with ferritic stainless steel with a varying slenderness in Class 1 (SHS 60x60x3).

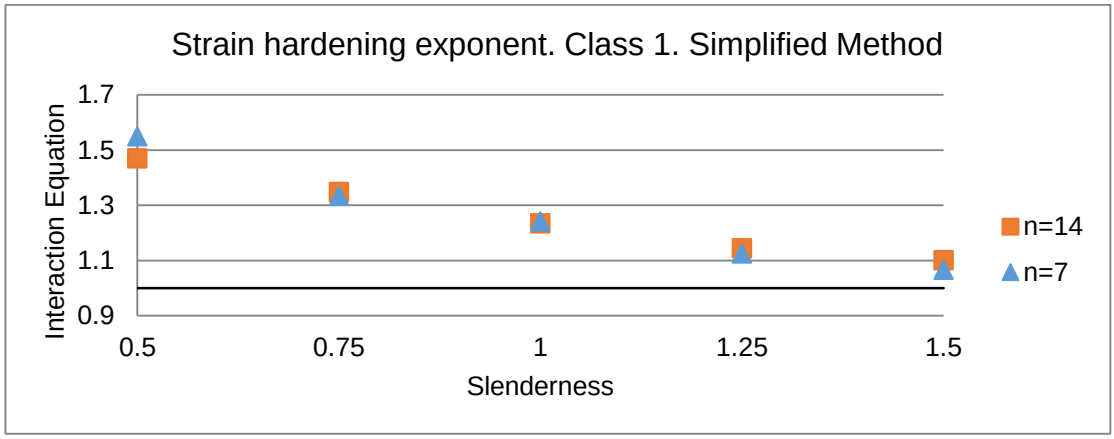

Figure 4.20. Comparison strain hardening exponent by Simplified Method. Class 1

The next Table 4.22 shows the mean average and the standard deviation for both strain hardening exponent.

n	Mean Av.	Standard D.
14.0	1.259	0.151
7.0	1.263	0.191

Table 4.22. Comparison strain hardening exponent by Simplified Method. Class 1

- Compact section Class 2

The Figure 4.21 represents how the Equation (2.34) works with ferritic stainless steel with a varying slenderness in Class 2 (SHS 100x100x3).

Figure 4.21. Comparison strain hardening exponent by Simplified Method. Class 2

The next Table 4.23 shows the mean average and the standard deviation for both strain hardening exponent.

n	Mean Av.	Standard D.
14.0	1.191	0.103
7.0	1.185	0.129

Table 4.23. Comparison strain hardening exponent by Simplified Method. Class 2

4.4.5. Concluding remarks

In the following Table 4.24, there is a summary where we can find the different mean averages and standard deviations for all different cases.

			n=14		n=7	
Formulation	**Cross-section**	**Material**	**Mean A.**	**Standard D.**	**Mean A.**	**Standard D.**
EN 1993 1-4	Class 1	Ferritic	1.064	0.032	1.064	0.039
	Class 2	Ferritic	1.018	0.043	1.009	0.023
Zhao, 2015	Class 1	Ferritic	0.998	0.007	0.999	0.027
	Class2	Ferritic	0.958	0.026	0.952	0.029
Arrayago et al., 2015	Class 1	Ferritic	0.949	0.017	0.95	0.04
	Class2	Ferritic	0.912	0.015	0.907	0.028
Simplified Method	Class 1	Ferritic	1.259	0.151	1.264	0.191
	Class2	Ferritic	1.191	0.103	1.185	0.129

Table 4.24. Summary of strain hardening exponent validation

The best results are those that have the mean average really close to the ideal value 1.0. So, using Zhao (2015) equations the Interaction Equation reaches values near to 1. For EN 1993-1-4 the values obtained are a little bit above from the ideal value but not too far. Then, for Arrayago et al. (2015) the outcomes are below 1.0 In both cross sections Class 1 and Class 2. This, as same that in the previous chapter, may be due to the calibration of the interaction factor *k* equation. Finally, for the Simplified Method, as it is not a formulation used for stainless steel, it is obtained values distant to the ideal value.

As it is possible to observe in the previous Table 4.24, all the standards deviations are lower when the strain hardening exponent equal to 14 is used. This means that the results are better than with the other parameter, n=7.0. Only in one case the standard deviation is higher with n=14, this is with the EN 1993-1-4 standards formulae in Class 2. This difference is of 0.02, so as it is not too high it can be assured that using the strain hardening exponent equal to 14 will give better results in ferritic stainless steel than using n=7.0 form the austenitic stainless steel.

5. BEHAVIOUR OF STAINLESS STEEL COLUMNS UNDER COMBINED BENDING AND AXIAL LOAD

5.1 Introduction

In this chapter a study of the behaviour of different stainless steel (Ferritic, Austenitic and Duplex) columns under combined bending and axial load is carried out. For elements subjected to combined compressive and bending load, the absence of buckling phenomena is really infrequent and so, the most significant verifications concern the bucking itself. The members subjected to combined compression and bending moment can buckle in different ways, depending on the cross-section geometry and on the boundary conditions. The study of members subjected to combined loading is done through interaction domains M-N. This study of the behaviour is done for square hollow section (SHS) of Class 1 and Class 2 (compact sections). For the first class we used the section 60x60x3 mm and for the second one 100x100x3 mm.

Numerical simulations were carried out on single span pin-ended stainless steel SHS beam-columns, accounting for initial geometric imperfections, with the member slenderness ranging between 0.5 and 1.5.

The following Figure 5.1 shows the different cross-section used in this analysis.

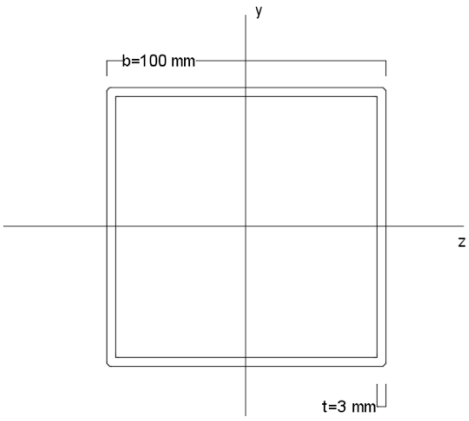

Figure 5.1a. SHS 100x100x3 mm

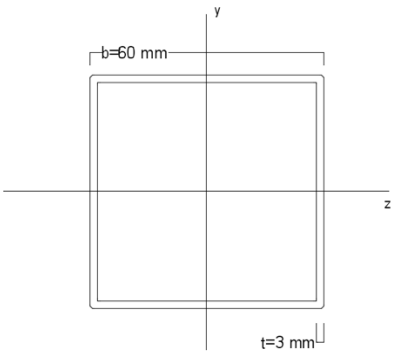

Figure 5.1b SHS 60x60x3 mm

Figure 5.1. Cross-sections

The main objective of this chapter is to make a comparison of four different methods, calculating in each case the interaction factor *k*. These methods will be explained later and they are:

- EN 1993-1-4
- Zhao, 2015
- Arrayago et al., 2015

- Simplified Method from Structural Steel Code EAE.

As it is explained before, it is taking into consideration the austenitic, duplex and ferritic stainless steel for this study. The main characteristics of this materials are proposed in Table 2.8.

In all the different cases and methods, we used the distribution of the bending moment taking into account ψ=1.0, so, a constant distribution of bending moment along the length member as could be seen from Figure 5.2.

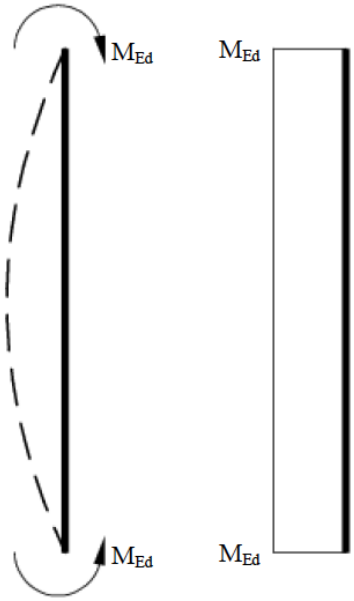

Figure 5.2: Bending moment diagram [Zhao, 2015]

5.2 Imperfections

Initial local geometric imperfections exist in all thin-walled structural members and can influence the development of local buckling, the load level at which plasticity initiates, the ultimate load-carrying capacity and the post-ultimate response. Hence, it is necessary to include suitable geometric imperfections into the FE models in order to accurately replicate the imperfections of the columns. The local imperfection that we used in this thesis is the imperfection amplitude $\omega_{D\&W}$ derived from the modified Dawson and Walker (D&W) predictive model, as given by Equation (5.1):

$$\omega_{D\&W} = 0.023 \left(\frac{\sigma_{0.2}}{\sigma_{cr,min}}\right) t \tag{5.1}$$

where t is the thickness of our section and $\sigma_{cr,min}$ is the lowest critical stress for local buckling. The way to know this stress is using the following Equation (5.2):

$$\sigma_{cr,min} = k \cdot \frac{\pi^2 \cdot E}{12(1-\nu^2)\left(\frac{b}{t}\right)^2} \quad (5.2)$$

in this case k=4.0 and the Poisson's ratio is 0.3.

Therefore, we have different local imperfections depending on the section that we are studying. In the following Table 5.1 we could see the different values of local imperfections.

	SHS 60x60x3 - Class 1	**SHS 100x100x3 – Class 2**
Local imperfection $\omega_{D\&W}$(mm)	0.0053	0.103

Table 5.1. Local imperfections in different cross-sections

For global imperfection, we are taking in consideration only one kind of imperfection, *L*/1000, for all the different analysis to study.

5.3 Previous Calculations

In this chapter, it is going to calculate the different lengths of the tests columns depending on its slenderness, $\bar{\lambda}$. It is possible to see by Equation (5.3) how to obtain this slenderness.

$$\bar{\lambda} = \sqrt{\frac{A \cdot \sigma_{0.2}}{N_{cr}}} \quad (5.3)$$

where $\sigma_{0.2}$ depends on the material used in the analyse.

There are two ways to find out the value of the critical load; by the Equation (44) of critical load of Euler or by finite elements in Abaqus.

$$N_{cr} = \frac{\pi^2 \cdot E \cdot I}{L^2} \quad (5.4)$$

As with FE Abaqus it is possible to obtain more accurate results, the critical load N_{cr} is going to obtained by it, and then the slenderness is going to be calculated.

It is important to remark that in order to calculate $A\sigma_{0.2}$ by Abaqus and not by hand, it needs to introduce in the code many restrictions along all the length of column in order to not have global buckling. The length of the column introduced is 4500 mm. In the following Figures 5.3 and 5.4 it is possible to see this effect:

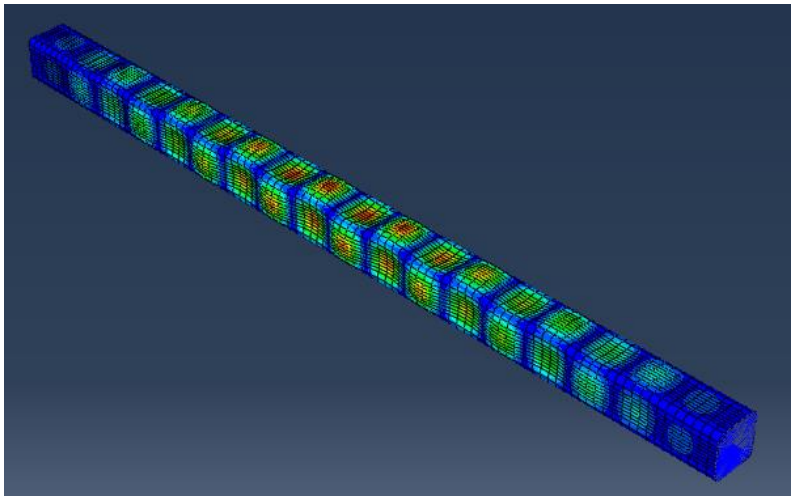

Figure 5.3. Local buckling $A\sigma_{0.2}$

In order to obtain N_{cr}, it is calculated the eigenvalue of our column introducing a load with a magnitude of 500 kN. Then, this eigenvalue given by Abaqus is multiplied by the load introduced and finally, the critical load for each material is obtained.

Once the results are obtained, it is possible to calculate the slenderness, $\bar{\lambda}$, for each particular case. Hence, this slenderness is interpolated in order to obtain different slenderness (from 0.5 to 1.5) and finally the different lengths for each slenderness are calculated

In the following Tables 5.2-5.3 there is a summarise of all the lengths (mm) for each material and cross-section.

SLENDERNESS	FERRITIC	DUPLEX	AUSTENITIC
0.5	1010	700	970
0.75	1520	1050	1450
1	2020	1500	1940
1.25	2540	1750	2430
1.5	3050	2100	2900

Table 5.2. Class 1 lengths

SLENDERNESS	FERRITIC	DUPLEX	AUSTENITIC
0.5	1840	1270	1780
0.75	2760	1910	2680
1	3570	2540	3570
1.25	4600	3180	4460
1.5	5520	3800	5350

Table 5.3. SHS Class 2 lengths

Therefore, Figures 5.4a-5.4c and 5.5a-5.5c represent the proposed beam-column design interaction curves for class 1 and class 2 corresponding to a range of member slenderness for ferritic, duplex and austenitic stainless steels, respectively, indicating and increasingly concave trend as the member slenderness increases.

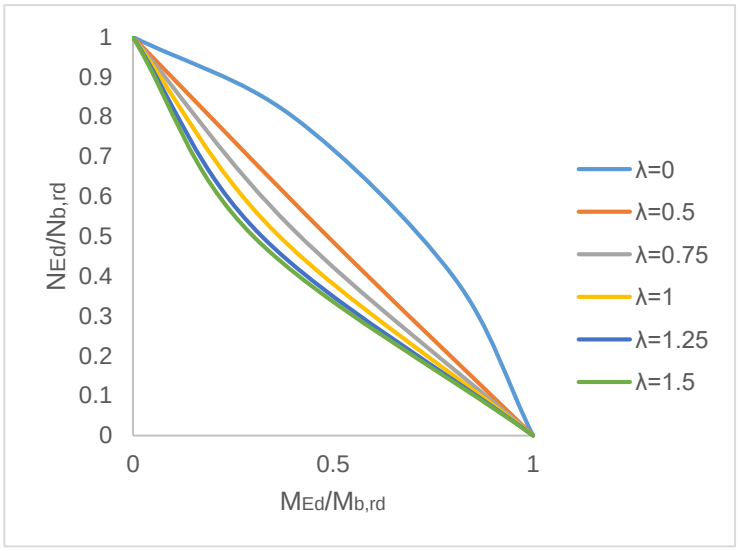

(a) Ferritic stainless steel. Class 1

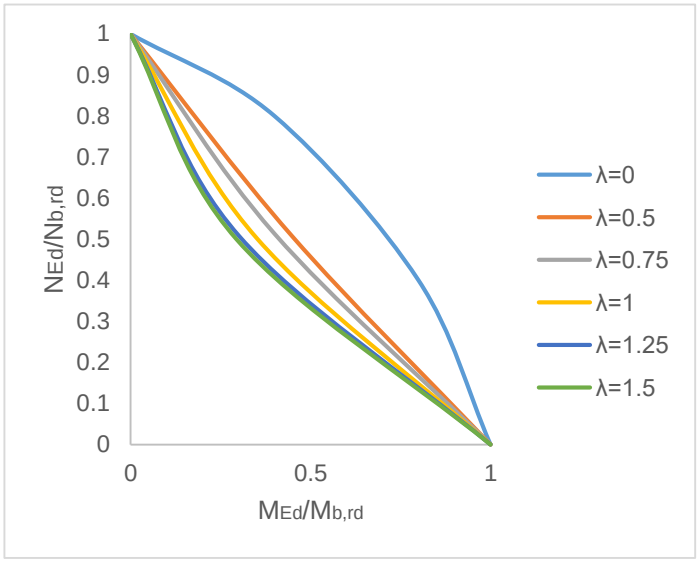

(b) Duplex stainless steel. Class 1

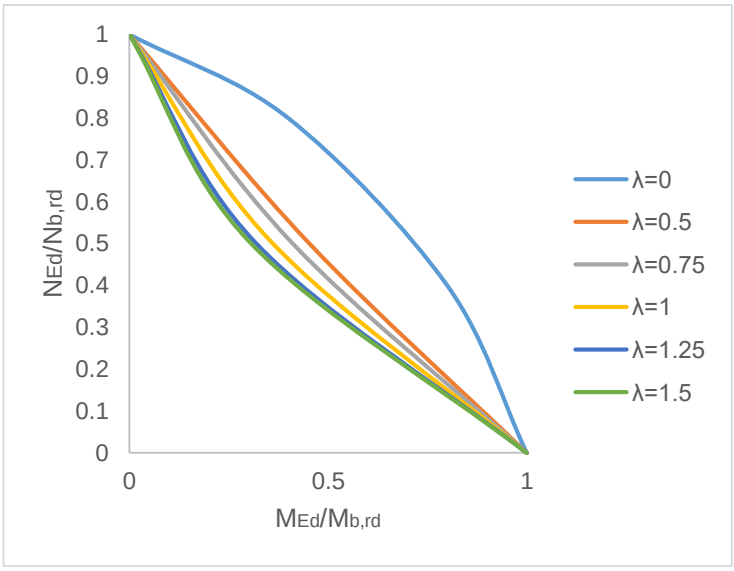

(c) Austenitic stainless steel. Class 1

Figure 5.4: Proposed beam-column design interaction curves for varying member slendernesses. Class 1

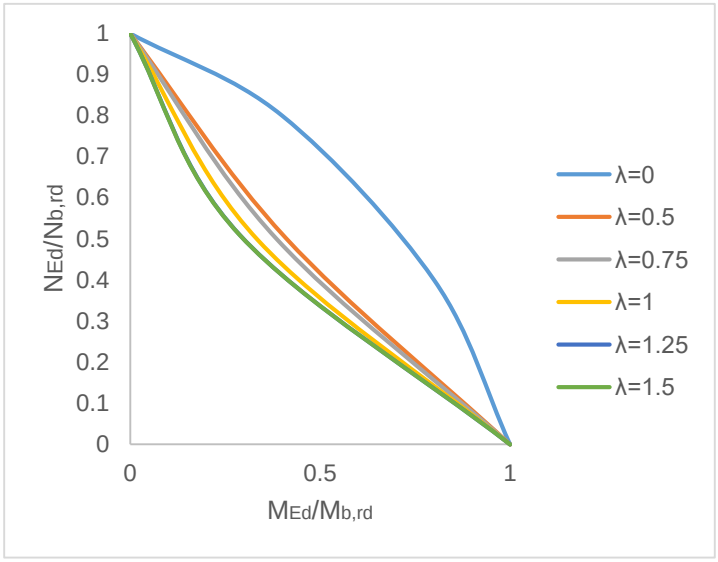

(a) Ferritic stainless steel. Class 2

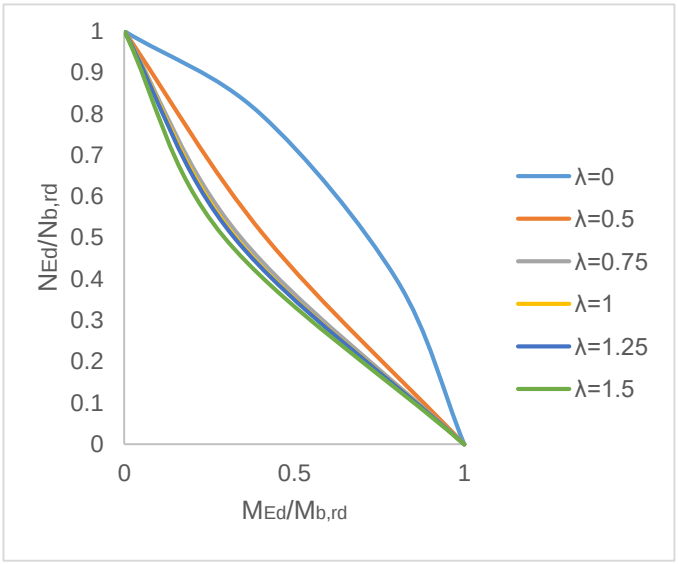

(b) Duplex stainless steel. Class 2

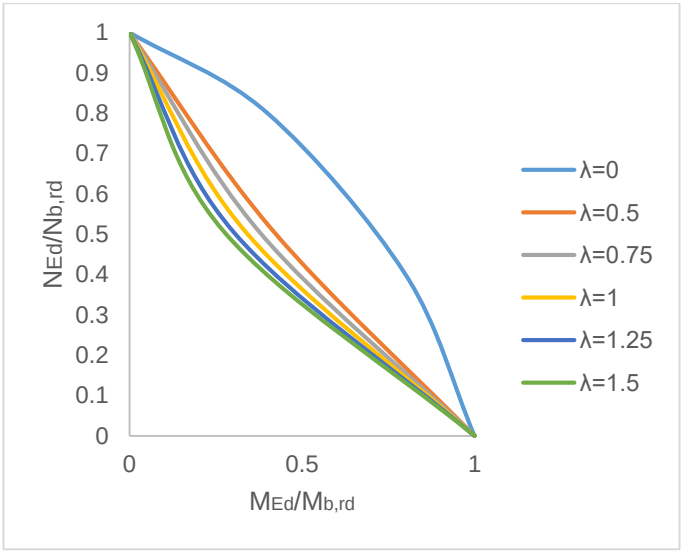

(c) Austenitic stainless steel. Class 1

Figure 5.5: Proposed beam-column design interaction curves for varying member slendernesses. Class 2

5.4 Interaction of axial compression and bending moment by EN 1993 1-4

In chapter 2.5.1. it is explained the formulation to use for EN 1993-1-4 [CEN, 2006]. So, the calculation of the interaction Equation (2.28) is worked out and then the results are compared.

- Compact section Class 1

The Figure 5.6 represents how the Equation (2.28) works with ferritic, duplex and austenitic stainless steel with a varying slenderness in Class 1 (SHS 60x60x3).

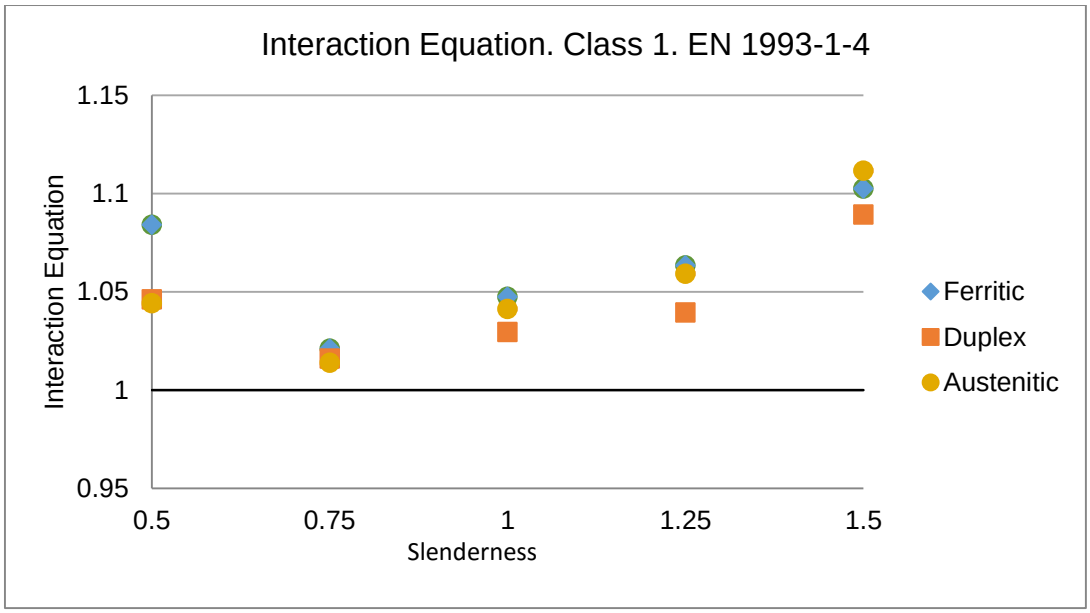

Figure 5.6. Interaction equation by EN 1993-1-4. Class 1

In Table 5.4 it is represented the mean average and standard deviation for these three different materials.

	FERRITIC	DUPLEX	AUSTENITIC
Mean Average	1.0638	1.0442	1.0542
Standard Deviation	0.0316	0.0276	0.0361
Coefficient of Variation (%)	2.97	2.64	3.42

Table 5.4. Mean average and standard deviation by EN 1993-1-4. Class 1

It is possible to observed that with EN 1993-1-4 in class 1 we have better results with duplex steel than with ferritic or austenitic steels

It is possible too to make a comparison of the three materials with the interaction factor *k* and the slenderness, in order to see if the Equation (2.29) is accurate enough. In Figure 5.7 it is represented this comparison.

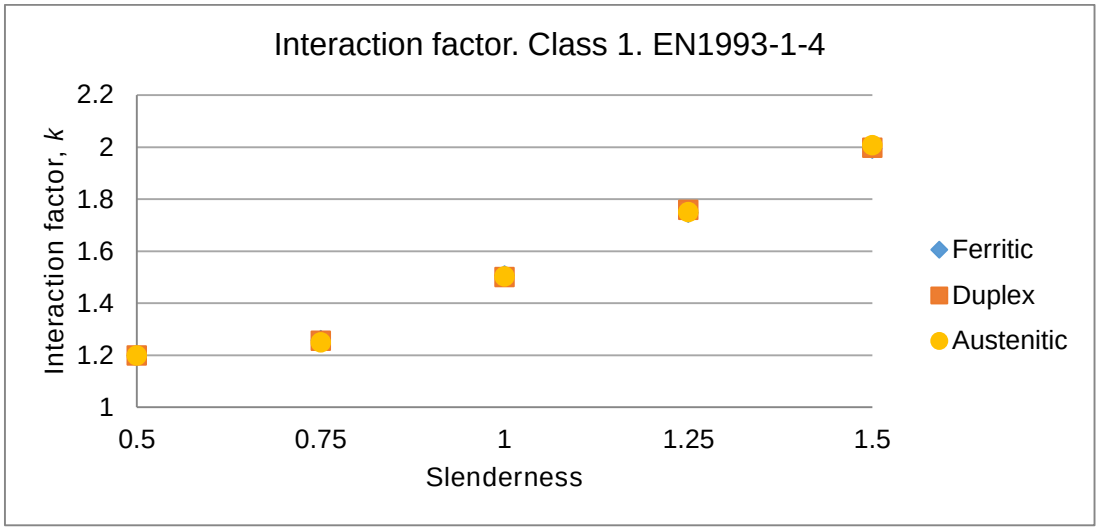

Figure 5.7. Interaction factor and slenderness. EN 1993-1-4. Class

In this case, the interaction factor *k* does not vary when the material is changed. This is something positive because it means that the method that it is used to calculate this interaction factor is robust. This means that no matter if the material is changed as so the interaction factor will be the same for each slenderness.

The following Figures are a comparison between the interaction factor *k* and the slenderness, but changing the ratio of applied axial force to column buckling strength, n_b. This ratio is expressed in Equation (5.5).

$$n_b = \frac{N_{ed}}{N_{b,rd}} \tag{5.5}$$

As observed in the following figures, the interaction factor will increase for the same slenderness at the same time that the ratio of applied axial force increases too.

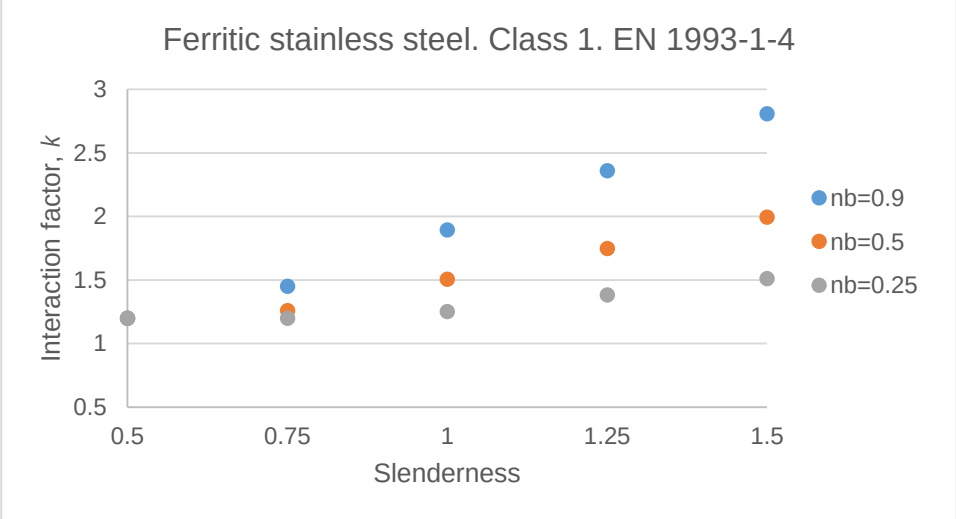

(a) Ferritic stainless steel

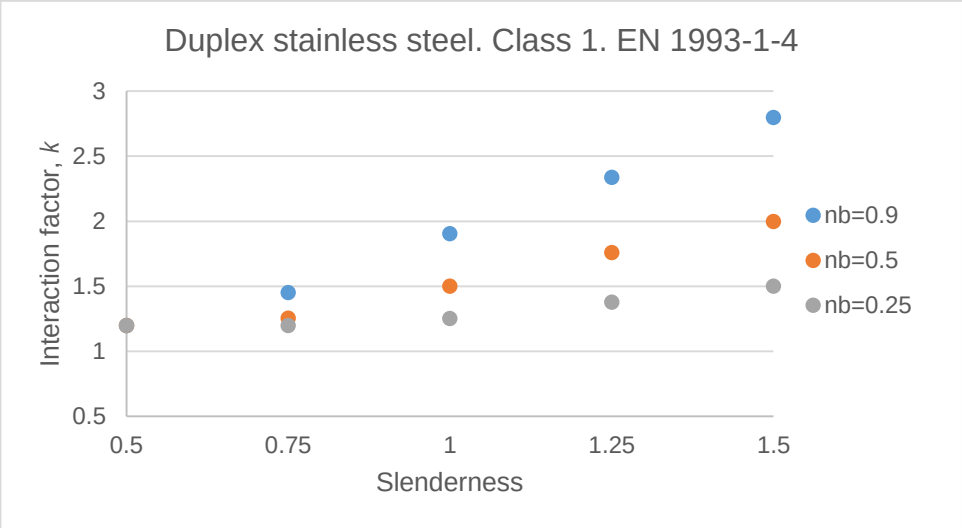

(b) Duplex stainless steel

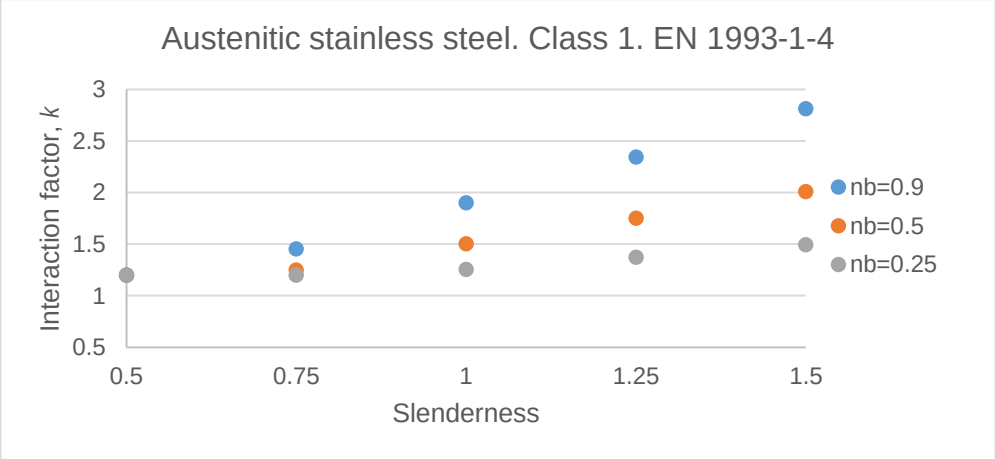

(c) Austenitic stainless steel

Figure 5.8. FE derived curves for interaction factors *k* by EN 1993-1-4. Class 1

- Compact section Class 2

The Figure 5.9 represents how the Equation (2.28) works with different materials (Ferritic, Duplex and Austenitic stainless steel) with a varying slenderness in Class 2 (SHS 100x100x3).

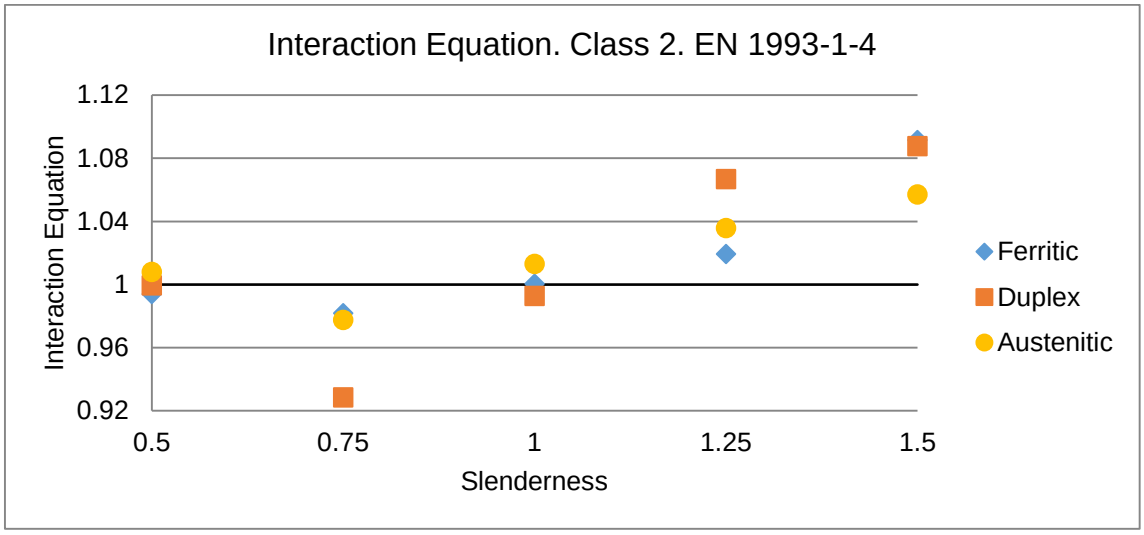

Figure 5.9. Interaction equation by EN 1993-1-4. Class 2

In Table 5.5 it is represented the mean average and standard deviation for this three materials.

	FERRITIC	DUPLEX	AUSTENITIC
Mean Average	1.0175	1.0151	1.0183
Standard Deviation	0.0436	0.0636	0.0299
Coefficient of Variation (%)	4.28	6.27	2.94

Table 5.5. Mean average and standard deviation by EN 1993-1-4. Class 1

As observed that with EN 1993-1-4 in Class 2 there are better results with austenitic stainless steel than with ferritic or duplex ones.

It is likely too to make a comparison of the three materials with the interaction factor *k* and the slenderness, in order to see if the Equation (2.29) is accurate enough.

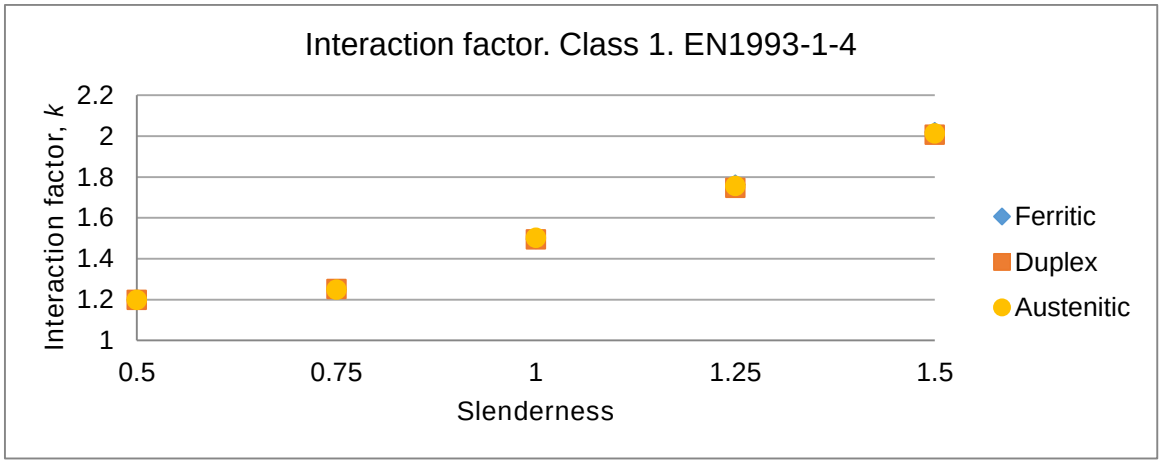

Figure 5.10. Interaction factor and slenderness. EN 1993 1-4. Class 2

For Class 2 the interaction factor *k* does not vary when the material is changed. This is something beneficial, as in Class 1, because it means that no matter if the material is changed as so the interaction factor will be the same for each slenderness.

The following Figures 5.11a-5.11c are a comparison between the interaction factor *k* and the slenderness, but changing the ratio of applied axial force to column buckling strength, n_b. This ratio is expressed in Equation (5.5). As it will be observed, the interaction factor will increase for the same slenderness at the same time that the ratio of applied axial force increases too.

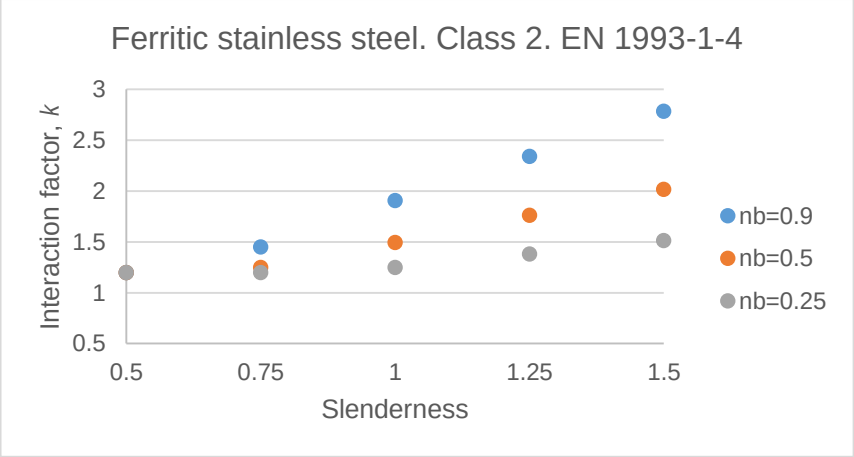

(a) Ferritic stainless steel

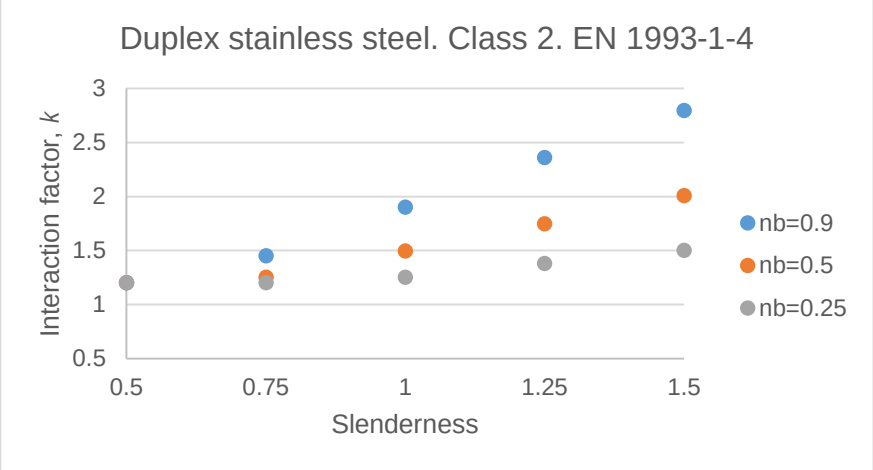

(b) Duplex stainless steel

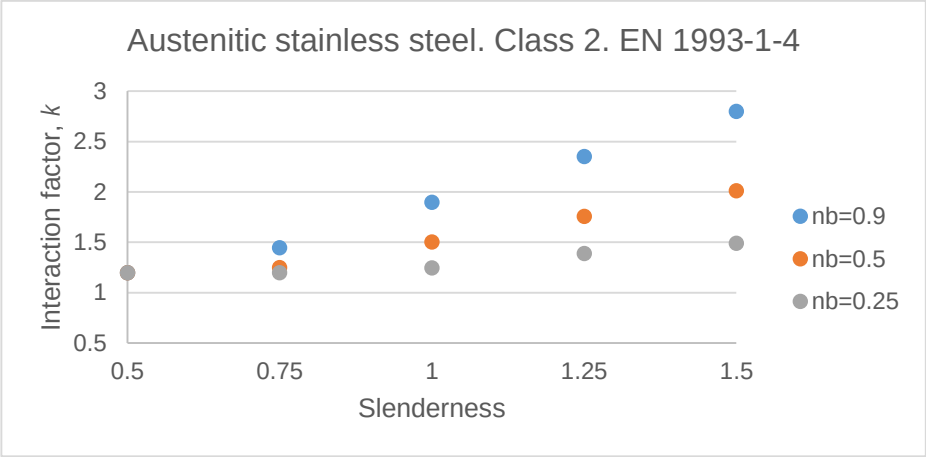

(c) Austenitic stainless steel

Figure 5.11. FE derived curves for interaction factors k by EN 1993-1-4. Class 2

5.5 Interaction of axial compression and bending moment by Zhao, 2015

In chapter 2.5.2. it is explained the designed formulae to use the interaction factor *k* for Ou Zhao [Zhao, 2015]. So, the calculation of the interaction Equation (2.28) is worked out and then the results are compared.

- Compact section Class 1

The Figure 5.12 represents how the Equation (2.28) works with different materials (Ferritic, Duplex and Austenitic stainless steel) with a varying slenderness in Class 1 (SHS 60x60x3).

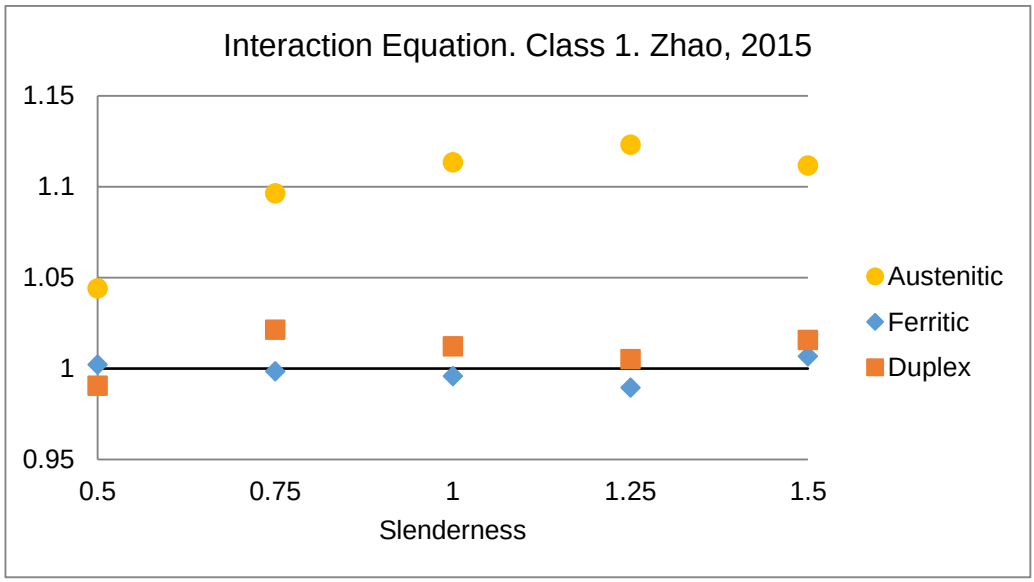

Figure 5.12. Interaction formula by Zhao, 2015. Class 1

In Table 5.6 it is represented the mean average and standard deviation for this three materials.

	FERRITIC	DUPLEX	AUSTENITIC
Mean Average	0.9985	1.0089	1.0977
Standard Deviation	0.0065	0.01185	0.0315
Coefficient of Variation (%)	0.65	1.17	2.87

Table 5.6. Mean average and standard deviation by Zhao, 2015. Class 1

The coefficient of variation in ferritic stainless steel shows that Zhao, 2015 is one of the best approaches in order to achieve the ideal value of the Interaction Equation 1.0.

It is possible too to make a comparison of the three materials with the interaction factor *k* and the slenderness, in order to see if the Equation (2.30) is accurate enough.

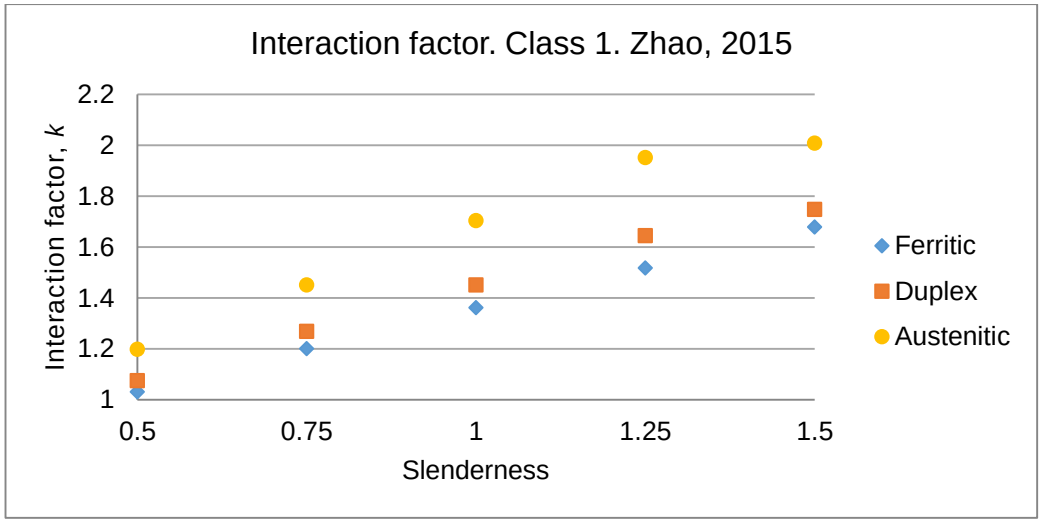

Figure 5.13. Interaction factor and slenderness. Zhao, 2015. Class 1

The interaction factor, *k*, does not vary when it is used ferritic and duplex stainless steel, but for austenitic there is a little variation from the other two. This is due to the change of the values of D_1, D_2 and D_3 for each material.

The following Figures 5.14a-5.14c are a comparison between the interaction factor *k* and the slenderness, but changing the ratio of applied axial force to column buckling strength, n_b. This ratio is expressed in Equation (5.5). As it is possible to observe, the interaction factor will increase for the same slenderness at the same time that the ratio of applied axial force increases too. For lower slenderness, the ratio of axial load will be more similar in three materials, but when the slenderness increases, the difference will be higher.

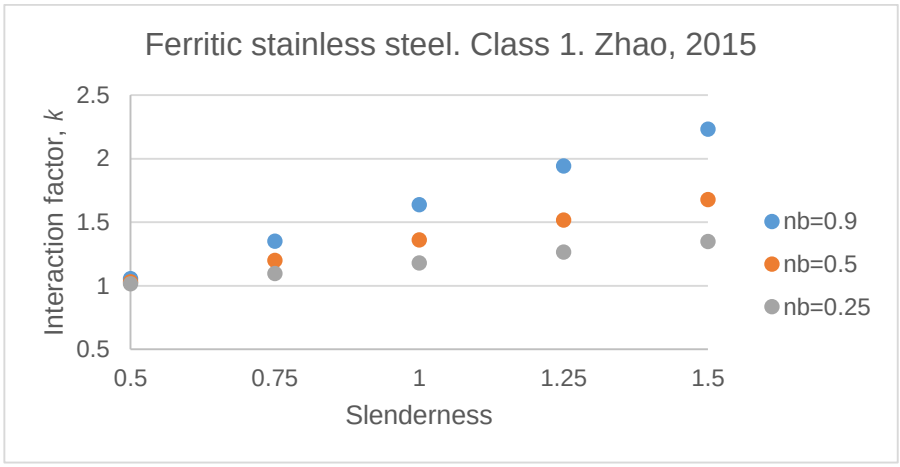

(a) Ferritic stainless steel

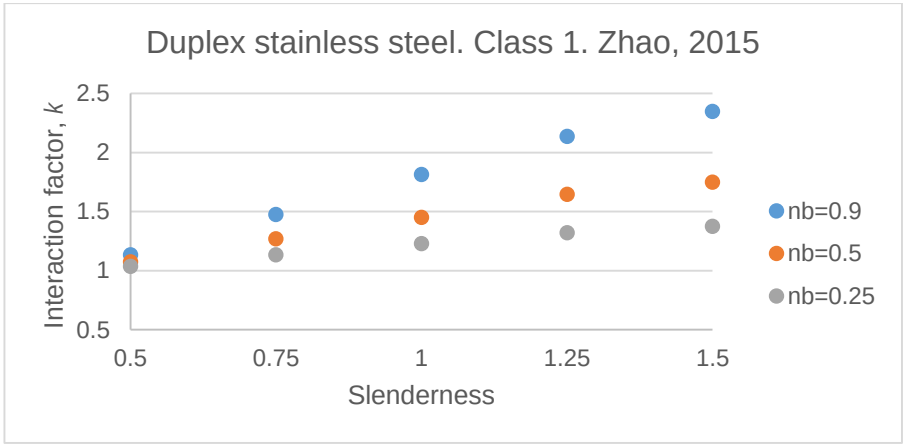

(b) Duplex stainless steel

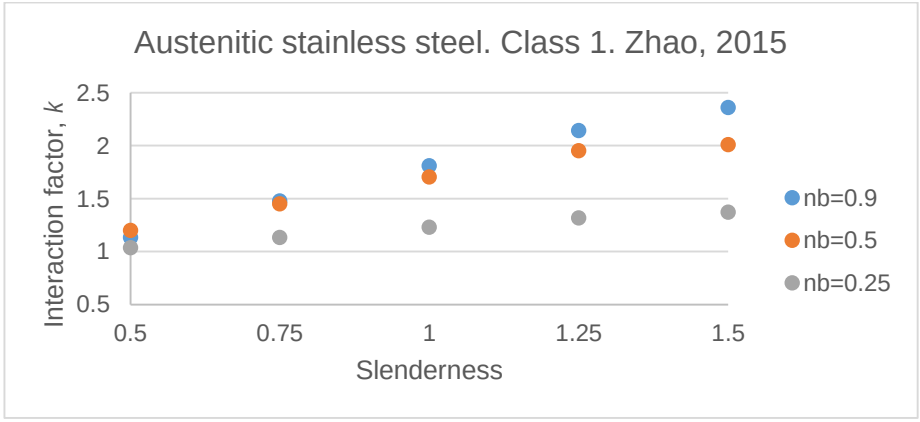

(c) Austenitic stainless steel

Figure 5.14. FE derived curves for interaction factors *k* by Zhao, 2015. Class 1

- Compact section Class 2

The Figure 5.15 represents how the Equation (2.28) works with different materials (Ferritic, Duplex and Austenitic stainless steel) with a varying slenderness in Class 2 (SHS 100x100x3).

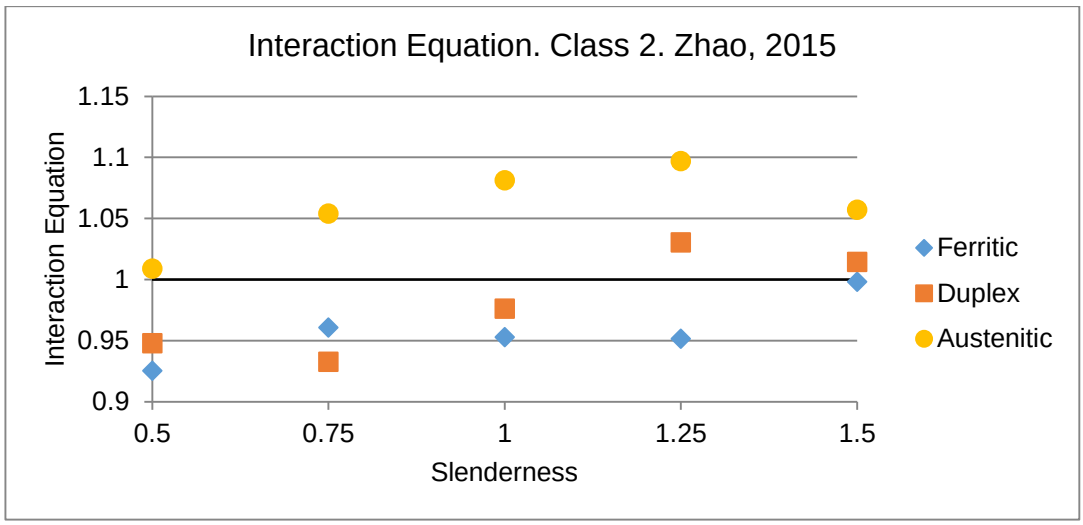

Figure 5.15. Interaction formula by Zhao, 2015. Class 2

In Table 5.7 it is represented the mean average and standard deviation for this three materials.

	FERRITIC	DUPLEX	AUSTENITIC
Mean Average	0.9578	0.9804	1.0596
Standard Deviation	0.0263	0.0418	0.0334
Coefficient of Variation (%)	2.75	4.26	3.15

Table 5.7. Mean average and standard deviation by Zhao, 2015. Class 2

As observed in the previous table, the interaction factor *k* of Zhao (2015) in Class 2 has the best result, as it happened in Class 1, in ferritic stainless steel. Hence, it is likely to affirm that ferritic stainless steel is the best material and the one that fits best when Zhao (2015) formulae is used.

It is possible too to make a comparison of the three materials with the interaction factor *k* and the slenderness, in order to see if the Equation (2.30) is accurate enough.

Figure 5.16. Interaction factor and slenderness. Zhao, 2015. Class 2

The interaction factor *k,* as it happens in Class 1, does not vary when it is used ferritic and duplex stainless steel, but for austenitic there is a little variation from the other two materials. This is due to the change of the values of D_1, D_2 and D_3 for each material. For lower slenderness, the interaction factor will be more similar in three materials, but when the slenderness increases, the difference will be higher.

The following Figures 5.17a-5.17c are a comparison between the interaction factor *k* and the slenderness, but changing the ratio of applied axial force to column buckling strength, n_b. This ratio is expressed in Equation (5.5). As it is possible to observe, the interaction factor will increase for the same slenderness at the same time that the ratio of applied axial force increases too.

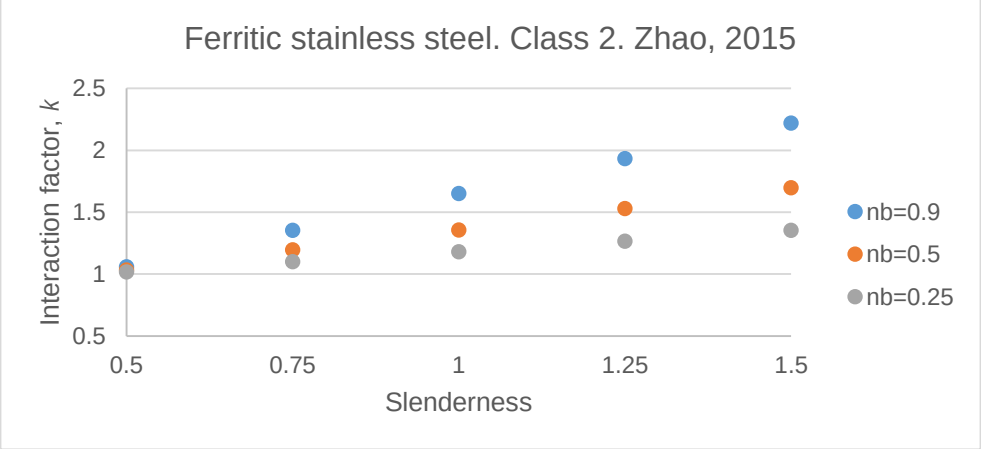

(a) Ferritic stainless steel

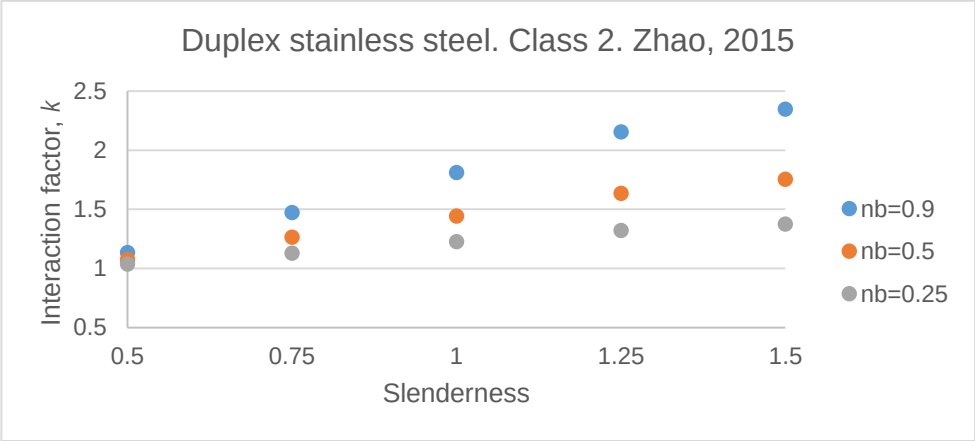

(b) Duplex stainless steel

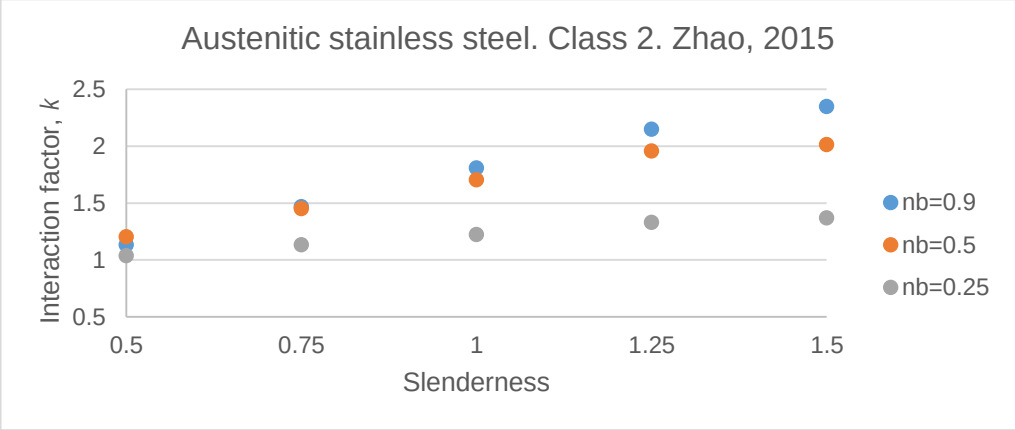

(c) Austenitic stainless steel

Figure 5.17. FE derived curves for interaction factors *k* by Zhao, 2015. Class 2

5.6 Interaction of axial compression and bending moment by Arrayago et al., 2015

In chapter 2.5.3. it is explained the designed formulae to use the interaction factor *k* for Arrayago et al. (2015). So, the calculation of the interaction Equation (2.28) is worked out and then the results are compared.

- Compact section Class 1

The Figure 5.18 represents how the Equation (45) works with different materials (Ferritic, Duplex and Austenitic) with a varying slenderness in class 1 (SHS 60x60x3).

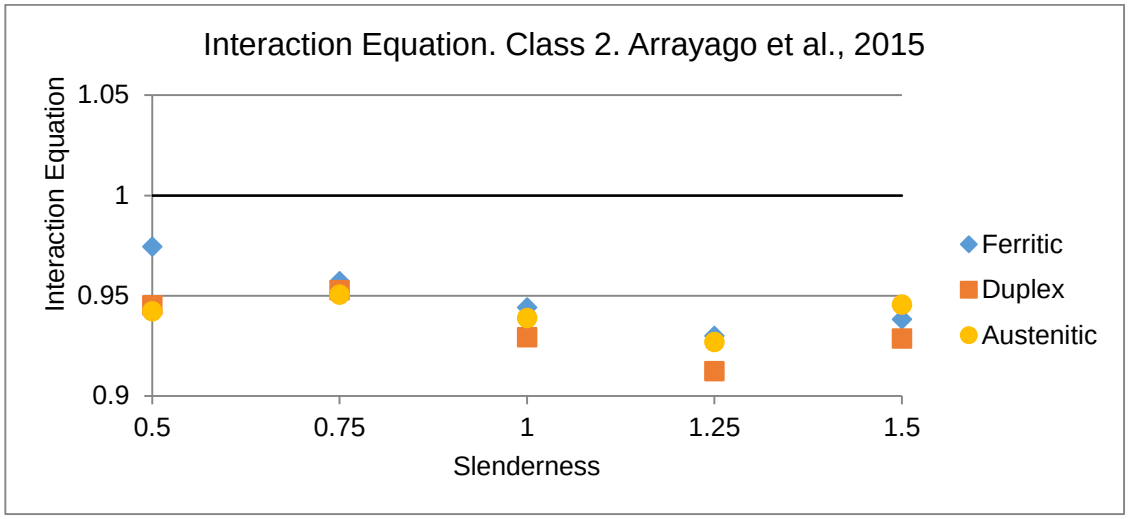

Figure 5.18. Interaction equation by Arrayago et al., 2015. Class 1

In Table 5.8 it is represented the mean average and standard deviation for this three materials.

	FERRITIC	DUPLEX	AUSTENITIC
Mean Average	0.9488	0.9338	0.9409
Standard Deviation	0.0174	0.0157	0.0089
Coefficient of Variation (%)	1.83	1.68	0.95

Table 5.8. Mean average and standard deviation by Arrayago et al., 2015. Class 1

As observed in the previous table the interaction factor *k* of Arrayago et al. have better results in austenitic stainless steel than in ferritic and duplex stainless steel. The coefficient of variation shows that the variation in austenitic stainless steel is minimum. So, as it is said before, this approach works really well for this kind of material.

It is possible too to make a comparison of the three materials with the interaction factor *k* and the slenderness, in order to see if the Equation (2.31) is accurate enough.

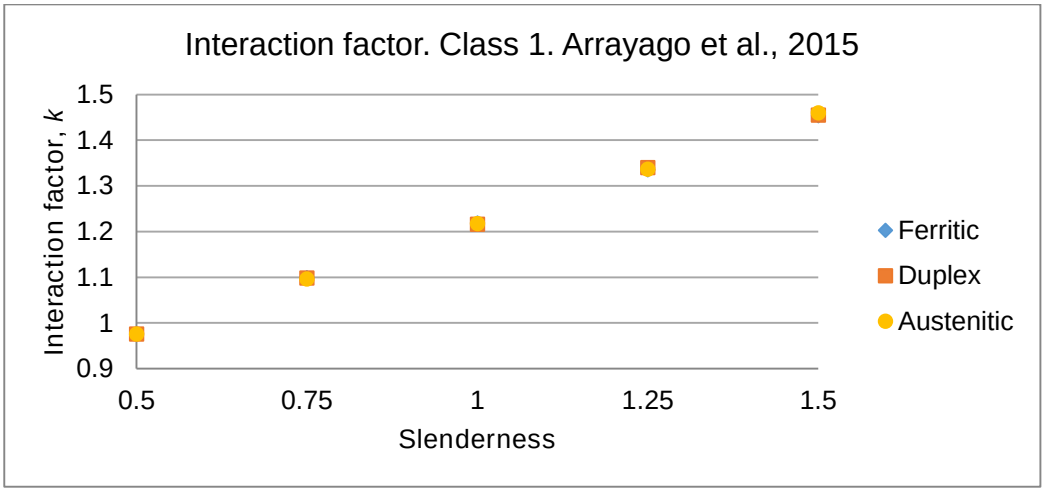

Figure 5.19. Interaction factor and slenderness. Arrayago et al., 2015. Class 1

The interaction factor, *k*, does not vary when the material is changed. As it happened with EN 1993-1-4, this non variation is really positive because it means that the interaction factor *k* will be always the same, no matter the material used, for each slenderness.

The following Figures 5.20a-5.20c are a comparison between the interaction factor *k* and the slenderness, but changing the ratio of applied axial force to column buckling strength, n_b. This ratio is expressed in Equation (5.5). As it is possible to observe, the interaction factor will increase for the same slenderness at the same time that the ratio of applied axial force increases too.

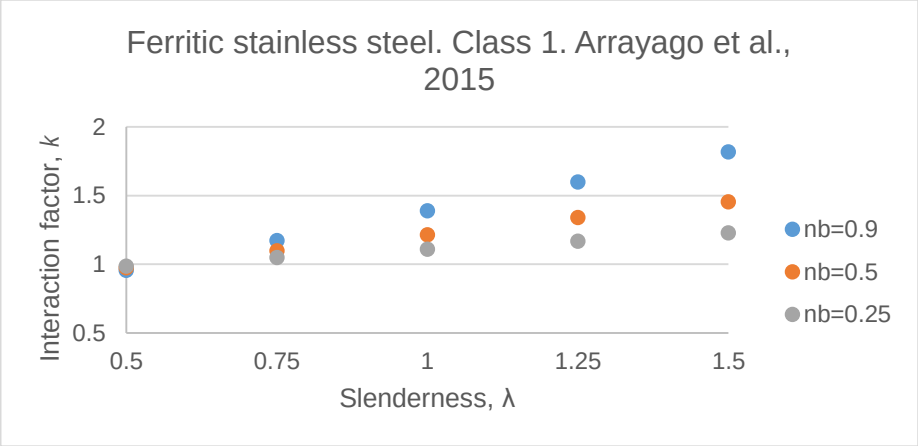

(a) Ferritic stainless steel

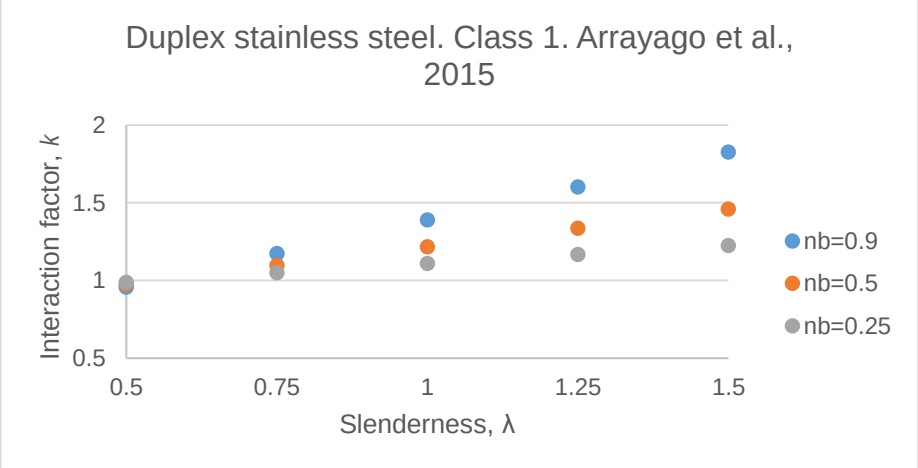

(b) Duplex stainless steel

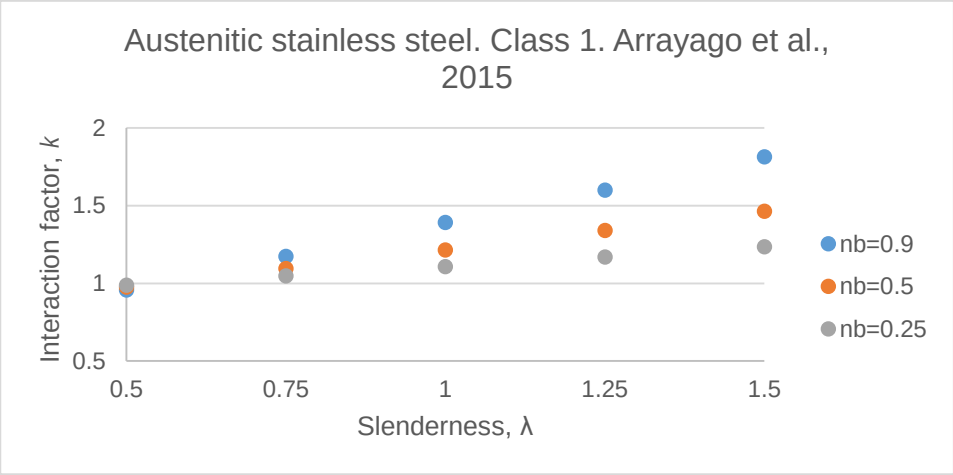

(c) Austenitic stainless steel

Figure 5.20. FE derived curves for interaction factors *k* by Arrayago et al., 2015. Class 1

- Compact section Class 2

The Figure 5.21 represents how the Equation (45) works with different materials (Ferritic, Duplex and Austenitic) with a varying slenderness in class 2 (SHS 100x100x3).

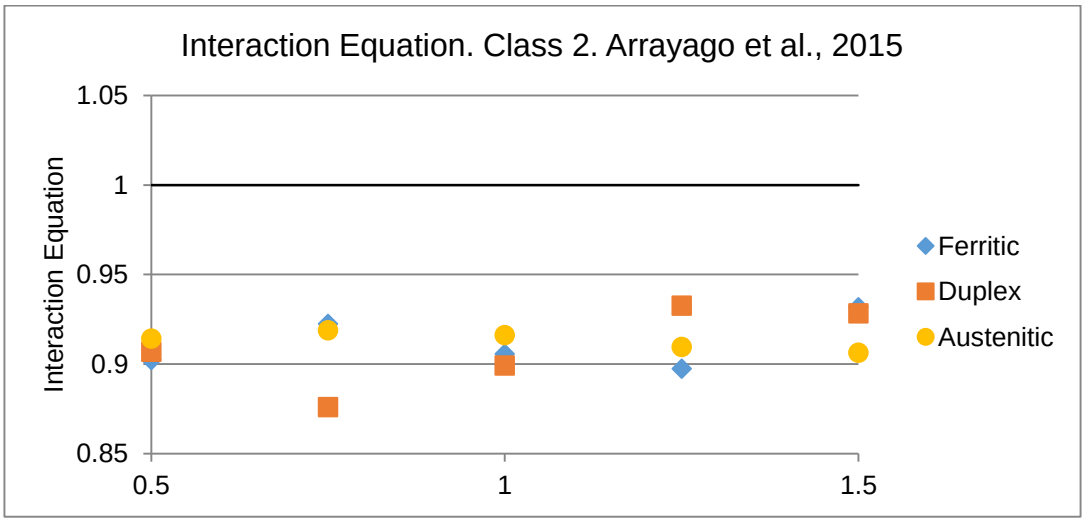

Figure 5.21. Interaction formula by Arrayago et al., 2015. Class 2

In Table 5.9 it is represented the mean average and standard deviation for this three materials.

	FERRITIC	DUPLEX	AUSTENITIC
Mean Average	0.9118	0.9085	0.91294
Standard Deviation	0.0146	0.023	0.005
Coefficient of Variation (%)	1.60	2.53	0.55

Table 5.9. Mean average and standard deviation by Arrayago et al., 2015. Class 2

As observed in the table, the interaction factor *k* in Class 2 has the best result, as it happened in Class 1, in austenitic stainless steel. Hence, it is likely to affirm that austenitic stainless steel is the best material and the one that fits best when Arrayago et al. formulae is used.

A comparison of the three materials is performed with the interaction factor *k* and the slenderness, in order to see if the Equation (2.31) is accurate enough.

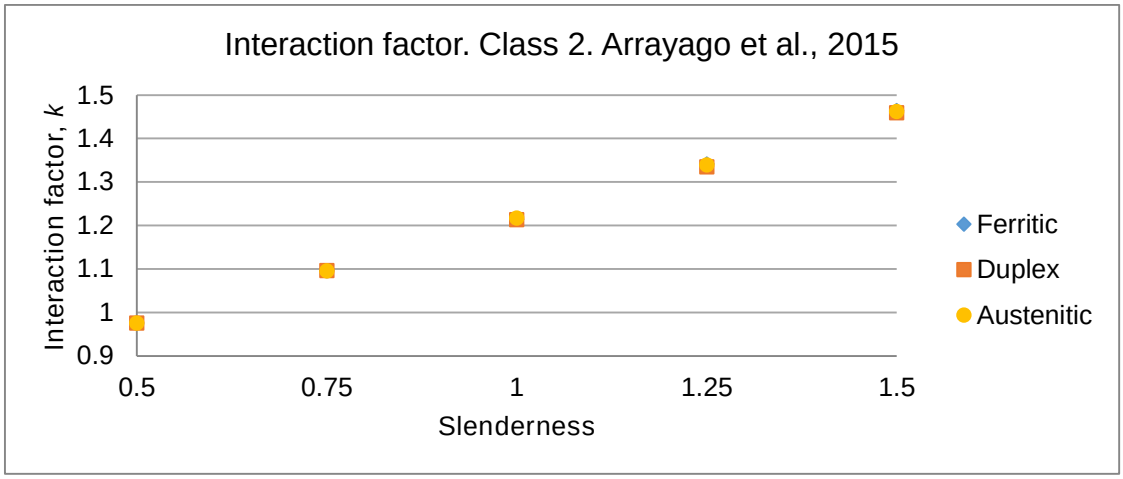

Figure 5.22. Interaction factor and slenderness. Arrayago et al., 2015. Class 2

The interaction factor, *k*, does not vary when the different stainless steel is used. As it happened with EN 1993-1-4, this non variation is really good for the analyse because it means that the interaction factor *k* will be always the same, no matter which material is used, for each slenderness.

The following Figures 5.23a-5.23c are a comparison between the interaction factor *k* and the slenderness, but changing the ratio of applied axial force to column buckling strength, n_b. This ratio is expressed in Equation (5.5). As we will observe, the interaction factor will increase for the same slenderness at the same time that the ratio of applied axial force increases too.

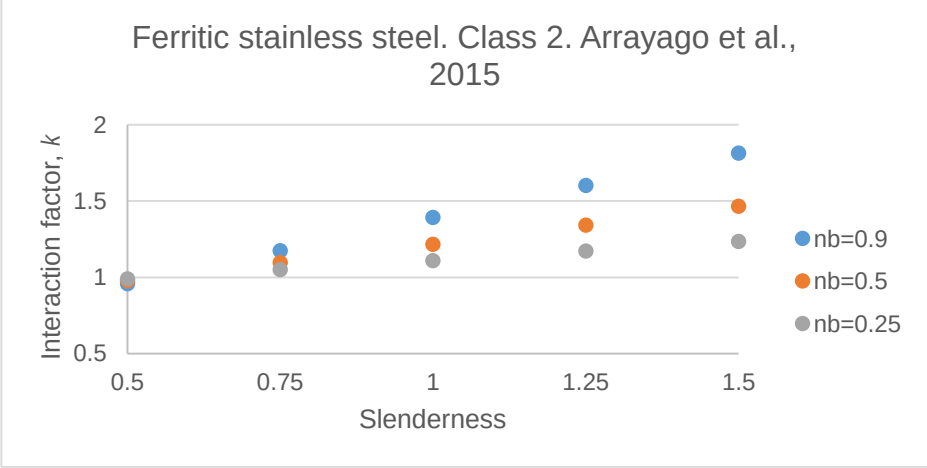

(a) Ferritic stainless steel

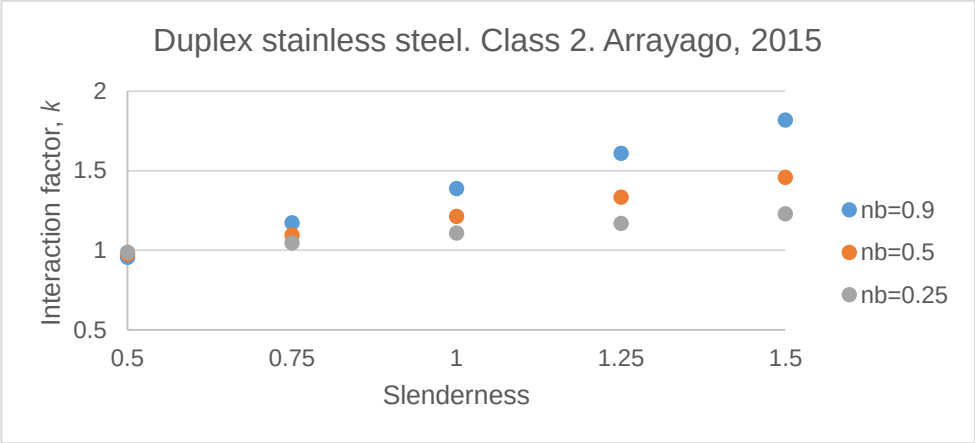

(b) Duplex stainless steel

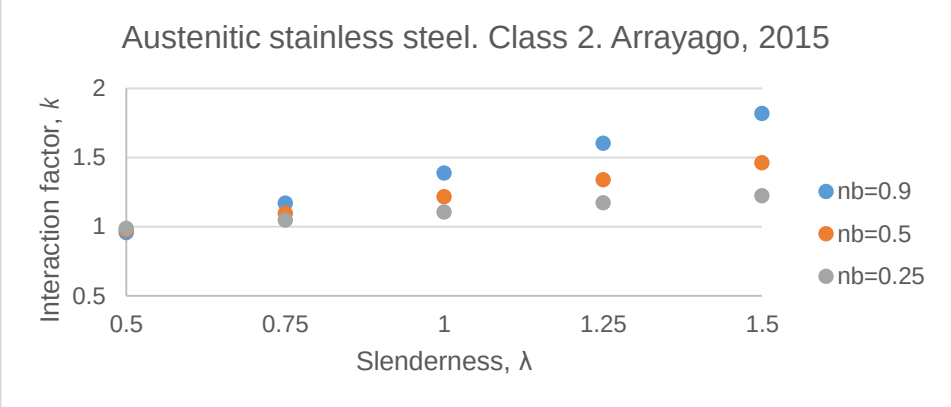

(c) Austenitic stainless steel

Figure 5.23. FE derived curves for interaction factors *k* by Arrayago et al., 2015. Class 2

5.7 Interaction of axial compression and bending moment by Simplified Method

In chapter 2.5.4. it is explained the designed formulae to use the interaction factor *k* for the Simplified Method. So, the calculation of the interaction Equation (2.28) is worked out and then the results are compared.

- Compact section Class 1

The Figure 5.24 represents how the Equation (2.34) works with different materials (Ferritic, Duplex and Austenitic) with a varying slenderness in class 1 (SHS 60x60x3).

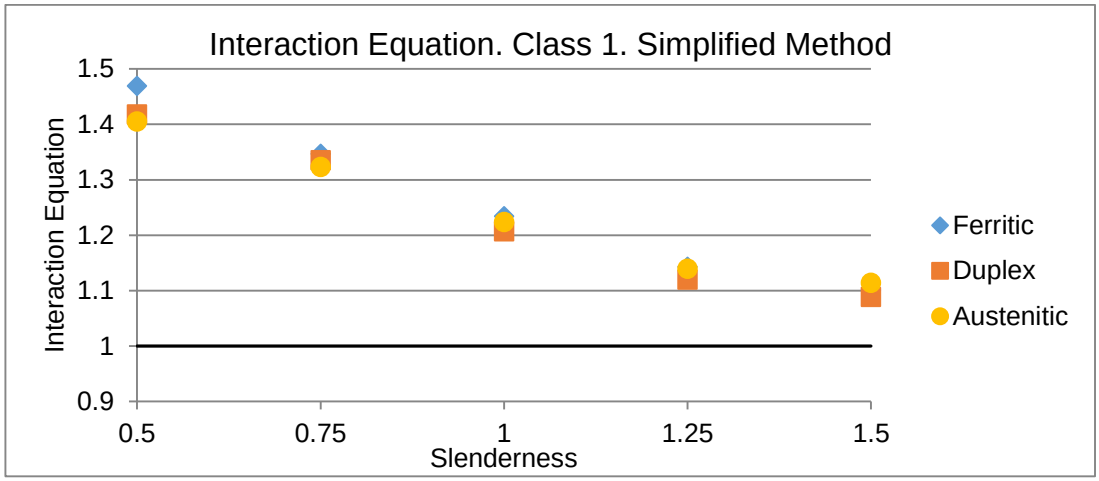

Figure 5.24. Interaction formula by Simplified Method. Class 1

In Table 5.10 it is represented the mean average and standard deviation for this three materials.

	FERRITIC	DUPLEX	AUSTENITIC
Mean Average	1.2591	1.2340	1.2414
Standard Deviation	0.1507	0.1404	0.1229
Coefficient of Variation (%)	11.97	11.38	9.90

Table 5.10. Mean average and standard deviation by Simplified Method. Class 1

As observed in the previous table the best result for interaction factor *k* of the Simplified Method is in austenitic stainless steel and not for ferritic and duplex stainless steel. Another point to take into account is that the results which are near to 1.0 are those that have the slenderness bigger, so when the length of the column is higher. For the three different materials the Interaction Equation results are similar.

It is possible too to make a comparison of the three materials with the interaction factor *k* and the slenderness, in order to see if the Equation (2.35) is accurate enough.

Figure 5.25. Interaction factor and slenderness. Simplified Method

It is observed that the interaction factor, *k*, does not vary when we change the material. Along all the different slenderness, this factor is always near to 2.0.

The following Figures 5.26a-5.26c are a comparison between the interaction factor *k* and the slenderness, but changing the ratio of applied axial force to column buckling strength, n_b. This ratio is expressed in Equation (5.5). As it will be observed in this case, the interaction factor k remains constant along all its slenderness for a ratio of 0.25 (approximately 1.3), for a ratio of 0.5 (approximately 2.0). and finally, for a ratio of 0.9 (approximately 9.5). This happens for all three materials, ferritic, duplex and austenitic stainless steel.

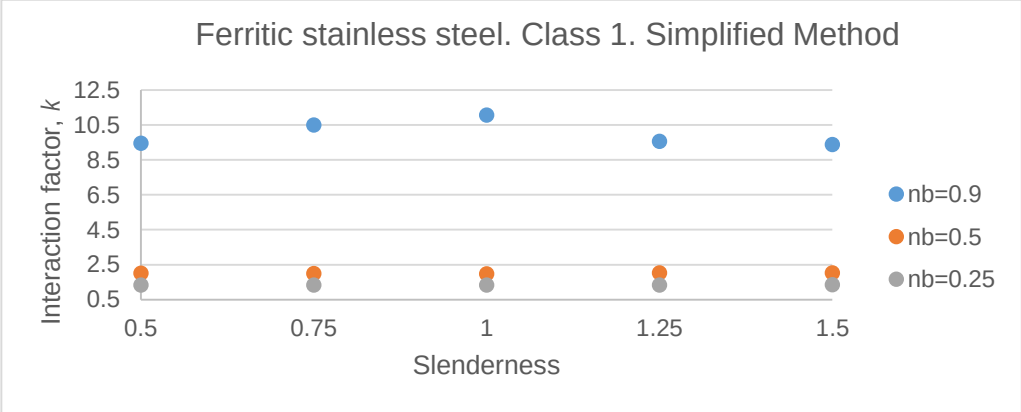

(a) Ferritic stainless steel

(b) Duplex stainless steel

(c) Austenitic stainless steel

Figure 5.26. FE derived curves for interaction factors *k* by Simplified Method. Class 1

- Compact section Class 2

The Figure 5.27 represents how the Equation (2.34) works with different materials (Ferritic, Duplex and Austenitic stainless steel) with a varying slenderness in class 2 (SHS 100x100x3).

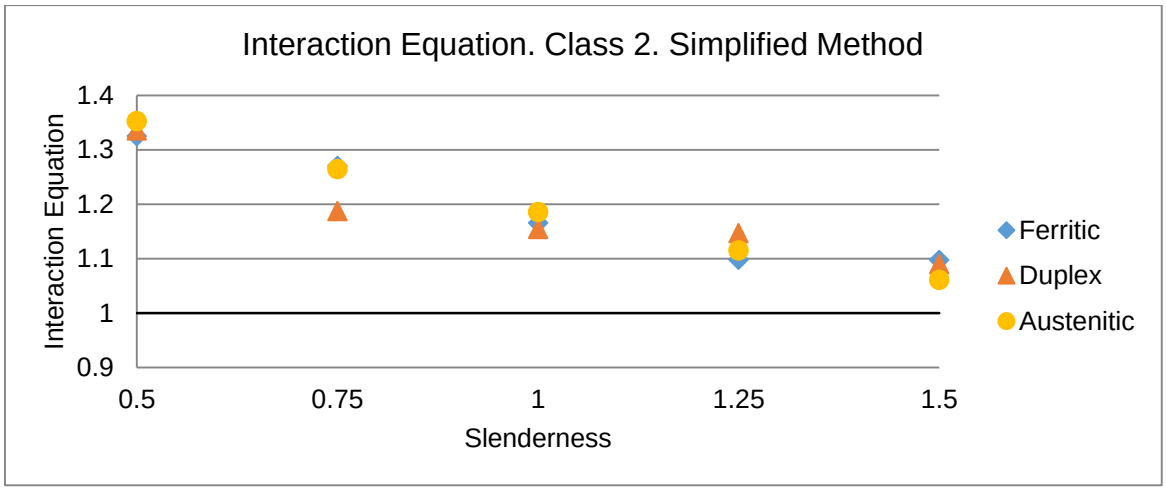

Figure 5.27. Interaction formula by Simplified Method. Class 2

In Table 5.11 it is represented the mean average and standard deviation for this three materials.

	FERRITIC	DUPLEX	AUSTENITIC
Mean Average	1.1915	1.1829	1.1959
Standard Deviation	0.1029	0.0925	0.1164
Coefficient of Variation (%)	8.64	7.82	9.73

Table 5.11. Mean average and standard deviation by Simplified Method. Class 2

As it is noticed in the previous table the best result interaction factor *k* in Class 2 is in the duplex stainless steel, followed by ferritic ant then austenitic stainless steel.

It is suitable too to make a comparison of the three materials with the interaction factor *k* and the slenderness, in order to see if the Equation (2.35) is accurate enough.

Figure 5.28. Interaction factor and slenderness. Simplified Method. Class 2

We observe that the interaction factor, *k*, does not vary when we change the material. Along all the different slenderness, this factor is near to 2.0. That means that no matter how high is the slenderness of the element that the interaction factor will be always around to 2.0.

The following Figures 5.29a-5.29c are a comparison between the interaction factor *k* and the slenderness, but changing the ratio of applied axial force to column buckling strength, n_b. This ratio is expressed in Equation (5.5). As it will be observed in this case, the interaction factor k remains constant along all its slenderness for a ratio of 0.25 (approximately 1.3), for a ratio of 0.5 (approximately 2.0). and finally, for a ratio of 0.9 (approximately 9.5). This happens for all three materials, ferritic, duplex and austenitic stainless steel.

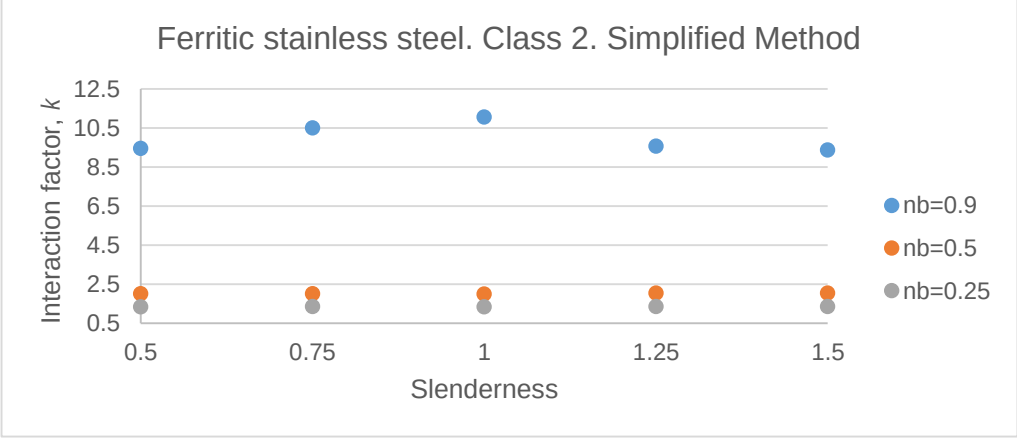

(a) Ferritic stainless steel

(b) Duplex stainless steel

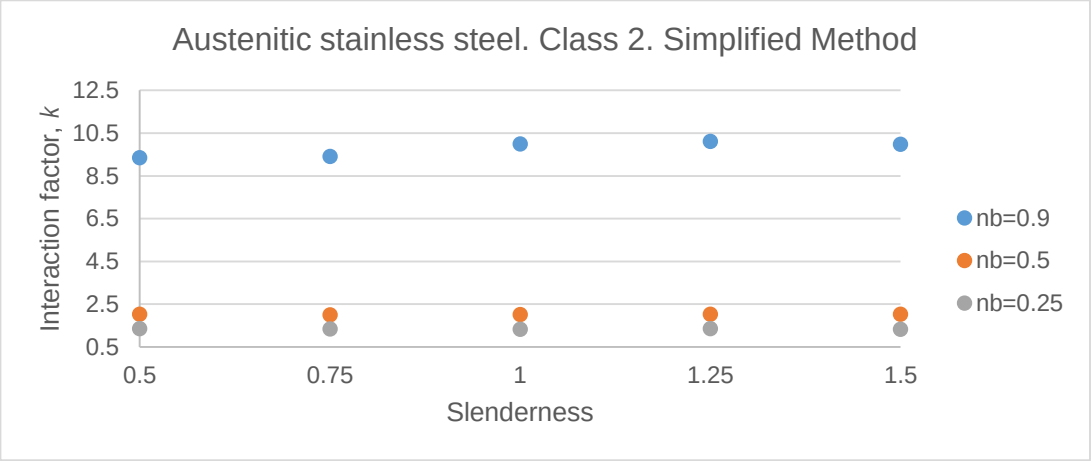

(c) Austenitic stainless steel

Figure 5.29. FE derived curves for interaction factors *k* by Simplified Method. Class 2

5.8 Concluding remarks

In the following Table 5.12a-5.12d there is a summary of all the different cases and materials where it is possible to find the standard deviation, the mean average and the coefficient of variation for each method used in this chapter. Therefore, there ratio of Mean Average can be compared and observed for distribution data with the ratio of axial force ($N_{Ed}/N_{b,Rd}$).

Formulation	Cross-section	Material	n_b	Mean Average, $\overline{x}$	Standard Deviation, σ_x	Coefficient of variation, V_x (%)
EN 1993 1-4	Class 1 60x60x3	Ferritic	0.9	1.0061	0.0119	1.18
			0.5	1.0638	0.0316	2.97
			0.25	1.0677	0.0392	3.67
		Duplex	0.9	0.9828	0.0055	0.56
			0.5	1.0442	0.0276	2.64
			0.25	1.0580	0.0320	3.03
		Austenitic	0.9	0.9827	0.0112	1.14
			0.5	1.0542	0.0361	3.42
			0.25	1.0349	0.0326	3.15
	Class 2 100x100x3	Ferritic	0.9	1.0043	0.0147	1.46
			0.5	1.0175	0.044	4.32
			0.25	1.0168	0.0261	2.57
		Duplex	0.9	0.9945	0.0089	0.89
			0.5	1.0151	0.0636	6.27
			0.25	1.0336	0.0612	5.92
		Austenitic	0.9	0.9942	0.0110	1.11
			0.5	1.0183	0.0299	2.94
			0.25	1.0125	0.0411	4.06

Table 5.12a. Summary results using EN 1993-1-4, 2006.

Formulation	Cross-section	Material	n_b	Mean Average, $\overline{x}$	Standard Deviation, σ_x	Coefficient of variation, V_x (%)
Zhao, 2015	Class 1 60x60x3	Ferritic	0.9	0.9917	0.0118	1.19
			0.5	0.9985	0.0065	0.65
			0.25	0.9874	0.0143	1.45
		Duplex	0.9	0.9773	0.0093	0.95
			0.5	1.0089	0.0118	1.17
			0.25	1.0032	0.0133	1.33
		Austenitic	0.9	1.0977	0.0315	2.87
			0.5	0.9772	0.0102	1.04
			0.25	0.9813	0.0126	1.28
	Class 2 100x100x3	Ferritic	0.9	0.9889	0.0084	0.85
			0.5	0.9578	0.0263	2.76
			0.25	0.9423	0.0236	2.50
		Duplex	0.9	0.9880	0.0056	0.57
			0.5	0.9804	0.0418	4.26
			0.25	0.9785	0.0389	3.97
		Austenitic	0.9	0.9874	0.0066	0.67
			0.5	1.0597	0.0334	3.15
			0.25	0.9604	0.0068	0.70

Table 5.12b. Summary results using Zhao, 2015.

Formulation	Cross-section	Material	n_b	Mean Average, $\overline{x}$	Standard Deviation, σ_x	Coefficient of variation, V_x (%)
Arrayago et al., 2015	Class 1 60x60x3	Ferritic	0.9	0.9786	0.0104	1.06
			0.5	0.9489	0.0174	1.83
			0.25	0.9440	0.0170	1.80
		Duplex	0.9	0.9609	0.0090	0.94
			0.5	0.9338	0.0157	1.68
			0.25	0.9366	0.0216	2.30
		Austenitic	0.9	0.9609	0.0059	0.61
			0.5	0.9409	0.0089	0.95
			0.25	0.9168	0.0107	1.17
	Class 2 100x100x3	Ferritic	0.9	0.9757	0.0078	0.79
			0.5	0.9118	0.0146	1.60
			0.25	0.9014	0.0196	2.17
		Duplex	0.9	0.9696	0.0068	0.70
			0.5	0.9085	0.0230	2.53
			0.25	0.9142	0.0293	3.20
		Austenitic	0.9	0.9684	0.0076	0.78
			0.5	0.9129	0.0050	0.55
			0.25	0.8978	0.0212	2.36

Table 5.12c. Summary results using Arrayago et al., 2015.

Formulation	Cross-section	Material	n_b	Mean Average, $\overline{x}$	Standard Deviation, σ_x	Coefficient of variation, V_x (%)
Simplified Method	Class 1 60x60x3	Ferritic	0.9	1.501	0.2009	13.38
			0.5	1.2591	0.1507	11.97
			0.25	1.0935	0.2009	18.37
		Duplex	0.9	1.3677	0.1553	11.35
			0.5	1.2340	0.1404	11.38
			0.25	1.0857	0.0967	8.91
		Austenitic	0.9	1.3585	0.1331	9.80
			0.5	1.2414	0.1229	9.90
			0.25	1.0586	0.0799	7.55
	Class 2 100x100x3	Ferritic	0.9	1.4776	0.1954	13.22
			0.5	1.1915	0.1029	8.64
			0.25	1.0413	0.0770	7.39
		Duplex	0.9	1.4334	0.1915	13.36
			0.5	1.1829	0.0925	7.82
			0.25	1.0521	0.0672	6.39
		Austenitic	0.9	1.4299	0.1935	13.53
			0.5	1.1959	0.1164	9.73
			0.25	1.0379	0.0944	9.09

Table 5.12d. Summary results using Simplified Method

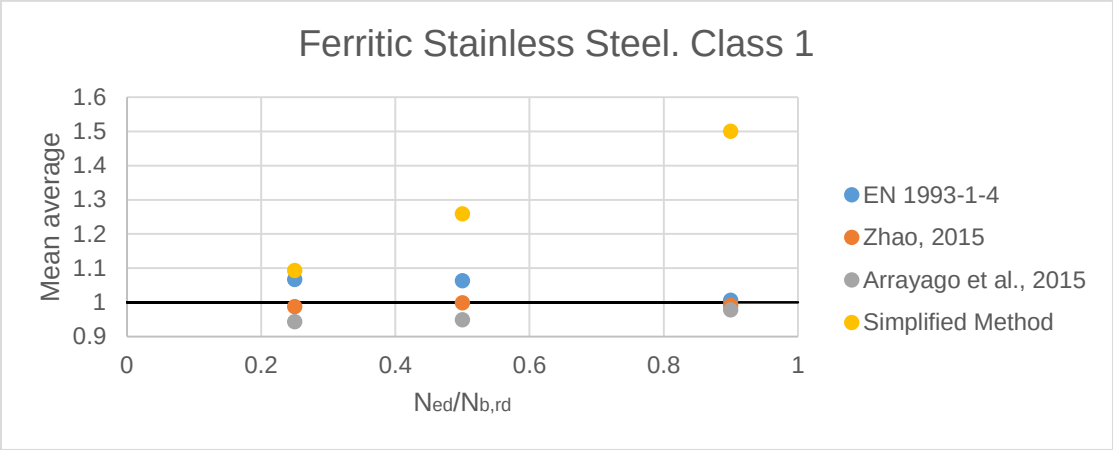

(a) Ferritic Stainless Steel. Class 1

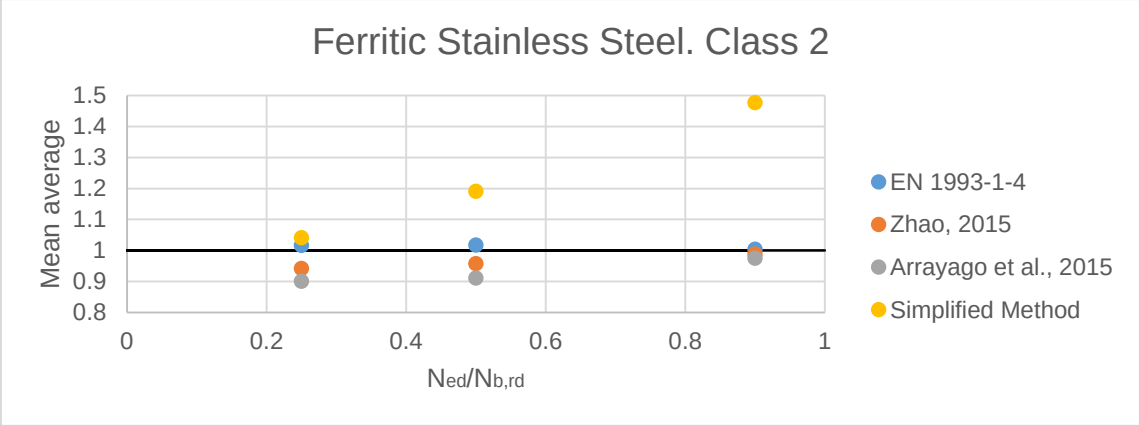

(b) Ferritic Stainless Steel. Class 2

Figure 5.30. Distribution data result for ratio Mean Average with $N_{Ed}/N_{b,Rd}$ Ferritic Stainless Steel

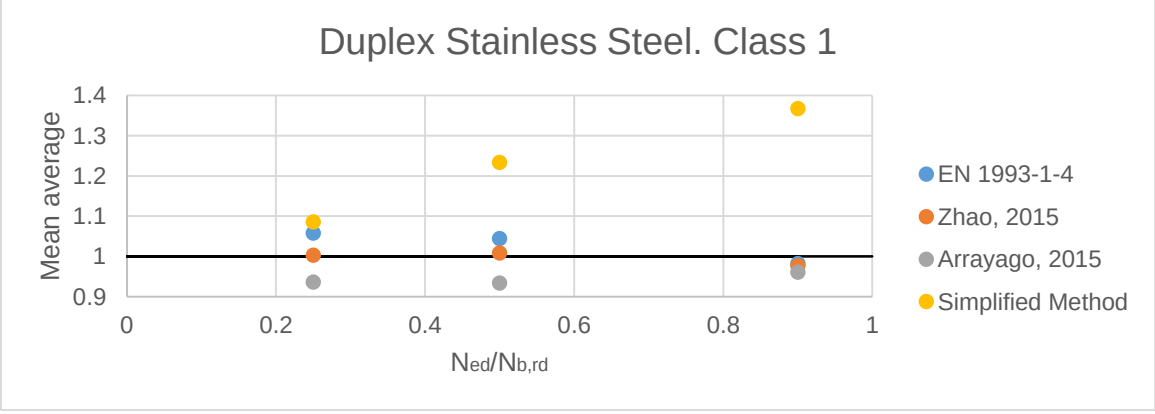

(a) Duplex Stainless Steel. Class 1

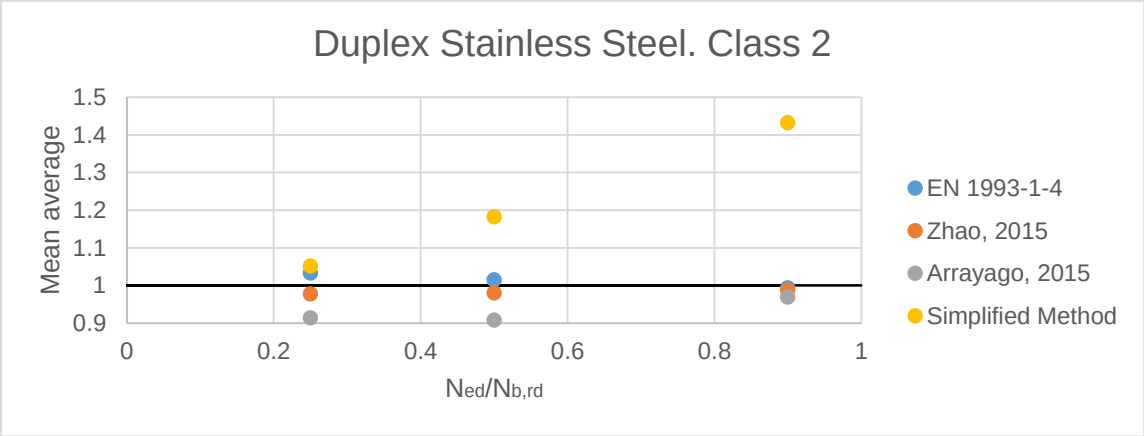

(b) Duplex Stainless Steel. Class 2

Figure 5.31. Distribution data result for ratio Mean Average with $N_{Ed}/N_{b,Rd}$ Duplex Stainless Steel

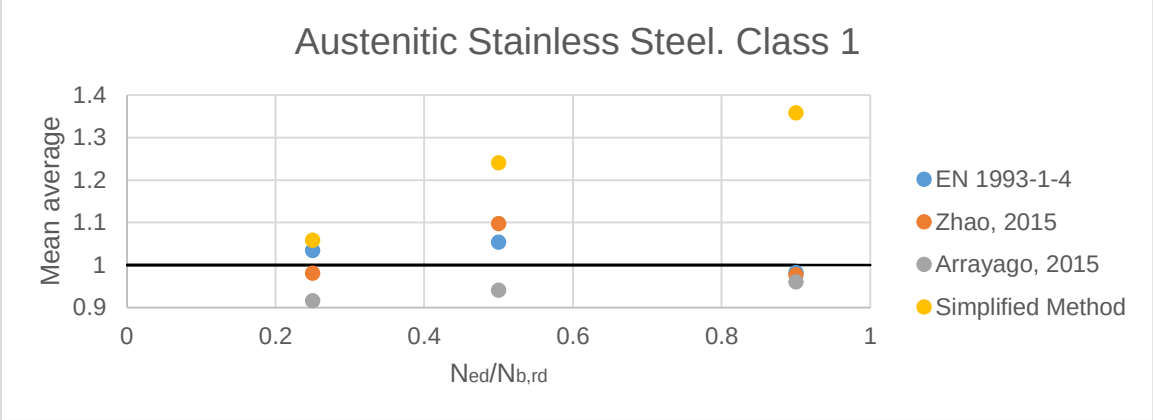

(a) Austenitic Stainless Steel. Class 1

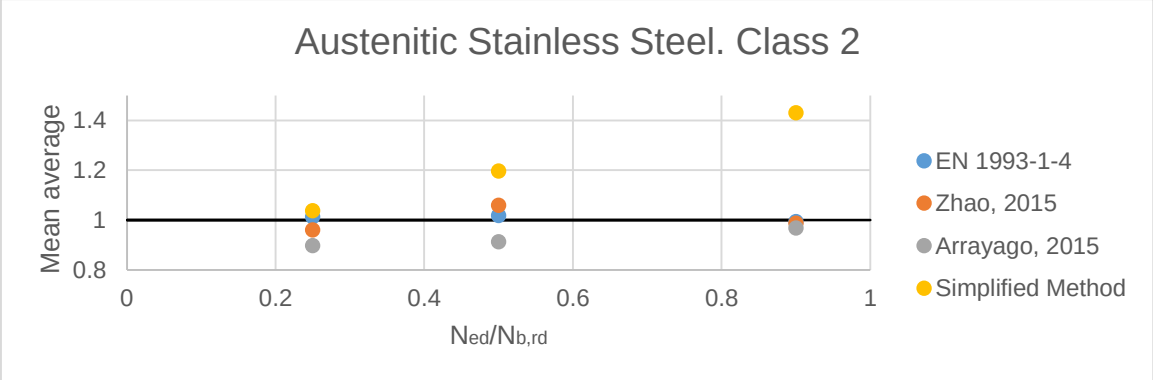

(b) Austenitic Stainless Steel. Class 2

(c) *Figure 5.32*. Distribution data result for ratio Mean Average with $N_{Ed}/N_{b,Rd}$ Austenitic Stainless Steel

First of all, it is important to remark that the designed formulae of the Simplified Method are used for non-stainless steel. This is why the results are a little bit different from the others approaches, but the aim of this study for Simplified Method was to observe how this interaction equation for non-stainless steel works for different stainless steel.

As it is possible to observe in tables and then in figures, the best approach for this material is when Zhao (2015) formulae it is used. The mean average gets closer to the ideal value 1.0 and the standard deviation and coefficient of variation are smaller than the other approaches. Then, with Arrayago et al. (2015) formulae, these statistics values are a little bit below the ideal value 1.0 for both Class 1 and Class 2. This difference could exist because when Arrayago et al. (2015) performed the research, they supposed the imperfection amplitudes due to they do not have them. In order to adopt the traditional L/1500, it was applied expressions from EN 1993-1-1 which gave some imperfections higher than L/1500, so the Equation was calibrated. This fact gives then, in some cases, unsafe results (values which are below 1.0). The contrary happens when EN 1993-1-4 is used, the results are just above the ideal value 1.0, this means that the formulae are conservatives and the results are safe. For the Simplified Method, as it is commented in the previously paragraph, for a low ratio of $N_{Ed}/N_{b,Rd}$ the value is near to 1.0 but when this ratio is increased, the mean average, standard and coefficient of variation increases.

6. PARAMETRIC STUDIES

6.1. Introduction

Once the finite elements model is validated, a parametric study was conducted to generate more beam-column data over a wide range of cross section sizes and slendernesses. This variation of slenderness is global but it is taken the compact sections Class 1 and Class 2. In this parametric study, the flat and corner section were considered to be equals for all different cross-sections and the material used is ferritic stainless steel, with a Young's modulus coefficient of 200 GPa and a Poisson's ratio of 0.3. The initial local amplitudes were predicted using the modified Dawson and Walker model (D&W), explained in chapter 5.2, while the global imperfection amplitudes were taken as 1/1000 of the effective member length. The modelled specimens covered the sections Class 1 and Class 2 (compact sections). The ratio c/t ranges from 8.0 to 30.0, where c is the flat element width and t the thickness width. The buckling lengths of the beam-column FE models were varied to cover a wide spectrum of member slendernesses $\bar{\lambda}$ between 0.34 and 2.75. It is introduced a bending moment which value is 1000 kNm, constant in all the length member, so ψ=1.0. The length member varies from 450 mm to 3500 mm. In total, 480 parametric results were generated for specimens with Class 1 or 2 cross-sections.

The specimens are all of them square hollow sections (SHS) with a variation in the flat element width *c* and in the the thickness width *t*. These variations are:

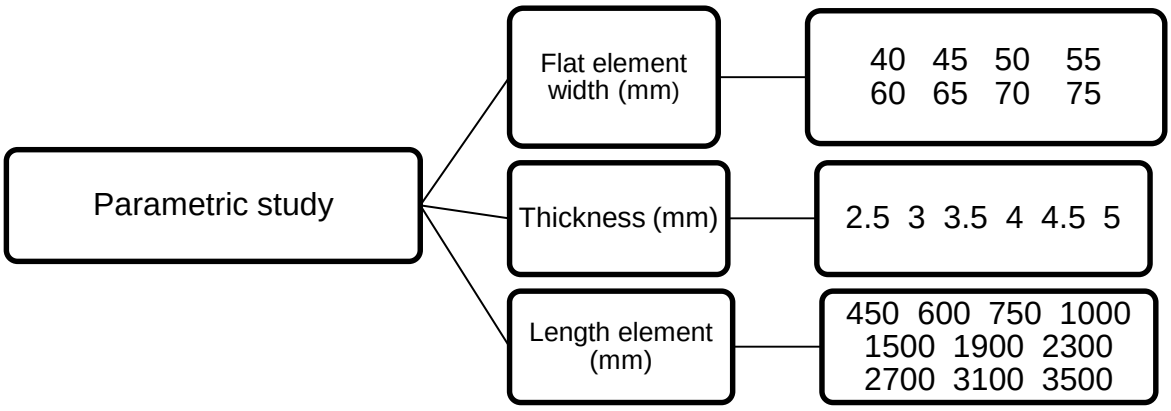

Figure 6.1. Different values for the parametric study

The main objective of this parametric study is to create a buckling curve and then compare it to the buckling curve for flexural buckling using the designed formulae for EN 1993-1-4 explained in chapter 2.5.1 and see if the wide range of points generated with the parametric study are above the curve of the European norm, so we would affirm that our parametric study is safe. The calculus resistance for buckling in an element subjected to axial load is the following Equation (6.1):

$$N_{b,rd} = \frac{\chi \cdot A \cdot \sigma_{0.2}}{\gamma_{M1}} \tag{6.1}$$

where γ_{M1} is equal to 1.0 for the Abaqus results and *A* is the cross-section area.

If the reduction coefficient is isolated, we have the following Equation (6.2)

$$\chi = \frac{N_{b,rd}}{A \cdot \sigma_{0.2}} \tag{6.2}$$

where $N_{b,rd}$ is the calculus resistance for buckling calculated by FE Abaqus.

This parametric study is done by a mesh combination, which means that it is analysed all different possibilities of flat elements and thickness. The other type of combination possible to do a is tuple mesh, but it was thought that with this kind of mesh would give much lower points to analyse and the main goal was to obtain a wide range of cross-section sizes, so this option was discarded it.

6.2. Results

The following Figure 6.1 shows, on the one hand, the European curve for buckling calculated following the equations from chapter 2.4.1. and, on the other hand, the buckling curve obtained by the parametric study done. This curve has the imperfection ratio α equals to 0.34 because the torsional and torsional-buckling for all members is taking into account. This means that it is used the buckling curve *b* in order to compare with the parametric study. Then, it is also compared with the different curves a, c and d for different imperfection ratio 0.21, 0.49 and 0.76, respectively.

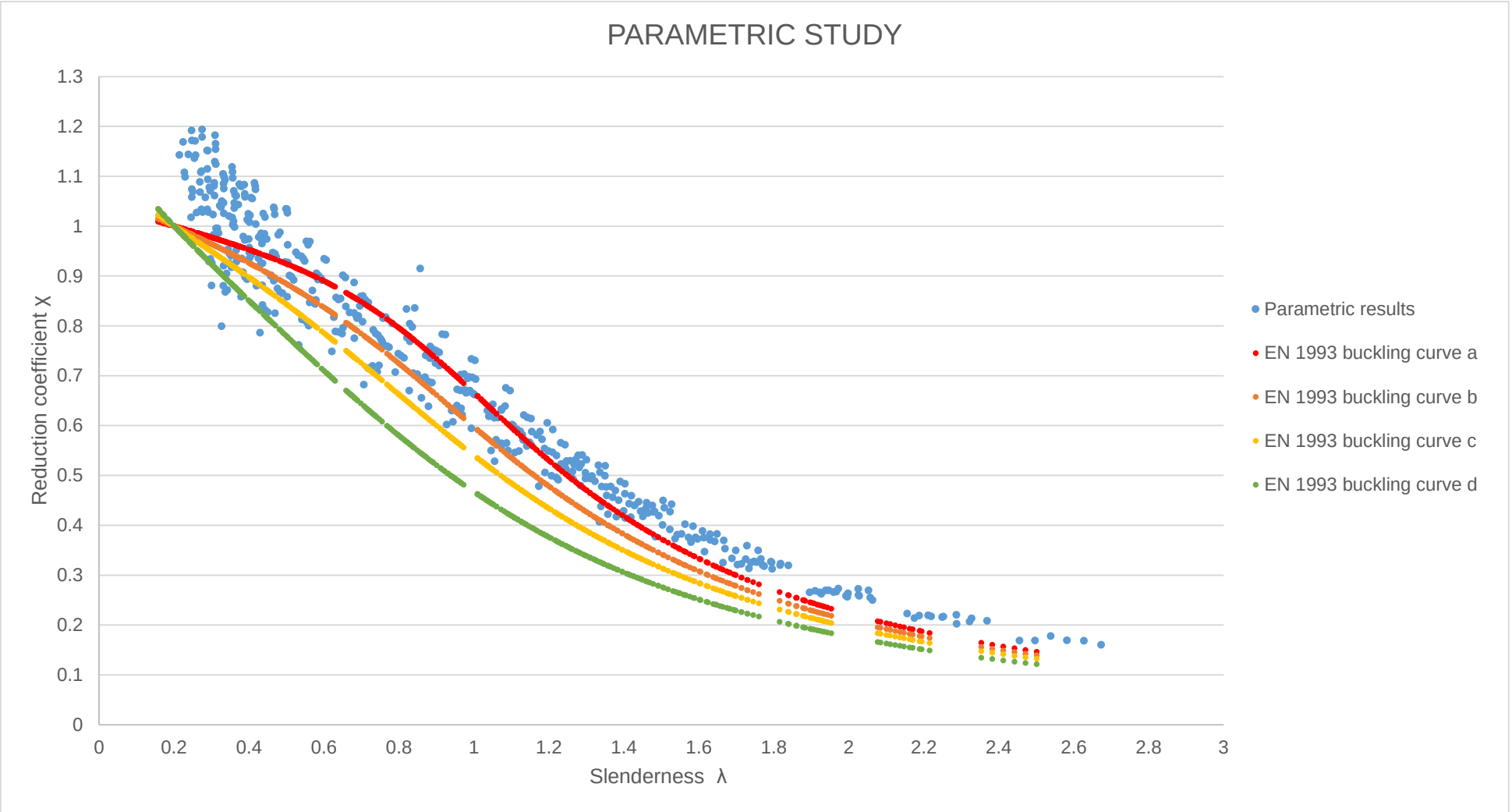

Figure 6.1. Curves for flexural buckling

6.3 Concluding remarks

The structural performance of ferritic stainless steel SHS beam-columns under axial compressive load and uniform bending moment has been investigated through numerical studies. The 480 finite elements results were employed to evaluate the accuracy of the European code EN 1993-1-4. It is proved with this parametric study that the European code leads to one of the most conservative strength predictions.

First of all, the EN 1993-1-4 curve buckling *b* is analysed. As is it possible to see in the previous chapter, for lowest slendernesses, the reduction coefficient is much higher than the European curve for buckling, so that means that it is safe, but for higher slendernesses the parametric results are closer to the actual curve for buckling, so for this values of slendernesses the parametric results are not as safe as for lower values of slendernesses. The parametric results that are below the European curve for buckling *b* are those which the cross-section has no sense. Due to the mesh that it has done in order to carry out this parametric study, it exists cross-section that in real life have no utility, for example the lowest value of flat element width (40 mm) and the highest value of thickness (5 mm). Those points exist in the parametric study but they have to be discarded.

Secondly, taking into account the comparison of the parametric results and the curve buckling *a*, there are between a range of slenderness from 0.4 to 0.8 some points which are below this curve. This buckling curve takes the lowest imperfection ratio of all the four curves, so the curve generated is the one which adjust best to the parametric results. For higher values of slenderness, the results points are all above the curve buckling *a*, and the same happens for slowest slendernesses.

Finally, for the other two curve buckling c and d all the parametric results are above them. This two curves have a high value for the imperfection ratio so the curves generated are more conservative than in the case *a* and *b*.

Also, there are points of the parametric study whose reduction factor are higher than 1.0. This is due to the length element low value of the beam-column.

7. CONCLUSIONS

This thesis has provided the summary of stainless steel nonlinearity behaviour with the wide range variety of wide range of mechanical properties for each stainless steel material (austenitic, duplex and ferritic) of various cross-section types observed (Class 1 and Class 2). Hence, the comparison observation and parametric study took the material properties values based on particular experimental test values which associates to particular investigations.

Finite element models were initially developed and validated against the experimental results and the used to conduct a parametric study to generate further structural performance data over a range of cross-section slendernesses. Analysis of the experimental and numerical results allowed the accuracy o0f the European code EN 1993-1-3.

Considering the higher comparative material cost of stainless steel relative to carbon steel and its excellent aesthetic and mechanical properties, it is important to remark the importance to verify and then improve the designed expressions contained in EN 1993-1-4 in order to obtain a more efficient use of this material in structural application and in constructions.

7.1 Specific conclusions

In this section the main specific conclusions obtained are explained just to prove that the proposed objectives have been achieved.

- A model validation has been made in order to carry out this thesis, so with this purpose, the results from the documents of *Arrayago, Real, Mirambell* [Arrayago et al.,2016] are used in order to verify the model. The comparison results show that there are no significant differences and the standard deviation is under 10, specifically 4.23. It is important to take into account that for this validation it has been taken the effective length (including the distance between knife-edges). The numerical model exploited has been demonstrated to be an adequate tool to reproduce the behaviour of plate elements loaded in compression. After that, with Rodríguez, who is doing the thesis in CTU in Prague, a procedure validation about the model has been done. A Class 1 (SHS 60x60x3) and a Class 4 (SHS 80x80x2) has been analysed with different materials (ferritic, duplex and austenitic stainless steel). The results obtained by Durán and Rodríguez are really similar, whether through Class 1 or Class 4 and for the different stainless steel materials. But for Arrayago et al. (2015), the results vary 0.2-0.3 in the mean average. These are not bad results but, just to remark, it has been obtained better outcomes with Eurocode and Zhao (2015) formulae than with Arrayago et al. (2015). This difference could exist because when Arrayago et al. (2015) performed the research, they supposed the imperfection amplitudes due to they do not have them. Instead of adopting the traditional L/1500, it was applied expressions from EN 1993-1-1 which gave some imperfections higher than L/1500, so the interaction factor *k* equation was calibrated.

- A validation of the strain hardening exponent *n* is done in this thesis. This validation is done using a cross-section Class 1 and another one for Class 2. It is wanted to observe how this change of parameter affected at the final results of the interaction formulas, using a n=14.0 (typical ferritic) and another n=7.0 (typical austenitic). The results confirm that all the standards deviations are lower when the strain hardening exponent equal to 14 is used. From the curve $\sigma_{nom} - \varepsilon_{true.pl}$ it was possible to affirm that with n=14.0, for a less strain the material will have a nominal stress higher. Hence, in this validation it has been studied how important is the strain hardening exponent in material equations.

- A study of the behaviour of different stainless steel (Ferritic, Austenitic and Duplex) beam-columns under combined bending and axial load is carried out. The members subjected to combined compression and bending moment can buckle in different ways, depending on the cross-section geometry and on the boundary conditions. This study of the behaviour is done for square hollow section (SHS) of Class 1 and Class 2 (compact sections). Numerical simulations were carried out on single span pin-ended stainless steel SHS beam-columns, accounting for initial geometric imperfections, with the member slenderness ranging between 0.5 and 1.5. The global imperfection was L/1000 and the local initial imperfection was taking into account using the Dawson and Walter formulation. The comparisons revealed that the proposals of Zhao (2015) and Arrayago (2015) provide more accurate and consistent beam column strength predictions than the current codified design approaches. In case of EN 1993-1-4 formulae, the mean average is above the ideal value 1.0 due to the European code use some conservative formulae. Finally, the formulae of the Simplified Method are used for non-stainless steel. This is why the results are a little bit different from the others approaches, but the aim of this study for Simplified Method was to observe how this interaction equation for non-stainless steel works for different stainless steel.

- A parametric study was conducted to generate more beam-columns data over a wide range of cross section sizes and slendernesses. The 480 finite elements results were employed to evaluate the accuracy of the European code EN 1993-1-4. It is proved with this parametric study that the European code leads to one of the most conservative strength predictions, for lowest slendernesses the reduction coefficient is much higher than the European curve for buckling, so that means that it is safe, but for higher slendernesses the parametric results are closer to the actual curve for buckling, so for this values of slendernesses the results are not as safe as for lower values of slendernesses.

7.2 Future research work

The main purpose of the master thesis has been to strengthen the knowledge of ferritic stainless steel structures behavior. Throughout the studies realized, the principal aim has been to analyze the response of ferritic stainless steel beam-columns subjected to combined loading and to compare the numerical results with the design formulae of EN 1993-1-4 literature and some others proposal researches (research performed at Imperial College of London by Zhao, 2015 and another research performed at UPC by Arrayago et al., 2015). Not every topic has been analyzed in this thesis so this has to encourage new future investigation.

- To study other SHS cross-sections in order to validate and prove the advanced proposals.
- In the parametric study, to consider a wide range of slenderness with more finite elements results.
- To realize some experimental tests in order to support the numerical results already obtained.

REFERENCES

Euro Inox and The Steel Construction Institute, Design manual for structural stainless steel, third edition *Euro Inox*, 2006.

Instrucción de Acero Estructural EAE, con comentarios de los miembros de la Comisión Permanente de Estructuras de Acero, tercera edición, Noviembre 2012.

SIMULIA. ABAQUS Standard user's manual and ABAQUS CAE manual, keywords edition, version 6.7, 2012.

S. Afshan and L. Gardner. Experimental study of cold-formed ferritic stainless steel hollow sections. *Journal of Structural Engineering*, 139 (special issue): 717-728, 2013.

I. Arrayago, F. Picci, E. Mirambell and E. Real. Interaction of bending and axial load for ferritic stainless steel RHS columns. *Thin-walled Structures*, 91: 96-107, 2015.

I. Arrayago, E. Real and L. Gardner. Description of stress-strain curves for stainless steel alloys. *Materials and Design,*87: 540-552*,* 2015.

I. Arrayago, E. Real and E. Mirambell. Experimental study on ferritic stainless steel RHS and SHS beam-columns. *Thin-walled Structures*. 100: 93-104, 2016.

I. Arrayago, E. Real and E. Mirambell, et al., Constitutive equations for stainless steels: experimental tests and new proposals. Proceedings of the Fifth International Conference on Structural Engineering, Mechanics and Computation. Cape Town, South Africa, pp 1435-1440, 2013.

R. Chacón, E. Mirambell and E. Real. Analysis of steel members using FEM and big data, *Proceedings of the International Colloquium of Stability and Ductility of Steel Structures,* Timisoara, Romania, 2016.

L. Gardner and M. Ashraf. Structural design for non linear metallic material. *Engineering Structures*, 28 (6): 926-934, 2006.

L. Gardner and M. Theofanous. Discrete and continuous treatment of local buckling in stainless steel elements. *Journal of Constructional Steel Research*, 64 (11), 2008.

R. Greiner and M. Kettler. Interaction of bending and axial compression of stainless steel members. *Journal of Constructional Steel Research*, 64: 1217-1224, 2008.

R. Greiner and J. Lindner. Interaction formulae for members subjected to bending and axial compression in EUROCODE 3-the Method 2 approach. Journal of Constructional Steel Research, 62(8), 757-770, 2005.

P. Hradil, A. Talja, E. Real, E. Mirambell and B. Rossi. Generalized multistage mechanical model for nonlinear metallic materials. *Thin-Walled Structures*, 63 (3): 63-69, 2013.

M. Jandera, D. Syamsuddin. Interaction formula for stainless steel beam-columns, *Recent research advances on thin-walled structures, in: Proceedings of the Seventh European Conference on Steel and Composite Structures (EURO-STEEL*), Napoli, Italy, 10-12 September 2014.

M. Jandera, D. Syamsuddin and B. Zidlicky. Stainless steel beam-columns behaviour. *The Open Civil Engineering Journal*, 2016.

N. Lopes, P. Vila Real and L. Simoes da Silva. Stainless steel beam-columns interaction curves with and without lateral torsional buckling. *Proceedings of the Seventh EUROMECH Solid Mechanics Conference*, Lisbon, Portugal, 2009.

E. Mirambell and E. Real. On the calculation of deflections in structural stainless steel beams: an experimental and numerical investigation. *Journal of Construction Steel Research*, 54(1):109-133, 2000.

F. Pizzi. Structural behaviour of ferritic stainless steel columns subjected to combined loading. *Master Thesis, UPC (Catalonia)*, 2014.

W. Quach, J. Teng and K. Chung. Three-stage full-range stress-strain model for stainless steels. *Journal of Structural Engineering*, 134 (9): 1518-1527, 2008.

W. Ramberg and W. Osgood. Description of strees-strain curves by three parameters. *Technical note No 902, Washington DC: National advirsorycommittee for aeronautics*, 1943.

KJR. Rasmussen. Full-range stress-strain curves for stainless steel alloys. *Journal of Constructional Steel Research*, 59(1):47-61, 2003.

E. Real, I. Arrayago, E. Mirambell and R. Westeel. Comparative study of analytical expressions for the modelling of stainless steel behaviour. *Thin-Walled Structures*. 83: 2-11, 2014.

M. Rodríguez. Structural behaviour of stainless steel slender sections beam-columns subjected to combined loading. *Master Thesis (under preparation in CTU Prague),* 2016.

A. Tajla and P. Salmi. Design of stainless steel RHS beam, columns and beam-columns. *Research note 1619*, VTT building technology, Finland, 1995.

O. Zhao, L. Gardner and B. Young. Buckling of ferritic stainless steel members under combined axial compression and bending. *Journal of Constructional Steel Research*, 117: 35-48, 2016.

O. Zhao. Structural behaviour of stainless steel elements subjected to combined loading. *Doctoral Thesis, Imperial College of Science, Technology and Medicine*, London, UK, 2015.